Lancaster University

Sodium Dichloroacetate (DCA) impairs β-secretase-mediated Proteolysis of the Alzheimer's Disease Amyloid Precursor Protein (APP)

Jessica Hammond MSci (Hons)

Supervisor: Dr Edward Parkin

This thesis is submitted in fulfilment of the degree of MSc (research) Biomedical Science

This thesis is entirely my own work and has not been submitted in full or in part for the award of a higher degree at any other educational institution.

September 2016

Abstract

Alzheimer's disease (AD) is caused by the accumulation of neurotoxic amyloid-beta (Aβ)-peptides in the brain. These peptides result from the amyloidogenic cleavage of the amyloid precursor protein (APP) by β-secretase yielding soluble APPbeta (sAPPβ) and a membrane-associated C-terminal fragment, C99. The latter fragment is then cleaved by γ-secretase liberating the toxic Aβ-peptides. Alternatively, APP can be cleaved non-amyloidogenically by an α-secretase activity (a member(s) of the a disintegrin and metalloproteinase, ADAM, family of zinc metalloproteinases) which cleaves within the Aβ region of the protein producing soluble APPalpha (sAPPα) and a membrane-associated C-terminal fragment (C83) and precluding the formation of intact Aβ-peptides.

In this study we show that, in human neuroblastoma SH-SY5Y cells, the mitochondrial modulator dichloroacetate (DCA) impairs the β-secretase-mediated processing of APP as determined by impaired sAPPβ production. Conversely, the non-amyloidogenic processing of APP was enhanced resulting in more sAPPα production. Over-expressing the β-secretase (BACE1) in SH-SY5Y cells partly reversed this phenomenon as sAPPα production did not significantly increase and $sAPP\beta_{751/770}$ levels were unaltered. Over-expressing APP_{695} resulted in unchanged sAPPβ generation following treatment with DCA. The effect of DCA on two further ADAM substrates, E-cadherin and Jagged1 was investigated in different cell lines in order to examine the substrate and cell-type specificity of DCA. Endogenous E-cadherin expression in both SW480 colorectal cancer cells and HEK-Jagged1 (HEK cells stably over-expressing Jagged1) was decreased following DCA treatment as was shedding of the protein. Endogenous APP expression and sAPPα shedding was increased in both cell lines, however it was not possible to detect sAPPβ in the samples. Conversely the expression and shedding of endogenous Jagged1 in SW480 cells was enhanced following DCA treatment whilst, in HEK-Jagged1 cells, expression of the transfected protein was unaltered but its shedding was enhanced. These data indicate that the effects of DCA on APP are not common to all ADAM substrates.

Thus, we postulate that the mode of activity of DCA involves the stimulation of APP release from the cell surface by α-secretase resulting in reduced internalisation and subsequent β-secretase-mediated proteolysis. When APP is over-expressed the α-secretase pathway becomes saturated resulting in more internalisation of intact APP and its availability for β-secretase cleavage Given that DCA is a very small molecule already used in humans for the treatment of specific medical conditions and can safely transit the blood brain barrier, it may be a suitable pharmaceutical candidate to delay or treat the development of AD.

Abbreviations

Aβ	amyloid beta
Ach	acetylcholine
AChE	acetylcholinesterase
AD	Alzheimer's Disease
ADAM	a disintegrin and metalloproteinase
AICD	APP intracellular domain
ApoE	apolipoprotein E
APP	amyloid precursor protein
BACE1	beta-site APP cleaving enzyme 1
CSF	cerebrospinal fluid
DCA	dichloroacetate
FAD	familial Alzheimer's disease
HEK	human embryonic kidney
iCLiP	intramembrane cleaving protease
IDE	insulin degrading enzyme
KPI	Kunitz protease inhibitor
LTP	long-term potentiation
MCI	mild cognitive impairment
NFT	neurofibrillary tangles
PDC	pyruvate dehydrogenase complex
PDH	pyruvate dehydrogenase
PDK	pyruvate dehydrogenase kinase
PHFs	paired helical filaments
PS1	presenilin-1
PS2	presenilin-2
RIP	regulated intramembrane proteolysis
SAD	sporadic Alzheimer's disease
sAPPα	soluble amyloid precursor protein alpha
sAPPβ	soluble amyloid precursor protein beta

Contents

Chapter 1: Literature Review

1.1 Introduction

Alzheimer's disease (AD), first described by Alois Alzheimer in 1906, is the most common form of dementia, primarily affecting the elderly. It is thought that an imbalance between the amyloidogenic and non-amyloidogenic processing of the amyloid precursor protein (APP) results in increased production of amyloid beta (Aβ) which, unless sufficiently cleared from the brain, aggregates into senile plaques and causes oxidative damage to surrounding neurons and synapses resulting in memory loss. The current study aims to characterise the role of the drug dichloroacetate (DCA) in the proteolysis of APP.

1.2 Alzheimer's disease

AD is a progressive neurodegenerative disease that accounts for more than 80% of dementia cases in the elderly worldwide (Anand *et al*., 2014). The age of onset is typically after 65 years with a life expectancy of 3-10 years (Zanetti *et al*., 2009). This devastating disease impacts on society in a number of ways; increasing the burden on the NHS, emotional stress on the patient and their immediate family and had an estimated global cost of $818 billion in 2015 (Prince *et al*., 2015). With an increase in life expectancy and growth in the ageing population, the number of patients is expected to increase from 46.8 million (as of 2015) to 131.5 million worldwide in 2050 (Prince *et al*., 2015).

AD progression is not linear; both the early and late stages of the disease progress slowly with the mid (moderate) stage progressing at a faster rate (Stern *et al*., 1994). AD progression is typically assessed by the mini mental state examination (MMSE) which is scored on a numerical scale; 20-24 mild, 11-20 moderate and 0-10 severe (Ercoli *et al*., 2003). AD presents in patients initially with memory loss in a stage referred to as mild cognitive impairment (MCI). 10-15% of people presenting with MCI go on to develop AD each year (Petersen, 2004), with their symptoms worsening to aphasia (inability to understand and form speech), agnosia (inability to recognise objects and people) and apraxia (inability to carry out voluntary movements) amongst other behavioural and memory issues (Blennow *et al*., 2006).

Current treatments for AD only attenuate these symptoms, with no real impact on disease progression. In addition to a lack of effective treatments, lack of effective diagnosis of AD further compounds the issue as many AD symptoms are common to other forms of dementia such as vascular dementia. The current gold standard diagnosis of AD is post-mortem examination of brain pathology but some advancements have been made such as the use of Pittsburgh Compound B (PiB). PiB binds to amyloid beta in affected regions of the brain

and can be detected by PET (positron emission tomography) scanning *in vivo* (Cohen and Klunk, 2014). A further understanding of the molecular mechanisms that underpin the pathology of the disease will no doubt lead to advancements in its diagnosis and treatment.

1.3 Neuropathology

On a pathological level, AD is characterised by the presence of extracellular deposits of Aβ protein in structures termed 'senile plaques' and the formation of intracellular neurofibrillary tangles (NFTs) composed of hyperphosphorylated tau protein (Fig. 1.1) (Braak and Braak, 1991). Additional structures of Aβ also accumulate in the vasculature of the brain, concentrating in small arteries and small arteriole walls.

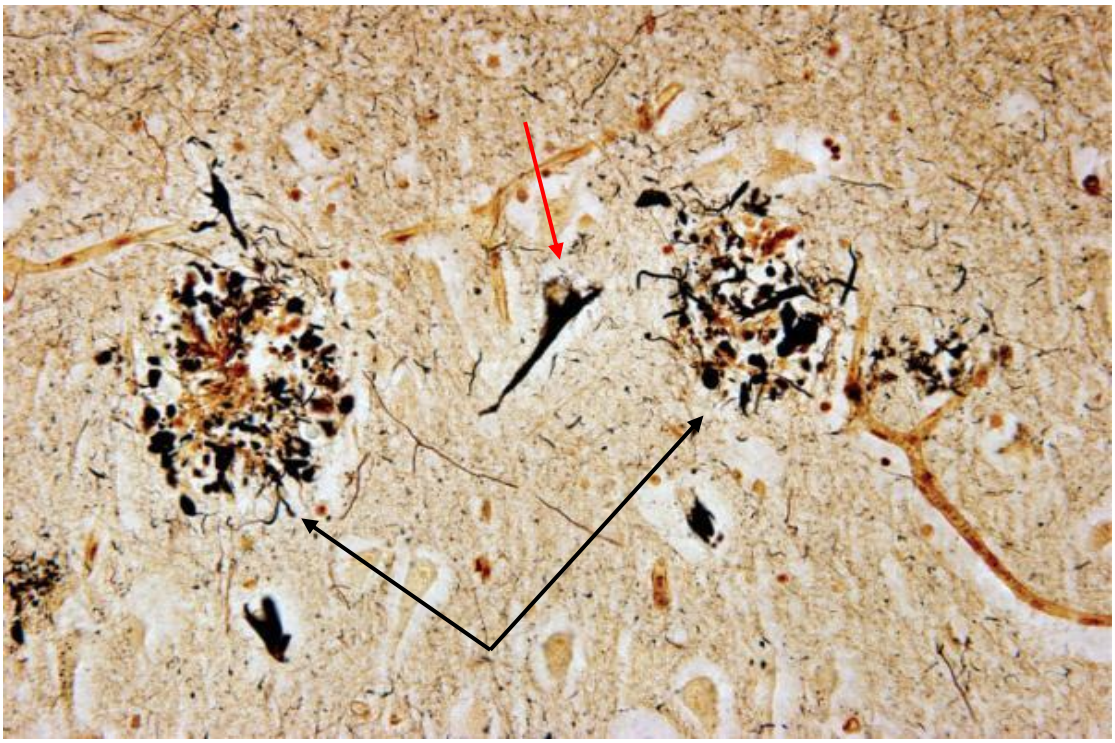

Figure 1.1. Neuropathological features of Alzheimer's disease. The micrograph shows the temporal cortex of an AD patient stained with modified Bielshowski stain at 400X objective. The black arrows indicate senile plaques whilst the red arrow indicates a neurofibrillary tangle. These two key histopathological features are characteristic of AD, with the appearance of senile plaques occurring before neurofibrillary tangles develop. Taken from (Perl, 2010).

These lesions are abundant in AD brains yet, interestingly, are also present in the normal ageing brain, but at a significantly lower level (Knopman *et al*., 2003). This raises the question as to at what point does plaque/NFT load constitute AD and how this is different to normal ageing. There is much debate as to whether these pathological markers are the tombstones of damage already done or are causing damage themselves.

A number of changes to brain structure are seen alongside the development of plaques and tangles; an overall decrease in brain mass is seen, which is primarily due to a loss of grey matter. Ventricles increase in size, due to a build-up in cerebrospinal fluid (Nestor *et al*., 2008). The cerebral cortex and cortical regions are starkly affected with the greatest change in mass observed in these regions (cortical atrophy) (Perl, 2010). The temporal and parietal lobes (part of the cortex) are affected in AD brains and are responsible for visual memory and language processing, so it is unsurprising that changes to these regions result in memory loss and problems processing and understanding speech (Wenk, 2003).

Spatially, AD pathology is spread throughout the brain, adding a layer of complexity when approaching treatments. The presence of cholinergic neurons is a common feature between areas of the brain afflicted, and these are typically damaged (Whitehouse *et al*., 1981). Both neurons and synapses are degraded in AD, and this neurotoxicity arises due to a combination of processes including oxidative damage and inflammation driven by Aβ oligomers and NFTs (Kumar *et al*., 2015).

1.4 Risk Factors associated with Alzheimer's disease

Whilst a definitive cause for Alzheimer's disease has not been identified, there are several known and suspected risk factors associated with this multifactorial disease. Factors include genetics, environmental factors (such as a toxin or specific metal imbalances) (Maher *et al*., 2016), head injury/trauma (Schofield *et al*., 1997), pre-existing conditions associated with vascular disease like type 2 diabetes, obesity, hypertension and atherosclerosis (O'Brien and Markus, 2014), and potentially bacterial/viral infections (Ellawanda and Wallace, 2013).

The majority of AD cases are sporadic (SAD) but 5% of cases are inherited and are referred to as Familial Alzheimer's disease (FAD) (Bird, 2008). FAD cases have a much earlier age of onset, usually between 40-50 years compared to 65 years for SAD and typically progress at a faster rate. Studies from FAD patients have elucidated genes linked to AD progression and have also identified specific mutations that cause early-onset AD such as the London mutation in *APP* (V717I) (Muratore *et al*., 2014). The majority of FAD cases are caused by mutations in *APP* (amyloid precursor protein), *PS1* (Presenilin-1) and *PS2* (Presenilin-2). Another subset of patients that have provided invaluable insight into the genetics behind AD are Down's Syndrome (DS) sufferers as they are at a much higher risk of developing AD than the general population. Individuals with Down's syndrome have trisomy of chromosome 21, which also happens to be the location of a major protein involved in Alzheimer's disease- the amyloid

precursor protein (APP). Studies in DS patients have contributed to our understanding of APP and the role it plays in AD pathogenesis (Wallace and Dalton, 2011).

The major genetic risk factor associated with sporadic cases of AD is the presence of the apolipoprotein E ε4 allele which increases the risk of developing AD 3-fold in heterozygotes and 15-fold in homozygotes (Farrer *et al*., 1997). Apolipoprotein E (ApoE) functions to transport lipids between tissues or different cells (Liu *et al*., 2013), however the ε4 form of the allele promotes fibrillation and plaque formation as it is necessary for amyloid beta deposition (Hartman *et al*., 2002, Holtzman *et al*., 2000).

1.5 Molecular theories behind Alzheimer's disease

The precise mechanism or cause of Alzheimer's disease is unknown; however, several different theories have been presented including the amyloid cascade hypothesis, the tau hypothesis, the cholinergic hypothesis and inflammation hypothesis. Current trends in the literature suggest the amyloid cascade hypothesis is the most widely accepted at present, and has been for the past two decades.

1.5.1 Tau Hypothesis

The tau hypothesis suggests that the primary cause of AD pathology is hyperphosphorylated tau aggregation into paired helical filaments (PHFs) and NFTs, with neuronal death and Aβ aggregation as downstream events. AD is considered a tauopathy, part of a group of diseases where tau is a key component of the pathology (Lee *et al*., 2001). Tau, encoded by the *MAPT* gene, is a microtubule associated protein which aids with assembly and stabilization of microtubules (Ittner and Gotz, 2011). The incorporation of tau into filamentous structures is dependent on its phosphorylation state; hyperphosphorylated tau aggregates whilst unphophorylated tau typically does not (Mukrasch *et al*., 2009). The phosphorylation state of tau is developmentally regulated with adult tau subject to fewer modifications than foetal tau (Kanemaru *et al*., 1992). The phosphorylation of tau is necessary for the regulation of microtubule stabilization and assembly, however it is the imbalance of this process (normal adult tau has 2 phosphates on average, whereas pathological tau has up to 8 phosphates) that lends to the formation of NFTs and PHFs (Wang and Mandelkow, 2016). NFTs are a classical hallmark of AD, and although an exact role for tau in AD pathology has not been pinpointed, several disease factors are attributed to tau. The hyperphosphorylation of tau is thought to prevent degradation of the protein (thereby disrupting axonal transport) (Rodriguez-Martin *et al*., 2013), cause tau to be missorted to the somatodendritic compartment where it impairs

synaptic signalling, and to increase aggregation of the protein into NFTs (Wang and Mandelkow, 2016). All of these processes result in neuronal degradation and AD pathology, although the precise mechanism by which tau aggregation leads to neuronal death is unknown. The tau hypothesis also acknowledges the existence of amyloid beta and senile plaques but frames them as a secondary consequence of NFT formation.

1.5.2 Amyloid Cascade

The amyloid cascade or amyloid hypothesis places amyloid beta (Aβ) as the causative agent of Alzheimer's disease with neurofibrillary tangles and oxidative damage as secondary downstream consequences of senile plaque generation (Hardy and Higgins, 1992). As the name suggests, amyloid beta is central to the development of AD which is just one of a number of diseases known collectively as amyloidoses where the underlying cause of the disease is aggregation of abnormal proteins into insoluble amyloid fibers (Ghiso and Frangione, 2002). Aβ aggregates in a gradual process or 'cascade'; Aβ monomers aggregate to form dimers which in turn aggregate into multimers through several steps eventually forming the mature fibrils that are interwoven into senile plaques (Fig. 1.2).

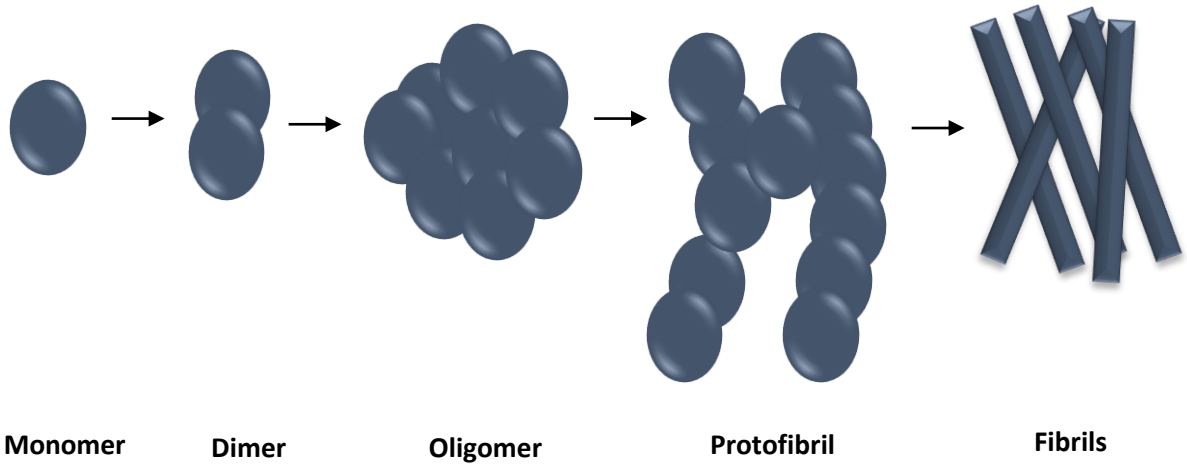

Figure 1.2. The amyloid cascade and aggregation of Aβ. The aggregation of Aβ is split into two phases; a nucleation phase and an elongation phase. The nucleation phase starts with a misfolded Aβ monomer self-aggregating to form a dimer and oligomers. The elongation phase refers to the stage whereby oligomers are extended by the addition of more Aβ and the oligomers elongate into protofibrils that develop into mature fibrils when no further Aβ can be added. Theses mature fibrils are usually composed of four protofibrils and are deposited extracellularly into senile plaques.

The aggregation of Aβ is thought, ultimately, to be due to the imbalance of Aβ generation and clearance. Aβ generation itself is thought to be due to the imbalance between two proteolytic processing pathways, one that generates Aβ – the amyloidogenic pathway and one that does not – the nonamyloidogenic pathway. Both pathways start with APP which is subject to a sequential cleavage steps (see section 1.7). The relationship between Aβ and the

brain (neurons in particular) is explored in section 1.8.3, but, briefly, it is thought that Aβ oligomers bind to receptors on neurons and alter synaptic shape and signalling as well as generating reactive oxygen species and causing oxidative damage to neurons (Lacor *et al*., 2007).

1.6 Amyloid precursor protein (APP)

APP is encoded on chromosome 21 and is part of a large family of APP related proteins which includes the APP-like proteins APLP1 and APLP2 (Jacobsen and Iverfeldt, 2009). The APP family of proteins are evolutionarily conserved from fly to mouse to human and share sequence homology. The key difference between APP and its related proteins is the presence of the internal Aβ domain within the former protein. APP is composed of a large extracellular domain, a single pass transmembrane region and a small cytoplasmic tail (Fig. 1.3) (Gralle and Ferreira, 2007). This structure is typical of cell surface receptors.

Figure 1.3. The domain structure of APP. All APP protein family members contain each of these regions bar the amyloid beta (Aβ) domain. The YENPTY motif shows highest homology across APP proteins (and species) and is the sequence where intracellular proteins interact with APP. The extracellular segment contains the E2 domain, Kunitz protease inhibitor (KPI) domain, acidic domain (Ac), copper binding domain (CuBD) and a heparin-binding domain (HBD). The KPI domain is not found in all APP isoforms as it is subject to alternative splicing. The heparin binding domain contains two heparin binding sites which are responsible for APP bioactivity.

The *APP* gene consists of 19 exons and undergoes alternative splicing of exons 7 and 8 to form 3 major isoforms; APP_{695}, APP_{751} and APP_{770} (numbers denote amino acid length). The isoforms have a similar domain structure, however APP_{695} doesn't contain a KPI (Kunitz protease inhibitor) or OX2 domain whereas APP_{770} contains both of these and APP_{751} has the KPI domain but lacks an OX2 domain. Although APP is ubiquitously expressed throughout the

body, the isoforms exhibit spatial distribution with APP_{695} primarily expressed in the brain and neurons, whilst APP_{751} and APP_{770} are primarily expressed in the periphery (Gralle and Ferreira, 2007). The ratio of APP isoforms (770:751:695) in the human cortex is approximately 1:10:20 (Nalivaeva and Turner, 2013) and this expression varies throughout brain maturation with *APP* expression beginning during early embryogenesis and brain development.

The exact function of APP has not been fully characterised, however it is thought to be involved in a host of processes including neurite outgrowth, axonal growth and guidance, calcium homeostasis, cell-cell adhesion, synaptogenesis, stem cell migration, learning and memory, carcinogenesis, and glucose homeostasis (Billnitzer *et al*., 2013, Song and Pimplikar, 2012, Hamid *et al*., 2007, Breen *et al*., 1991, Wang *et al*., 2009, Freude *et al*., 2011, Weyer *et al*., 2011, Krause *et al*., 2008, Needham *et al*., 2008). As many of these processes shape and regulate the development of the brain, APP has been described as morphoregulatory (Alpar *et al*., 2006). A number of these processes involve metabolites of APP produced from APP proteolysis (section 1.7). The role of APP in neurite outgrowth is perplexing with some studies showing APP inhibits outgrowth whilst others show the protein stimulates neurite outgrowth (Allinquant *et al*., 1995, Hoareau *et al*., 2008). It has been proposed that the influence of APP on neurite outgrowth varies according to cell type and stage of development, as well as the suggestion that a metabolite of APP (sAPPα) may serve to enhance neuritic outgrowth by inhibiting APP holoprotein (Young-Pearse *et al*., 2008). A contrasting role for APP is in cell death. APP is also subject to cleavage by caspases and cleavage of APP by caspases can trigger cell death, but in a controlled manner and is thought to be a selective process during brain maturation (De Strooper and Annaert, 2000).

APP has the typical structure of a receptor, forms homodimers and heterodimers, and has a role in cell-cell adhesion all of which suggest it may transduce signals by acting as a receptor, however a definitive ligand for APP has yet to be characterised (Deyts *et al*., 2016). F-spondin is a proposed ligand for APP and it binds to APP on the first heparin binding site within the heparin binding domain (HBD) (Ho and Sudhof, 2004). F-spondin is known to be involved in neuronal development and repair, however the necessity of APP in these particular processes has not been identified.

Although it is uncertain as to what stimulates the transduction of a signal from APP, it is undisputed that it plays a vital role in normal brain development and processes. The dysregulation of APP can lead to diseases like AD, type 2 diabetes and cancer. Approximately 32 mutations in *APP* have been linked to FAD cases (O'Brien and Wong, 2011), the majority of

which are mutations near the γ-secretase cleavage site. APP is regulated by interactions with various proteins such as p53, but is also influenced by copper and iron (Acevedo *et al*., 2011, Rogers *et al*., 2008). *APP* promoter activity is repressed by p53 when p53 binds to the transcription factor Sp1 (stimulating protein 1) preventing it from stimulating the *APP* promoter (Cuesta *et al*., 2009).

1.7 APP Proteolysis

APP undergoes proteolysis via one of two different pathways; the amyloidogenic pathway and the non-amyloidogenic pathway (Fig. 1.4). As the name suggests, the amyloidogenic pathway results in the production of amyloid beta whereas the non-amyloidogenic pathway does not. The majority (~90%) of APP proteolysis occurs via the non-amyloidogenic pathway and the remaining 10% of APP is processed to yield amyloid beta amongst other products (Octave *et al*., 2013).

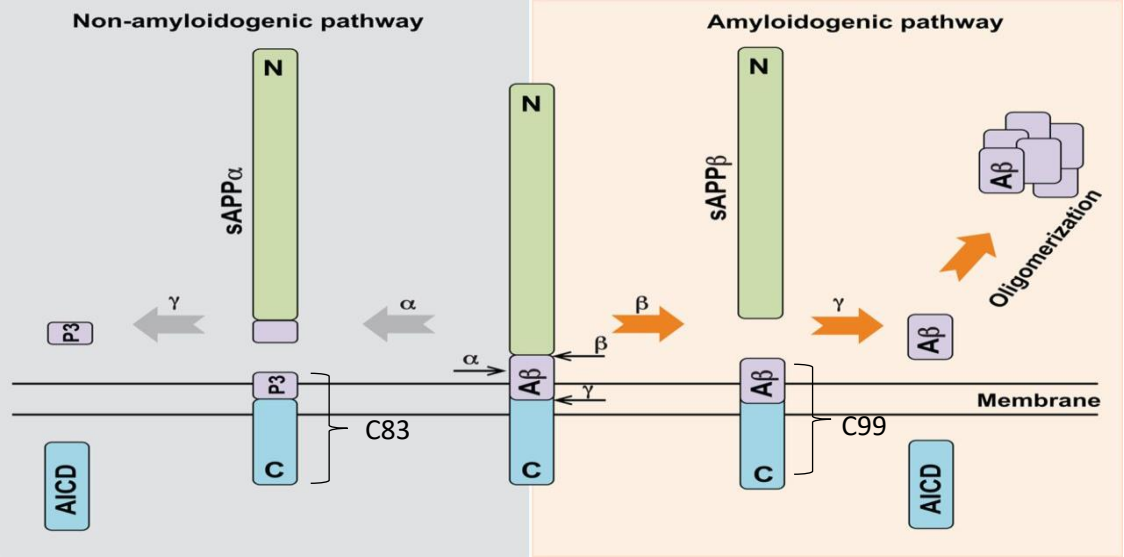

Figure 1.4. APP proteolysis. APP can be cleaved, in the amyloidogenic pathway, by β-secretase (BACE1) yielding soluble APP beta (sAPPβ) and a C-terminal fragment (C99). The latter fragment is then cleaved by γ-secretase to liberate intact Aβ-peptides. Alternatively, APP can be cleaved non-amyloidogenically by an α-secretase to yield soluble APP alpha (sAPPα) and an alternative C-terminal fragment (C83). Membrane-bound C83 is then cleaved by γ-secretase to release a small fragment, P3. Cleavage of both C83 and C99 by γ-secretase also yields a soluble APP intracellular domain (AICD) fragment. Adapted from (Nicolas and Hassan, 2014).

Of note is spatial separation of the two pathways, alpha cleavage occurs at the membrane surface (Lammich *et al*., 1999) whilst beta cleavage occurs in endocytic compartments (Fuentealba *et al*., 2007) or in lipid rafts. Lipid rafts are present at the cell surface, but are a distinct microenvironment enriched in cholesterol and glycosphingolipids

that facilitate amyloidogenic processing (Hicks *et al*., 2012). The generation of APP fragments via the two pathways is regulated by enzymes known as secretases.

The proteolysis of APP is one example of regulated intramembrane proteolysis (RIP). Regulated intramembrane proteolysis (RIP) is a signalling paradigm for which there are over 60 current known substrates (Lichtenthaler *et al*., 2011), including E-cadherin, Jagged1 and Notch (Marambaud *et al*., 2002, LaVoie and Selkoe, 2003). RIP is characterised by the cleavage of a transmembrane protein by an iCLiP (intramembrane cleaving protease) within the transmembrane domain to yield a cytosolic fragment. This cleavage step is usually preceded by another cleavage step in a process known as ectodomain shedding whereby the transmembrane substrate is cleaved near the transmembrane domain by a membrane bound protease (sheddase) to leave a membrane bound fragment of 30 amino acids or less and a soluble ectodomain fragment that is shed into the extracellular space (Landman and Kim, 2004). For APP, the cytosolic fragment is AICD (APP intracellular domain) and the ectodomain fragment is sAPPα for the non-amyloidogenic pathway and sAPPβ in the amyloidogenic pathway.

1.7.1 Alpha secretases

Alpha secretase (α-secretase) was the generic term given to the enzyme(s) responsible for the initial cleavage of APP within the Aβ sequence, which generates sAPPα and C83 and prevents Aβ generation. It is known that the α-secretase in question belongs to the ADAM (**a** **d**isintegrin **a**nd **m**etalloprotease domain) family of enzymes. The ADAMs are transmembrane proteins characterized by a specific domain organization; pro-domain, metalloprotease, disintegrin, cysteine-rich, epidermal-growth factor like, transmembrane, and cytoplasmic domains (Seals and Courtneidge, 2003). Catalytically active ADAMs share a common HEXGHXXGXXHD motif .There are around 40 mammalian ADAMs, only a select number of which have catalytic activity and are involved in the cleavage of transmembrane proteins like APP. APP can be cleaved by ADAM9, ADAM10 or ADAM17 (Deuss *et al*., 2008), however ADAM10 was identified as the α-secretase involved in non-amyloidogenic processing of APP (Kuhn *et al*., 2010).

ADAM10 (EC 3.4.24.81) is a type 1 transmembrane glycoprotein encoded by the *ADAM10* gene on chromosome 15 (Yamazaki *et al*., 1997). Part of the ADAM family of zinc metalloproteases, it is ubiquitously expressed and is evolutionarily conserved (Becherer and Blobel, 2003). Transcription of ADAM10 is upregulated by the X-box binding protein 1 (XBP1)

transcription factor (Reinhardt *et al*., 2014) as well as by the hormone melatonin which stimulates the ADAM10 promoter region (Shukla *et al*., 2015). ADAM10 transcription is also upregulated by a heteromer of RAR (Retinoic Acid Receptor) and RXR (Retinoid X Receptor), when all-trans retinoic acid is bound to the heteromer (Prinzen *et al*., 2005). ADAM10 is synthesized as a 748 amino acid precursor which, after undergoing proteolysis in the Golgi body, matures into the catalytically active form (Anders *et al*., 2001). One region that is removed during this process is the prodomain. The prodomain controls ADAM10 function as expression of only the prodomain inhibits ADAM10 activity (Moss *et al*., 2007) and it is required for correct protein folding of ADAM10 (Anders *et al*., 2001). The importance of the prodomain is highlighted by the presence of the Q170H and R181G mutations within the domain in patients with SAD (Kim *et al*., 2009). Recapitulation of these mutations in cellular models showed a 2-3-fold increase in Aβ levels suggesting functional ADAM10 (as controlled by the prodomain) is a key part of preventing AD pathology. It is worth noting that decreased ADAM10 activity is a risk factor for SAD (Kim *et al*., 2009) and that lower levels of XBP1 are observed in AD patients (Reinhardt *et al*., 2014). Dysregulation of ADAM10 has been associated with numerous diseases including Alzheimer's disease, Prion disease, Huntington's disease, bipolar disorder, and fragile X syndrome (Lo Sardo *et al*., 2012, Altmeppen *et al*., 2015, Jian *et al*., 2011, Pasciuto *et al*., 2015).

ADAM10 functions to cleave a range of transmembrane proteins including APP, E-cadherin, Jagged1 and Notch (Allinson *et al*., 2003). In addition to carrying out ectodomain shedding of protein substrates, ADAM10 itself is also subject to ectodomain shedding (Parkin and Harris, 2009). Due to its involvement in signalling processes that control development, adhesion and proliferation, it is unsurprising that ADAM10 knockout mice are early embryonic lethal (Hartmann *et al*., 2002). This presented a challenge when trying to identify which ADAM was responsible for the α-secretase cleavage of APP, but this has now been confirmed to be ADAM10. ADAM10 was confirmed as the α-secretase by RNAi knockdown of ADAM10 in primary murine neurons which showed supressed α-cleavage when ADAM10 was knocked down but not ADAM9 or ADAM17 (Kuhn *et al*., 2010). ADAM10 cleaves the bond between lys16 and leu17 in APP (within the Aβ sequence), to produce sAPPα and C83, whilst precluding generation of Aβ (Allinson *et al*., 2003). It is co-expressed with APP and BACE1, and competes with BACE1 for APP (Colombo *et al*., 2013).

As ADAM10 competes with BACE1 for APP, and precludes the generation of Aβ, it has been proposed as a potential therapeutic target in AD, as it is thought stimulation of the alpha pathway may reduce Aβ production and thereby slow disease progression. This has been

evidenced in transgenic mice overexpressing ADAM10, as they had increased sAPPα levels which coincided with decreased Aβ production (Postina *et al*., 2004). Other studies have shown that transgenic mice that express a mutant form of ADAM10 which does not possess catalytic activity show increased senile plaque load (Postina *et al*., 2004), and HEK (human embryonic kidney) cells overexpressing ADAM10 show increased alpha shedding of APP (Lammich *et al*., 1999). A clinical trial aimed at increasing ADAM10 activity has also shown promise; acitretin (an all-trans retinoic acid derivative) increased sAPPα shedding but did not alter Aβ significantly in humans (Tippmann *et al*., 2009). Acitretin was the first ADAM10 substrate validated in humans, and may affect Aβ levels if used for a longer period than that used in the trial. Together, these studies suggest stimulation of the non-amyloidogenic pathway by up-regulating ADAM10 activity/expression would increase sAPPα, preclude Aβ generation and slow AD disease progression.

ADAM17 is also a catalytically active ADAM involved in APP ectodomain shedding. ADAM17 is also referred to as TACE – tumour necrosis factor-α-converting enzyme, as TNF-α was the first substrate identified for ADAM17 (Black *et al*., 1997). ADAM17 was also the first enzyme to be identified as a sheddase; an enzyme that is responsible for ectodomain shedding. Prior to this discovery, ADAMs were thought to solely act as adhesion molecules. Despite the fact that they share a substrate (APP), ADAM17 and ADAM10 only share 30% protein sequence homology and ADAM17 is not very similar to any other members of the ADAM family (Gooz, 2010). Like ADAM10, ADAM17 undergoes proteolysis to remove its prodomain to become a mature catalytically active enzyme. Other ADAM17 substrates include adhesion proteins L-selectin and CAM-1 and cytokine receptors like TNF-receptor and IL-6R (interleukin 6 receptor) (Scheller *et al*., 2011).

1.7.2 Beta Secretase

BACE1 (beta-site APP cleaving enzyme 1) was identified in 1999 as the β-secretase responsible for cleaving APP to form sAPPβ and C99 (Hussain *et al*., 1999). The enzyme is a type I transmembrane aspartyl protease that is ubiquitously expressed with particularly high levels expressed in the pancreas and the brain (Ehehalt *et al*., 2002). Structurally, BACE1 has two catalytic sites located in the 'flap' region which is composed of a flexible β-hairpin loop and only the full length enzyme (501 amino acids) possesses catalytic activity (Wang *et al*., 2013). BACE1 is subject to different post-translational modifications as well as existing as different isoforms and is regulated by a host of interactions.

In addition to cleaving APP, BACE1 has other substrates including neuregulin1, neuregulin3 (Cheret *et al*., 2013), and low density lipoprotein receptor-related protein (von Arnim *et al*., 2005). There are no known mutations in *BACE1* associated with AD (Sathya *et al*., 2012), however increased BACE1 levels in the cortex are associated with sporadic AD (Sathya *et al*., 2012) and BACE1 exhibits maximal activity in neurons (Seubert *et al*., 1993). Elevated levels of BACE1 have also been associated with other neurological conditions such as brain injury, cerebral hypometabolism and ischaemia (Wang *et al*., 2013). Furthermore, BACE1 enzyme activity increases in response to various stresses (all of which have been implicated in AD pathogenesis) including oxidative stress, metabolic stress and inflammatory stress (Findlay *et al*., 2015).

1.7.3 Gamma secretase complex

The γ-secretase is a 170 kDa multi-protein complex composed of four hydrophobic proteins; presenilin-1 (or presenilin-2), nicastrin, APH-1 (anterior-pharynx defective 1) and PEN-2 (presenilin enhancer 2) (Tolia and De Strooper, 2009). Presenilin-1, the catalytically active subunit, is a membrane-bound aspartyl protease with nine-transmembrane topology found in the endoplasmic reticulum and trans-golgi network (De Strooper, 2003). Presenilin-2 is a homolog of presenilin-1 and the two share 67% of their DNA sequence (Zhang *et al*., 2013). Whilst the two are similar, differential cleavage of APP C99 is observed with presenilin-1 and presenilin-2 γ-secretase complexes (Bentahir *et al*., 2006). Nicastrin is the largest γ-secretase subunit and is a scaffolding protein which also binds to ligands acting as a receptor for ectodomain shed proteins (Dries *et al*., 2009). APH-1 and PEN-2 co-operate to interact with presenilin-1 and regulate proteolysis of presenilin-1 (Luo *et al*., 2003). It is thought that each of the γ-secretase subunits cross-regulate each other as well as being subject to regulation by other proteins (Zhang *et al*., 2014).

The complex functions as a protease, cleaving numerous transmembrane proteins within their transmembrane domains. The most notable substrates of γ-secretase include APP, Notch, E-cadherin, N-cadherin, and Jagged1 (Krishnaswamy *et al*., 2009, De Strooper *et al*., 1999, Marambaud *et al*., 2002, Marambaud *et al*., 2003, LaVoie and Selkoe, 2003).

Presenilin-1 has long been implicated in AD pathology due to mutations in the presenilin gene *PS1* being identified in autosomal dominant familial cases of AD (Hutton and Hardy, 1997). There have been over 150 mutations in the presenilin genes (*PS1* and *PS2*) associated with AD pathology (Zhang *et al*., 2014). There have also been studies implicating presenilin in cancer development due to the fact that the γ-secretase complex also cleaves

Notch and aberrant Notch signalling is implicated in several types of cancer (Capaccione and Pine, 2013).

1.8 APP fragments

Proteolysis of APP generates a number of different fragments, both intracellular and extracellular (see Fig. 1.4.). The extracellular ectodomain fragments sAPPα and sAPPβ have been implicated in neuroprotective processes (Chasseigneaux and Allinquant, 2012) and have been proposed as potential biomarkers of AD progression (Lewczuk *et al*., 2010). Less is known about p3, a fragment produced after γ-secretase cleavage of C83, but it may also be neuroprotective (Han *et al*., 2011). Aβ is another extracellular fragment of APP and is thought to be responsible for AD pathology. Lastly, the APP intracellular domain (AICD) is liberated from C83 and C99 following γ-secretase cleavage and is thought to partake in nuclear and cytosolic signalling (Beckett *et al*., 2012).

1.8.1 sAPPα

Following cleavage of APP by the α-secretase, two fragments are produced; C83 and sAPPα. sAPPα has been reported to have a role in many processes including neuroprotection, proliferation of neural stem cells, regulation of cell division and enhancement of cognition via long term potentiation (Chasseigneaux and Allinquant, 2012). One particularly neuroprotective form of sAPPα is a 17mer peptide (composed of residues 319-335) which was found to increase synaptic density as well as improving memory retention (Roch *et al*., 1994). The generation of sAPPα is observed in embryonic brains and is required for normal brain development (Guenette *et al*., 2006). It has also been shown to protect against glutamate excitotoxicity and oxidative damage induced by Aβ (Barger and Harmon, 1997, Chasseigneaux and Allinquant, 2012) but the mechanistic action behind these effects is poorly defined although several pathways have been implicated including the MAPK (Gakhar-Koppole *et al*., 2008), PI3K, and AKT kinase pathways (Cheng *et al*., 2002).

Another function of sAPPα in protecting against neurodegeneration is via the regulation of CDK5 (cyclin-dependent kinase 5) in neurons (Hartl *et al*., 2013). CDK5 normally functions to keep neurons in a post-mitotic state by inhibiting cell cycle progression (Zhang and Herrup, 2011) and regulates neuronal morphology, but has also been associated with AD pathology by aberrant phosphorylation of APP, BACE1 and tau (Cheung and Ip, 2012). CDK5 is activated by Aβ (Shukla *et al*., 2012) but is downregulated in primary cortical mouse neurons

treated with sAPPα, suggesting CDK5 is a downstream target of sAPPα signalling (Hartl *et al*., 2013).

1.8.2 sAPPβ

In contrast to sAPPα, sAPPβ has been the subject of fewer studies and not much is known about its physiological function. Both sAPPα and sAPPβ are identical in sequence with the exception of the additional 16 C-terminal amino acids found in the former fragment. For functions mediated by regions of the protein other than the last 16 C-terminal amino acids, sAPPα and sAPPβ largely act in the same way. Unlike sAPPα, sAPPβ has not been shown to be beneficial with regards to long term potentiation (Taylor *et al*., 2008). The neuroprotective effects of sAPPβ are also several magnitudes smaller than that of sAPPα, with a 50 to 100-fold decrease in neuroprotective action (Barger and Harmon, 1997, Furukawa *et al*., 1996). These findings together suggest that the final 16 amino acids are crucial for the neuroprotection and cognition enhancing effects of sAPPα (Chasseigneaux and Allinquant, 2012).

Other roles for sAPPβ have also been described including the triggering of cell death in peripheral neurons via the death receptor DR6 in response to a lack of growth factors (Nikolaev *et al*., 2009). Decreased levels of sAPPβ are present in cerebrospinal fluid (CSF) from patients with rapid onset amyotrophic lateral sclerosis (ALS), another neurological condition (Steinacker *et al*., 2011). It is thought that the decrease in sAPPβ (which also coincided with a decrease in sAPPα) in CSF of ALS patients reflects a loss of functional neurons, as neurons are responsible for sAPP generation (Chyung *et al*., 1997). Rather than a general decrease in sAPP fragments, CSF of AD patients shows a shift in sAPP levels with increased sAPPβ and no significant difference in sAPPα levels (Lewczuk *et al*., 2010). For this reason, the soluble ectodomain fragments have been explored as biomarkers for AD disease progression, with sAPPβ levels of particular interest. However, biomarker studies of sAPPα and sAPPβ in CSF have been inconclusive, as others have shown there may be no detectable difference in sAPP fragments in CSF of AD patients (Brinkmalm *et al*., 2013). sAPPα and sAPPβ levels in plasma have also been investigated in the same vein (Perneczky *et al*., 2013). This study showed that sAPPβ levels in plasma are slightly decreased in AD patients relative to controls (whilst no significant change in sAPPα was seen) and may be a potential biomarker for AD.

1.8.3 Amyloid beta (Aβ)

Amyloid beta has been the focus of a large proportion of AD research given its central role in disease pathogenesis. Levels of Aβ are elevated in the brains of SAD and FAD cases

(Hellstrom-Lindahl *et al*., 2009) and FAD-associated mutations in both *APP* and *PS1* have been shown to increase levels of Aβ42 (Blennow *et al*., 2006). Aβ is produced when C99 is cleaved by γ-secretase and, in ~90% of cases, the fragment produced is Aβ40 but other isoforms of Aβ exist including Aβ42 and Aβ38 which are produced when γ-secretase cleaves at different sites in the C99 fragment (Zou *et al*., 2002). The Aβ42 isoform is the most neurotoxic of the isoforms, is the major form present in senile plaques and encourages the aggregation of other Aβ monomers (Sakono and Zako, 2010). On the other hand, Aβ38 is not associated with AD pathology (Branca *et al*., 2014). The neurotoxicity of Aβ is thought to be due to the self-aggregation of Aβ monomers into soluble oligomers (Fig. 1.2). The aggregation of oligomers may rely on the neuronal cell membrane to form oligomers and protofibrils (Salay *et al*., 2009). The soluble oligomers may exert their toxic effects by increasing production of ROS leading to oxidative damage, mitochondrial dysfunction, and cell death. It is thought this oxidative damage is due to Aβ generating hydroxyl radicals using Fe (II) ions via Fenton's reaction (Tabner *et al*., 2002). A subset of cells within the brain exhibit resistance to this toxicity which may be due to a shift in cell metabolism as the Aβ-resistant cells primarily carry out glycolysis (Newington *et al*., 2011). The shift in metabolism precludes generation of reactive oxygen species within mitochondria and makes cells more resistant to apoptosis in the presence of Aβ.

Aβ is not purely a toxic entity and has some physiological roles ascribed to it such as modulation of synaptic activity and stimulating neurogenesis (Parihar and Brewer, 2010). The importance of normal Aβ is evident as it is produced during embryogenesis and is required for normal brain development (Guenette *et al*., 2006). Aβ is also present in low levels in normal healthy individuals and is constitutively produced throughout the body (Haass *et al*., 1992). Low concentrations of Aβ do not aggregate into oligomers; in fact, picomolar levels enhance long-term potentiation (LTP) whilst nanomolar levels reduce potentiation in the hippocampus (Puzzo *et al*., 2008). Aβ is cleared from the cell via one of three enzymes; insulin-degrading enzyme (IDE), neprilysin or endothelin-converting enzyme (Chasseigneaux and Allinquant, 2012). AD pathology is likely a failure of the clearance of Aβ coupled with increased production of Aβ giving rise to neurotoxic effects. Given that Aβ also has an important physiological role, strategies targeting Aβ must carefully consider the wider impact that this will have on the brain in general.

1.8.4 APP Intracellular Domain (AICD)

The APP intracellular domain (AICD) is a 5 kDa cytosolic fragment of APP released following γ-secretase cleavage of C99 or C83 with the majority of AICD *in vivo* being derived

from the processing of C99 (Goodger *et al*., 2009). There has been much controversy surrounding the exact physiological function of AICD as it has been shown to contribute to AD pathogenesis as well as being neuroprotective (Belyaev *et al*., 2010). AICD has been implicated in several processes including apoptosis, synaptic plasticity, neural development, neurite outgrowth and regulation of APP (Müller *et al*., 2008, Beckett *et al*., 2012, Zhou *et al*., 2012). There are multiple isoforms of AICD including AICD50 which is produced when γ-secretase cleaves at the ε site and the theoretical AICD57 and AICD59 which have not yet been detected experimentally (Müller *et al*., 2008). These small peptides are short-lived in the cytosol, making it difficult to detect and study their function (AICD degradation is controlled by IDE, and it may also be degraded by the proteasome) (Edbauer *et al*., 2002, Nunan *et al*., 2001). AICD interacts with numerous adapter proteins via its ^{681}YENPTY^{687} motif and forms transcriptionally active complexes (Beckett *et al*., 2012). The most well-characterized of these interactions is with Fe65, binding of Fe65 to AICD promotes AICD localisation to the nucleus (Kimberly *et al*., 2001). Genes regulated by AICD include *APP*, *BACE1*, *p53*, *MME* (neprilysin), and *GSK3-β* (Zhang *et al*., 2014). Interestingly, AICD levels are elevated in AD brains (Ghosal *et al*., 2009) suggesting that levels may be linked to increased Aβ (perhaps not surprising considering the involvement of the AICD in the regulation of several genes involved in Aβ production and degradation). The non-steroidal anti-inflammatory (NSAID) CHF5074 has been shown to lower AICD levels *in vivo* and concomitantly reduce Aβ42 levels whilst increasing levels of the non-pathogenic Aβ38 (Branca *et al*., 2014). This suggests CHF5074 exerts its neuroprotective effects via reduction of AICD resulting in altered cleavage of C99 to yield non-toxic forms of Aβ peptides. On the other hand, AICD has been shown to down regulate Wasf1 transcription and expression, which resulted in reduced Aβ levels in mice suggesting that AICD has a beneficial effect on Aβ modulation (Ceglia *et al*., 2015).It is clear that AICD interacts with many targets and it is likely that it is the balance (or rather imbalance) of these interactions that contributes to AD pathology.

1.9 Treatments for AD

A small number of drugs are currently available which address the symptoms of AD and delay disease progression. However, current treatments do not address the underlying cause of the disease so there is an unmet medical need in this respect.

Treatments currently used in the UK for the management of AD fall in to two categories; acetylcholinesterase (AChE) inhibitors and glutamate antagonists, both of which provide

symptomatic relief as opposed to being curative. They are available through the NHS as monotherapies and are also being explored as combination therapies given that they have different therapeutic targets. The treatments only help a specific subset of patients, with half of patients showing no response (Kumar *et al*., 2015). The reason as to why only some patients respond is unknown.

1.9.1 Acetylcholinesterase Inhibitors

There are four different acetylcholinesterase (AChE) inhibitors used for the management of mild to moderate AD; rivastigmine, donepezil, galantamine, and tacrine. Tacrine has been discontinued due to severe side effects associated with it (hepatotoxicity & liver damage), but the other 3 are still in use (Gao *et al*., 2014). AChE inhibitors target AChE, preventing the breakdown of acetylcholine (ACh). Aβ peptides supress release, synthesis, and transport of ACh (Pedersen *et al*., 1996, Auld *et al*., 2002), so it is present at reduced levels in AD and in other dementias (Parsons *et al*., 2013). AChE inhibitors attempt to maintain ACh levels, and increased ACh improves signalling and cognitive function (Barnes *et al*., 2000). All three inhibitors show similar efficacy, but have different modes of action. Rivastigmine exhibits pseudo-irreversible binding and inhibits butyrylcholinesterase (BuChE). BuChE is a non-specific cholinesterase present at elevated levels in AD brains (Wong, 2016). Conversely, AChE levels are usually depleted in AD brains by as much as 90% (Giacobini, 2003). It is possible that the benefits of rivastigmine treatment are due to the inhibition of BuChE in addition to AChE inhibition as ACh is also a substrate for BuChE. Donepezil is a specific reversible inhibitor, solely targeting AChE without any additional interactions known. Galantamine is a selective and reversible inhibitor that also has a secondary target; nicotinic acetylcholine receptors. It is thought that the interaction between galantamine and these receptors promotes neuronal signalling by increasing ACh release and inhibiting AChE (Woodruff-Pak *et al*., 2001), adding an additional benefit to the direct AChE inhibition by galantamine.

There are some side effects associated with use of AChE inhibitors that are mainly gastrointestinal and are linked to increased cholinergic signalling. Gastrointestinal side effects include vomiting and diarrhoea, whilst other side effects also include weight loss and incontinence. To minimize the risk of side effects, patients typically are given a low dose which is then increased gradually over a period of time (Wong, 2016). Furthermore, a transdermal patch has been developed for the application of rivastigmine and donepezil which is currently only available in the USA but does not have gastrointestinal side effects (3 times fewer side effects reported) and has the benefit of not relying on the patient to remember to take medicine although fresh patches do need to be applied (Winblad and Machado, 2008).

1.9.2 Glutamate Antagonists

At present, memantine is the only approved glutamate antagonist in use for the management of moderate to severe AD and is also prescribed in cases where AChE inhibitors have been ineffective. In contrast to AChE inhibitors, memantine has a better safety profile and tolerability with side effects including headache vomiting and dizziness (Reisberg *et al*., 2003). Memantine is a non-competitive NMDA (N-methyl-D-aspartate) receptor antagonist for which it shows weak affinity. Glutamate accounts for 70% of excitatory signalling in the brain (Danysz *et al*., 2000) and is overstimulated in the AD brain leading to Ca^{2+} surges that result in numerous changes including increased reactive oxygen species (ROS) production leading to tau hyperphosphorylation (Kumar *et al*., 2015). Memantine has been shown to exert its protective effects on neurons in rats by decreasing apoptosis, free radical oxidative damage and Aβ toxicity (Javier Miguel-Hidalgo *et al*., 2012). To achieve these effects, memantine binds to the NMDA receptor, trapping it in an open confirmation preventing glutamate binding. However, normal glutamate signalling is not disturbed as memantine has a weak affinity for NMDA receptors, resulting in a restoration of normal glutamate signalling levels as opposed to over-excitatory levels. In addition to briefly delaying AD progression, memantine has also proved beneficial in addressing behavioural symptoms of AD, reducing aggression and agitation in some cases (Wilcock *et al*., 2008). New methods for the delivery of memantine are also being explored including memogain (GLN-1062), a nasal spray that is a prodrug of memantine which is 15 times more efficient at penetrating to the brain (Maelicke *et al*., 2010) and sparks neurogenesis in the dentate gyrus of the hippocampus, something which memantine is not capable of when administered orally (Van Kampen *et al*., 2012). Memantine does not interfere with AChE inhibitors and clinical trials for a dual treatment of memantine and donepezil have shown promising, with an increase in efficacy at least 50% greater than either treatment in isolation (Atri *et al*., 2015). In fact, it has been suggested that a multi-target drug is necessary for AD to address the numerous contributory pathways involved (Hughes *et al*., 2016).

1.9.3 Emerging Therapeutics

There is a great need for disease modifying drugs to treat Alzheimer's disease. Given that AD has a complex of mechanisms and pathways that contribute to pathogenesis, there have been numerous different approaches to develop corresponding treatments (Fig. 1.5).

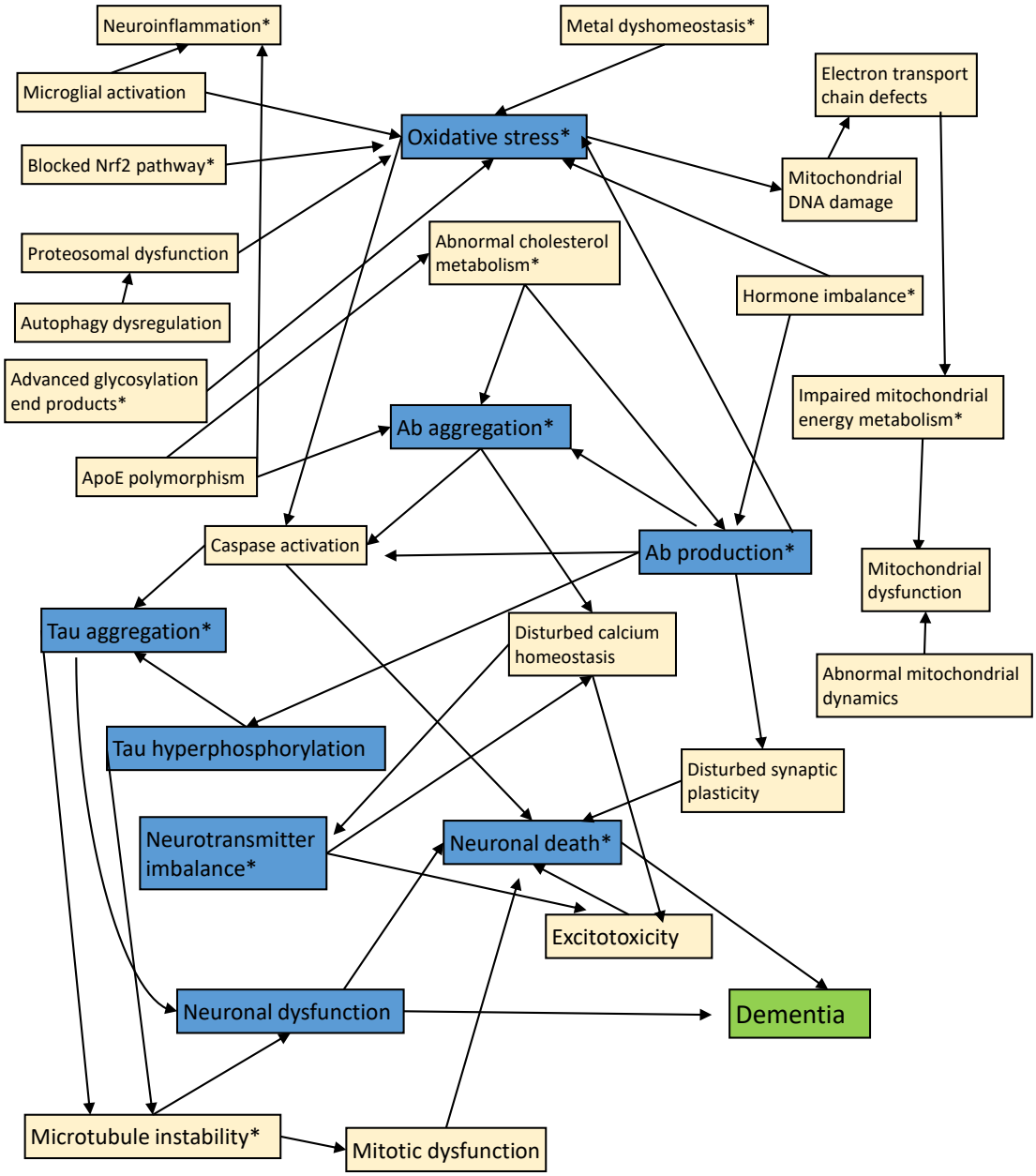

Figure 1.5. Alzheimer's disease pathogenesis and therapeutic targets. There are numerous mechanisms that contribute to the pathogenesis of Alzheimer's disease with a complex interplay between these mechanisms. The mechanisms central to pathogenesis are indicated by bold outlines, whilst * are indicative of mechanisms for which therapeutics are in development. Adapted from (Anand *et al.*, 2014).

1.9.4 Targeting Aβ Aggregation

Part of the logic behind targeting Aβ aggregation is that the peptide has a normal physiological function and that removing the peptide completely could interfere with this function. Additionally, it is believed that the oligomers or protofibrils are the toxic species, so preventing aggregation would prevent development of both these structures. One such example of a potential therapeutic that targets Aβ aggregation is RI-OR2-TAT. RI-OR2-TAT is a retro-inverso peptide inhibitor that penetrates the blood brain barrier and was found to

prevent Aβ aggregation into oligomers and fibrils *in vitro* (Taylor *et al*., 2010) as well as reducing senile plaque numbers and Aβ oligomers in the APPswe/PS1ΔE9 mouse model of AD (Parthsarathy *et al*., 2013). The drug is currently undergoing further testing for its suitability as a therapeutic and for clinical trials. Tramiprosate is another inhibitor of Aβ aggregation which is a glycosaminoglycan that binds to monomeric Aβ (Gervais *et al*., 2007). It has been shown to decrease Aβ in CSF by ~70 % (Aisen *et al*., 2011) and has been through two phase III trials but only showed significant impact in ApoE ε4 homozygotes (Abushakra *et al*., 2016). ELND005 (Scyllo-Inositol) also acts to prevent Aβ oligomerisation and the benefits have been shown in transgenic mice where cognitive decline reversed and a decrease in Aβ oligomers was seen (DaSilva *et al*., 2009).

1.9.5 Immunotherapy

Both active and passive immunization methods are being developed for AD; active immunization involves stimulating a patient's immune system to produce antibodies against a specific antigen whilst passive immunization involves the delivery of antibodies raised to specific antigens outside of the host. Concerns have been raised as to whether or not an ageing immune system is capable of mounting an effective response with either method. There are two main approaches to AD immunotherapy; targeting tau or targeting Aβ (whether that is at the peptide or oligomeric level). For Aβ vaccines, the target is usually Aβ oligomers with the view of inhibiting aggregation and clearing Aβ from the body using the immune system. The AN-1792 vaccine is composed of synthetic Aβ42, targets Aβ oligomers and was the first vaccine to reach clinical trials. The trials were stopped at phase 2A due to some participants developing brain inflammation, however follow-up studies and post-mortem analysis showed decreased cognitive decline compared to placebo treated patients (Vellas *et al*., 2009) and a decrease in amyloid plaque load (Holmes *et al*., 2008). Whilst these indications seem promising, it is only a small part of the story; NFTs were unaffected, and during phase 1 trials, 8 patients died from AD despite decreasing plaque load. There may be some long-term benefits from Aβ vaccination, however numerous aspects of the treatment need further characterisation.

Tau immunotherapy aims to decrease NFTs by targeting and clearing tau from the cell. The ACI-35 vaccine is liposome-based and is a synthetic phosphorylated peptide that imitates residues pS396/pS404 of tau (Theunis *et al*., 2013). Initial studies in Tau.P301L mice treated with ACI-35 showed high titers of IgG antibodies, which bound to phosphorylated tau and reduced soluble and insoluble tau in the brain. Vaccinations remain an attractive therapeutic possibility for AD but have several complications such as the need for a persistent response

and the challenges of an ageing immune system, which make development of vaccines a more trying and expensive process.

1.9.6 β-secretase inhibitors

One strategy to prevent Aβ aggregation and its downstream toxic effects is to reduce generation of Aβ by inhibiting β-secretase. Studies with *BACE1* knockout mice show no detectable forms of Aβ in the brain (Sathya *et al*., 2012) and APP/PS-1 transgenic mouse models of AD have been used to show that BACE1 deficiency stopped the progression of memory loss and halted degeneration of cholinergic neurotransmission (Ohno *et al*., 2004) suggesting β-secretase is a rational target for therapeutic intervention. GRL-8234 is one such example of a β-secretase inhibitor which showed promising results *in vivo*, reducing Aβ40 levels by 65% in Tg2576 mice, just 3 hours after injection (Ghosh *et al*., 2008).The initial study was taken further and, using the same mouse model, the authors were able to demonstrate that, after 5 to 7.5 months of treatment, cognitive decline halted and there was no Aβ accumulation (Chang *et al*., 2011). More recently, similar beneficial effects have also been demonstrated in 5XFAD mouse models, however the effects are age-dependent and if administered in later stages of the disease are no longer effaceable (Devi *et al*., 2015).

1.9.7 γ-secretase inhibitors and modulators

The rationale behind inhibition γ-secretase for the treatment of AD, is similar to the rationale of inhibiting β-secretase; γ-secretase cleaves C99 to form Aβ so inhibition of this process should result in reduced Aβ production. γ-secretase is known to regulate over 90 intramembrane signalling proteins, most notably Notch which is critical for growth, proliferation and differentiation (Haapasalo and Kovacs, 2011). As a result, studies with non-specific γ-secretase inhibitors like semagacestat have had several issues with adverse effects including haematological disorders (Doody *et al*., 2013). To address this, newer inhibitors are being developed that avoid affecting Notch in order to improve safety and tolerability. In addition to these new inhibitors, modulators of γ-secretase activity are also under investigation. Modulators alter the activity of γ-secretase so that it cleaves short Aβ peptides without altering Notch signalling (Godyń *et al*., 2016). These modulators were developed due to the fact that although γ-secretase inhibitors generally decrease Aβ production, an accompanying shift in production towards toxic Aβ42 was also observed in response to treatment (Golde *et al*., 2013). The results of modulators and inhibitory molecules have not been very promising with adverse effects still present and poor efficacy of the drugs identified.

1.9.8 Tau targeting Therapies

In addition to vaccines against tau, other strategies to target tau include prevention of tau aggregation, enhancing degradation of tau, microtubule stabilisation, and inhibition of tau phosphorylation. As Tau is an important part of the microtubules and the cytoskeleton, strategies targeting tau must be considered carefully. One example of a tau-targeted therapy is paclitaxel (Taxol®). Paclitaxel is a microtubule stabilising drug which has been used effectively for the treatment of different cancers. It promotes microtubule assembly and protects microtubules from disassembly by microtubule poisons (Horwitz, 1994). Paclitaxel has an application in AD, compensating for the disruption of microtubule stability by hyperphosphorylated tau; injections of paclitaxel in tau transgenic mice resulted in stabilisation of microtubules, improved fast axonal transport and motor function (Zhang *et al*., 2005). However, paclitaxel is poor at crossing the blood brain barrier so alternatives like epothioline D may be more effective whilst still having the same microtubule stabilization effect (Das and Miller, 2012).

1.9.9 Other therapeutics

A number of other strategies for developing disease-modifying drugs are also under investigation, targeting other aspects of AD pathophysiology such as reducing oxidative stress, increasing neurogenesis, altering neurotransmitter levels and targeting apolipoprotein E. The re-purposing of drugs used for the treatment of pre-existing conditions may expedite the drug development process, given that safety trials will have already been undertaken. One example of this is the re-purposing of liraglutide, a glucagon-like peptide-1 (GLP-1) receptor agonist normally used for the treatment of type 2 diabetes which has been shown to decrease plaque numbers by 40-50% in APP/PS1 mouse models of AD and prevent synaptic degradation and memory loss (McClean *et al*., 2011). Another class of drugs that may be re-purposed in AD are the cholesterol lowering drugs, statins. Hypercholesterolemia is a risk factor for AD and statins have been shown to have beneficial effects on cognition, memory and neuroprotection (Li *et al*., 2006), lowering the risk of developing AD by up to 75% (Wolozin *et al*., 2000). Aside from lowering risk, statins also may inhibit Aβ formation *in vitro*, however the results from a 2007 phase III trial indicated no significant efficacy of simvastatin on AD (Jacobson and Sabbagh, 2011) so statins may attenuate risk rather than modify the disease. Other novel strategies include extracts of the Gingko Biloba leaf which has positive effects on learning and memory in the brain as well as acting as an anti-inflammatory (Osman *et al*., 2016). Mixed results have been seen in clinical trials however, with no improvement over placebos observed (Vellas *et al*., 2012). Another molecule derived from plant sources, curcumin, has been explored for its

ability to enhance tau degradation; curcumin inhibits heat shock protein 90 (Hsp 90) which is thought to result in inhibition of tau aggregation (Ma *et al*., 2013).

1.10 Glucose Metabolism and dichloroacetate (DCA) as a potential AD therapy

The brain utilizes glucose as its sole energetic substrate (except during starvation) in order to meet the high energetic demands of neurological processes such as synaptic signalling (Mosconi *et al*., 2008). Some of the first biochemical indications in AD are a decline in the utilization of glucose, a decrease in the consumption of oxygen by the brain, and improper mitochondrial functioning. These metabolic changes can occur decades before symptoms or pathological hallmarks are displayed in a patient, making glucose consumption a potential biomarker for the disease (Mosconi *et al*., 2008). Decrease in glucose metabolism has also been identified in Apolipoprotein E ε4 homozygotes in the same regions of the brain that show decrease glucose consumption in AD (Reiman *et al*., 1996, Jagust and Landau, 2012). It is hoped that patterns in changes to glucose metabolism in AD brains can be pinpointed with enough precision for use with FDG-PET (2-[18F]fluoro-2-Deoxy-D-glucose Positron emission tomography) scanning as an early diagnostic tool for AD (Mosconi *et al*., 2010). Early detection of AD would allow for intervention before irreversible neuronal damage occurs, if suitable interventions were developed.

Aβ potentially exerts its toxic effects by producing ROS that disrupt key metabolic enzymes such as a ketoglutarate dehydrogenase and pyruvate dehydrogenase (PDH) as well as damaging mitochondrial membranes, releasing electrons to cause further oxidative damage (Reddy and Beal, 2008). The pyruvate dehydrogenase complex (PDC), which includes PDH and is a key regulator of entry into oxidative phosphorylation, is predominantly inactive in the AD brain and has been postulated as a target for therapeutic intervention in a number of age-related diseases (Stacpoole, 2012). Other metabolic pathways in AD brains compensate for the loss of ATP that would have been produced by glucose metabolism, usually through utilization of alternative substrates such as ketone bodies (Jha *et al*., 2012).

1.10.1 Dichloroacetate

Dichloroacetate (DCA) is a small 150 kDa organohalide that has been used for over 30 years in humans for the treatment of lactic acidosis and inherited mitochondrial disorders (Stacpoole *et al*., 1988). In previous years, DCA has also been explored as a treatment for sepsis, cirrhosis, congestive heart failure and burns (Michelakis *et al*., 2008) with varying degrees of success. More recently, DCA has also been explored as an anti-cancer therapeutic

against a number of types of cancer such as breast and ovarian cancer (Xintaropoulou *et al*., 2015), colorectal cancer (Madhok *et al*., 2010) and multiple myeloma (Sanchez *et al*., 2013) as well as for neurological diseases such as Huntington's disease (Andreassen *et al*., 2001) and amyotrophic lateral sclerosis (Miquel *et al*., 2012).

DCA is a modulator of metabolism; it inhibits the activity of pyruvate dehydrogenase kinases (PDKs) in a dose-dependent manner (10-250μM) (Stacpoole, 1989). PDKs usually phosphorylate and inactivate pyruvate dehydrogenase (PDH), a key enzyme involved in the link reaction between glycolysis in the cytoplasm and oxidative phosphorylation in the mitochondria. DCA concentrates in the mitochondria of cells, crossing the plasma membrane via the monocarboxylate transporter system and passes from the cytoplasm through the mitochondrial membrane via the pyruvate transporter system (Kankotia and Stacpoole, 2014). DCA inhibits all four isoforms of PDK (PDK 1-4) but has a different KI (inhibitor constant) value for each, with PDK2 the most sensitive to DCA treatment (Bonnet *et al*., 2007). PDK2 is ubiquitously expressed throughout the body (Bowker-Kinley *et al*., 1998) and DCA binds to it via its carboxylate group, creating a salt-bridge with the N-terminal domain of PDK2 at Arg154 (Knoechel *et al*., 2006), preventing pyruvate from binding thereby inactivating the enzyme.

A summary of normal metabolism and DCA interaction can be seen in figure 1.6. In short, DCA restores the balance of metabolism in cells from primarily glycolysis back to a combination of glycolysis and oxidative phosphorylation. The restoration of oxidative phosphorylation is a factor which is desirable in a cancer treatment as many cancer cells are subjected to the Warburg effect whereby they alter their metabolism to primarily undergo glycolysis to avoid producing reactive oxygen species (ROS) which can trigger ROS-linked apoptotic mechanisms within the cell (Vander Heiden *et al*., 2009). Interestingly, an age-related shift towards glycolysis has been observed in rodent brains (Yao *et al*., 2010) as well as a decrease in glucose utilization and oxygen consumption in the ageing human brain (Stacpoole, 2012), which may result in impairment of normal neuronal activity.

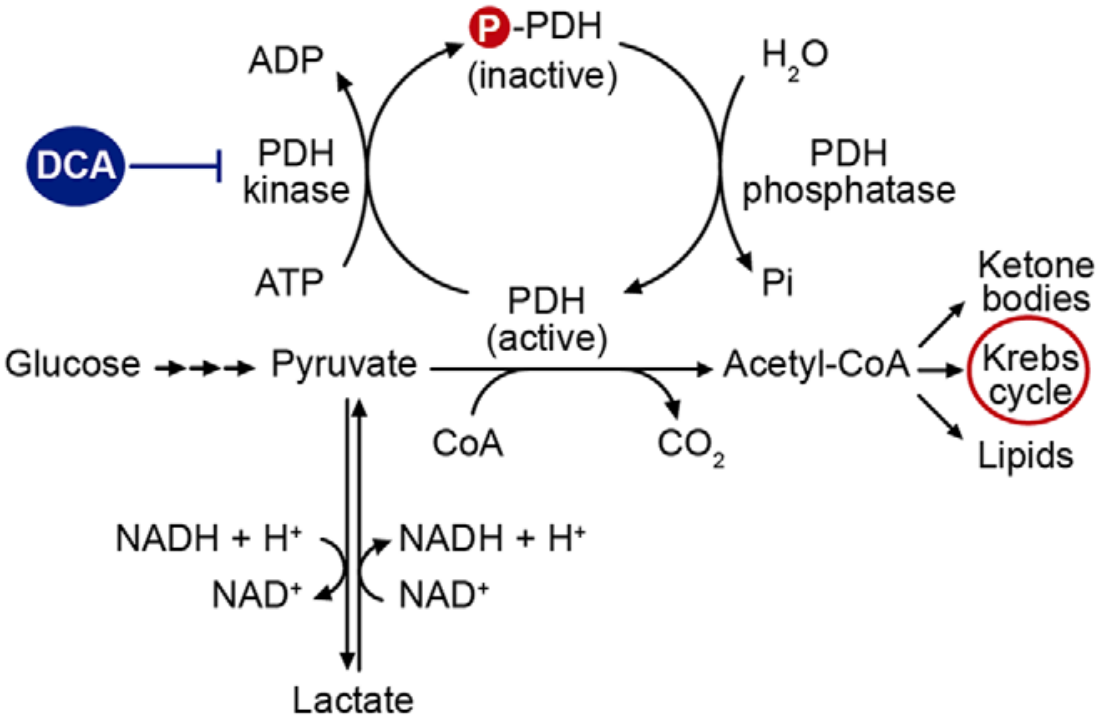

Figure 1.6. Dichloroacetate and metabolism. Glucose is converted to pyruvate during glycolysis. At this point, metabolism can either proceed to the Krebs cycle via the link reaction or pyruvate can be converted to lactate. The pyruvate dehydrogenase complex (PDH) catalyses the conversion of pyruvate to Acetyl-CoA and determines entry into the Krebs cycle. PDH is active when unphophorylated and inactive in a phosphorylated state. The phosphorylation state is controlled by PDH kinase and PDH phosphatase. Dichloroacetate (DCA) modulates metabolism by inhibiting PDH kinase in mitochondria to ensure PDH remains in its active state for glucose oxidation. Taken from (Miquel *et al*., 2012).

In addition to rebalancing the ratio of oxidative phosphorylation to glycolysis, DCA has been found to have a number of other effects on metabolism; DCA stimulates reorganization of the mitochondrial network, inhibits lipogenesis, cholesterolgenesis and gluconeogenesis and stimulates glucose utilization in the periphery (Pajuelo-Reguera *et al*., 2015). Administration of DCA also enhanced activation of the tumour suppressor p53 both *in vivo* and *in vitro* in glioblastoma tumour cells (Michelakis *et al*., 2010). More recently, p53 has been identified as playing a key role in metabolic homeostasis potentially reversing the Warburg effect by promoting oxidative phosphorylation over glycolysis (as DCA does) (Allende-Vega *et al*., 2015). Increased levels of p53 in DCA treated cancer cells may work alongside the inhibition of PDK by DCA to shift the balance towards oxidative phosphorylation in a complimentary manner.

DCA exerts an anti-proliferative effect on cells in a dose-dependent manner, slowing cancer cell proliferation and having no significant impact on growth of non-cancerous cells (Madhok *et al*., 2010). Madhok *et al* also demonstrated that 20 mM DCA is sufficient to promote apoptosis in cancerous cells with no significant increase in the number of cells

undergoing apoptosis in the non-cancerous cell lines HEK293 and HB2. However, another study showed that DCA treatment has a minimal effect on colorectal cancer cell lines and instead induced reversible autophagy (Lin *et al*., 2014). There is controversy surrounding the anti-neoplastic effects of DCA due to the discrepancy in anti-proliferative and apoptotic effects seen in experiments with different cell lines (Bell and Parkin, 2016). One reason for this discrepancy could be the difference in distribution of PDK isoenzymes in different cells, resulting in varying impact on glycolysis and induction of death via apoptosis in cancerous cell lines. Furthermore, in a trial of 5 glioblastoma patients treated with DCA alongside other therapies, a regression in tumour growth was seen and PDK2 is highly expressed in glioblastoma multiforme cells, further indicating that the distribution of PDK isoenzymes may be linked to the anti-neoplastic effect of DCA in cancer cells (Michelakis *et al*., 2010).

DCA has several characteristics that lend it to being a good pharmaceutical treatment; it is small, crosses the blood brain barrier (Abemayor *et al*., 1984), is cheap, is readily available (by-product of the chlorination of water), exhibits a high bioavailability (100% oral bioavailability seen) (Michelakis *et al*., 2008), and has been used concurrently in humans for several decades. However, as with any treatment, there are side effects; peripheral neuropathy was observed in patients receiving 25mg/Kg/day DCA in a double-blind randomized trial for the treatment of a mitochondrial disorder, MELAS (mitochondrial myopathy, encephalopathy, lactic acidosis and stroke-like episodes) (Kaufmann *et al*., 2006). However, in another trial which was also a randomised double-blind placebo controlled trial, peripheral neuropathy was only observed in 1 out of 21 children participating and there were no significant toxic effects associated with DCA (Stacpoole *et al*., 2006). The peripheral neuropathy observed in the MELAS trial may be due to a predisposition to developing peripheral neuropathy present in MELAS patients. The doses used both *in vitro* and *in vivo* are usually much higher than the normal doses used for lactic acidosis treatment, meaning that side effects are more likely to occur given the doses are up to 10x more than current treatments. Furthermore, DCA inhibits its own metabolism; DCA is converted to gloxylate by glutathione transferase zeta 1 (GSTZ1-1) which is inhibited by DCA (Li *et al*., 2011).The clearance of DCA decreases after subsequent doses; after several doses the half-life increases however levels plateau and levels of DCA present in the blood after 5 years of oral DCA treatment at 25 mg/Kg/day are only marginally elevated above levels observed after the first few doses (Mori *et al*., 2004). The clearance of DCA from blood plasma is age-linked with younger children (such as those in the MELAS trial) less able to clear DCA than adults or adolescents (Shroads *et al*., 2008). In the clinical trial involving glioblastoma patients, the

safety profile overall was good with peripheral neuropathy (nondemyelinating neurotoxicity) either being minimal or absent in patients and was reversible by withdrawal of treatment (Dunbar *et al*., 2014). The sample size in the glioblastoma trial was only 5 (and one patient died before completion of the trial, unrelated to DCA) so it is not possible to draw definitive conclusions about the safety of DCA from such a small sample size (Michelakis *et al*., 2010). Although peripheral neuropathy is an undesired side-effect, the reasons outlined above may explain why such events occurred during clinical trials and when considering the impact a chronic disease such as cancer or Huntington's disease would have on quality of life (including the side-effects of treatments like radiotherapy or chemotherapy), the risk of developing peripheral neuropathy would likely outweigh the symptoms of the disease.

1.11 Summary

Alzheimer's disease is a devastating chronic neurological disorder involving a complex of biochemical pathways, the interactions of which are not fully understood. Progress has been made in multiple areas from diagnosis and management to mechanistic elucidations. Novel treatments, pathways and interactions associated with AD are still being characterised and here we present a possible novel treatment for AD; dichloroacetate.

1.12 Outline of the project

The current project aims to investigate the effect of DCA on the proteolysis of APP in a variety of cell lines. Previous unpublished results have suggested that this orphan drug might promote α-secretase activity in the colorectal cancer cell line SW480. This phenomenon will be investigated further in relation to APP with a concomitant determination of whether the compound also exerts reciprocal inhibitory effects on the amyloidogenic processing of APP.

Chapter 2: Materials and Methods

2.1 Materials

All cell culture materials were purchased from Lonza Ltd. (Basel, Switzerland) and all other reagents were purchased from Sigma (Poole, UK) unless stated otherwise. Mouse monoclonal anti-actin, rabbit polyclonal anti-ADAM10, rabbit polyclonal anti-APP C-terminus and rabbit polyclonal anti-BACE1(EE17) antibodies were purchased from Sigma-Aldrich Company Ltd. (Gillingham U.K.). Mouse monoclonal anti-sAPPα 6E10, rabbit polyclonal anti-sAPPβ, rabbit polyclonal anti-presenilin-1 C-terminus, and mouse monoclonal anti-p53 antibodies were purchased from BioLegend (San Diego California, USA). Goat polyclonal anti-Jagged1 C-terminus antibody was purchased from Santa Cruz Biotechnology Inc. (Santa Cruz, U.S.A). Goat polyclonal anti-E-cadherin, goat polyclonal anti-ADAM17, and goat polyclonal anti-Jagged1 N-terminus antibodies were purchased from R&D Systems Europe Ltd. (Abingdon, U.K.).

2.2 Methods

2.2.1 Cell culture

Human embryonic kidney (HEK) cells overexpressing full-length human Jagged1 were generated by stable transfection as previously described (Delury *et al*., 2013). The SH-SY5Y neuroblastoma cells stably overexpressing APP_{695} or BACE1 have been characterised and reported previously (Hicks *et al*., 2013) (Parkin *et al*., 2007). These cell lines along with untransfected SH-SY5Y cells and the Dukes B colorectal cancer cell line, SW480, were cultured, essentially, in the same manner. Growth medium consisted of Dulbecco's modified Eagle's medium (DMEM) supplemented with 25 mM glucose, 4 mM L-glutamine, 10% (v/v) filter-sterilized foetal bovine serum (FBS), penicillin (50 units/mL), streptomycin (50 μg/mL) and the cells were maintained at 37°C and 5% CO_2. Cells were passaged when they reached confluency by removing medium and rinsing with 2 ml trypsin (Trypsin EDTA 200 mg/L, 170,000 U Trypsin/L) before adding a fresh 2ml trypsin and incubating at 37°C for approximately 5 min (20-30 min for SW480 cells) until cells detached. The trypsin was neutralised by the addition of 20 ml growth medium and the suspension was centrifuged at 800 rpm for 5 minutes in an Allegra X-22R centrifuge (Beckman Coulter, California U.S.A). Cells were reseeded in flasks at the required density.

2.2.2 Freezing and resurrecting cell lines

Once a flask reached confluency, the cells were trypsinised as described in section 2.2.1. and the cell pellet was resuspended in 1.5 ml of 10% (v/v) DMSO (Dimethyl sulphoxide)

in DMEM. This resuspension was transferred to a cryovial and frozen at -80°C for at least 24 hours before being transferred into liquid nitrogen. When resurrecting cells, the cryovials were thawed at 37°C. The cell suspension was transferred to a Falcon tube containing 20 ml pre-warmed growth medium and centrifuged at 800 rpm (Allegra X-22R centrifuge) for 5 min. The supernatant was discarded and the pellet resuspended in 2 ml of growth medium before transferring 1 ml to a culture flask containing 10 ml of growth medium.

2.2.3 DCA treatment of cells

For the extended growth period experiments a stock flask of cells was grown to confluency and then harvested as described in section 2.1.1. The pellet was resuspended in 10 ml of growth medium (15 ml for the SW480 cells) and 1 ml of the resuspension was seeded into each of ten flasks containing 9 ml of growth medium. A 400 mM stock solution of filter-sterilized sodium DCA was prepared (fresh for each experiment) in growth medium and 250 µl or 500 µl of the stock was added to the 10 ml cell cultures in order to obtain final DCA concentrations of 10 and 20 mM, respectively. Control (0 mM DCA) flasks were cultured alongside the DCA-treated cells. The medium was changed every two days until the quickest growing flask reached 100% confluency. At this point, the growth medium was removed and replaced cells were washed with 10 ml of UltraMem before adding a fresh 10 ml of the same medium containing DCA at the concentrations described above (DCA stock prepared in UltraMem). The cells were then incubated for a further 24 hours in order to conditioned the UltraMem.

For the 24 hour DCA treatments, SH-SY5Y cells were grown to confluence in growth medium lacking DCA before performing the 24 h UltraMem incubation in the absence or presence of DCA as described above.

2.2.4 Preparation of conditioned medium samples

The conditioned UltraMem was collected from cell cultures and centrifuged at 3000 rpm in a Hettich Rotanta 460R centrifuge (Hettich, Tuttlingen Germany) for 5 min at 4°C to remove cell debris. The supernatant was concentrated to a volume of 250 µl using Amicon Ultra-4 centrifugal filters (Merck Millipore, Ireland).

2.2.5 Preparation of cell lysates

Conditioned medium was decanted into Falcon tubes and the cells were rinsed *in situ* with 10 ml PBS (20 mM Na_2HPO_4, 2 mM NaH_2PO4, 150 mM NaCl pH 7.4). The cells were then scraped into a fresh 10 ml of PBS and transferred into a Falcon tube. Residual cells were washed from the culture flask with a further 10 ml of PBS which was combined in the same Falcon tube. Cells were pelleted by centrifugation at 1500*g* for 3 min at 4°C. The supernatant was discarded and the pellets were resuspended in 1 ml of lysis buffer (0.1 M Tris, 0.15 M NaCl, 1% (v/v) Triton X-100, 0.1% (v/v) Nonidet P-40, pH 7.4) containing 1% v/v protease inhibitor cocktail (P8340, Sigma Aldrich). Resuspended cells were sonicated at half power for 30 s using a probe sonicator (MSE, Crawley U.K.) and insoluble material was pelleted by centrifugation at 11,600 *g* for 10 min and the supernatant (lysate) was transferred to a fresh Eppendorf tube. Lysates were assayed for protein content via Bicinchoninic acid assay (see section 2.2.6.) and equalized to the same concentration by dilution with lysis buffer containing 1% (v/v) protease inhibitor cocktail before freezing at -80°C in 200 μl aliquots.

2.2.6 Bicinchoninic acid (BCA) protein assay

Bovine serum albumin (BSA) standards ranging from 0-1 mg/ml were prepared by dissolving BSA in distilled water. Standards (10 μl) and lysate samples (3 μl) were pipetted in duplicate into the wells of a 96-well microtiter plate. Assay working reagent was prepared immediately prior to use by the addition of BCA protein assay reagent (Pierce, Illinois, U.S.A) to 4% (w/v) $CuSO_4.5H_20$ in a ratio of 50:1, and 200μl of working reagent added to each well. The contents of the wells were mixed briefly before incubating the plate at 37°C for 30 min. Absorbance (570 nm) was then read using a Victor2 1420 microplate reader (Perkin Elmer, Waltham, U.S.A.). Duplicate readings were averaged for each standard and sample. A BSA standard calibration graph was then used to extrapolate the protein concentrations of the lysate samples.

2.2.7 Sodium dodecylsulphate-polyacrylamide gel electrophoresis (SDS-PAGE)

Gradient gels (5-20% 7-17% and 7-20%) were hand cast prior to use, using the solution compositions detailed in Tables 2.1.-2.3.

Table 2.1 Resolving Gel - High concentration

Resolving Gel (High concentration)		
	17%	20%
Sucrose	0.37g	0.37g
Solution I (1M Tris, pH 8.8)	1.39 ml	-
Special Solution X (1.5M Tris, pH 8.8)	-	0.93 ml
Solution III (30% acrylamide)	2.10 ml	2.5 ml
Solution V (1.5% w/v Ammonium Persulphate)	0.22 ml	0.22 ml
Solution II (10% SDS)	37 µl	37 µl
TEMED (Tetramethylethylenediamine)	3 µl	3 µl

Table 2.2 Resolving Gel - Low concentration

Resolving Gel (Low concentration)		
	5%	7%
Solution I (1M Tris, pH 8.8)	1.39 ml	1.39 ml
Solution III (30% acrylamide)	0.63 ml	0.88 ml
H_2O	1.64 ml	1.36 ml
Solution V (1.5% w/v Ammonium Persulphate)	71 µl	0.1 ml
Solution II (10% SDS)	37 µl	37 µl
TEMED	3 µl	3 µl

Table 2.3 Stacking Gel

Stacking Gel	
Solution IV (1M Tris, pH 6.8)	0.63 ml
Solution III (30% Acrylamide)	0.5 ml
H_2O	3.83 ml
Solution V (1.5% w/v Ammonium Persulphate)	0.25 ml
Solution II (10% SDS)	50 µl
TEMED	5 µl

The relevant high and low concentration resolving gel solutions were prepared as detailed in Tables 2.1 and 2.2 and the gradient gel poured using a mixing chamber and peristaltic pump. The poured gel was layered with isopropanol in order to facilitate polymerisation. Once set the isopropanol was removed and the stacking gel poured (Table 2.3). Gels were either used immediately or stored at 4°C for use the following day. Samples were mixed with dissociation buffer (3.5 ml 1 M Tris/HCl, pH 6.8, 2.5g SDS, 0.3085 g dithiothreitol, 5 ml glycerol, 0.05 mg bromophenol blue, made up to 25 ml with dH20) in a ratio of 2:1 (sample: dissociation buffer) and heated at 90°C for 3 min with the exception of samples being tested for presenilin which were heated to 55°C for 5 min. Molecular weight markers (Amersham Low Molecular Weight Calibration Kit; Phophorylase b 97 kDa, Albumin 66 kDa, Ovalbumin 45 kDa, Carbonic anhydrase 30 kDa , Trypsin inhibitor 20.1 kDa, and α-Lactalbumin 14.4 kDa) were prepared in the same manner. The volume of sample loaded is

indicated alongside each result but was 20-30µl. Equal volume of molecular weight markers was also loaded on each gel. Gels were run at 40 mA per gel in 1X Tris/glycine/SDS running buffer (Geneflow Ltd. Bradley, U.K.) until the dye front reached the base of the gel.

2.2.8 Immunoblotting

Proteins from SDS-PAGE gels were transferred to Immobilon P polyvinylidene difluoride membrane (Millipore, Massachusetts U.S.A). Prior to transfer, membranes were activated by submerging in methanol for 10 s, water for 2 min, and then Towbin transfer buffer (20 mM Tris, 150 mM glycine, 800 ml methanol made up to 4 L with dH_2O) for at least 15 min. Membranes were sandwiched together with SDS-PAGE gels and blotting paper (also equilibrated in transfer buffer) and placed in a transfer kit containing transfer buffer at 115V for 1 h. Following transfer, membranes were rinsed in PBS for 5 min before an hour incubation at room temperature in 5% (w/v) Marvel milk powder in PBS containing 0.2% (v/v) Tween-20 (PBS-Tween). The membranes were rinsed again for 5 min in PBS before the addition of primary antibody (Table 2.4) diluted in 2% (w/v) BSA in PBS-Tween with subsequent incubation overnight at 4^{o}C on a rocking platform. The membranes were then subjected to 1 x 1 min and 2 x 15 min washes in PBS-Tween before the addition of secondary antibody (Table 2.5) diluted in 2% (w/v) BSA in PBS-Tween. Following incubation for 1 h at room temperature, the membranes were then washed for 1 x 1 min and 2 x 15 min periods in PBS. All rinses and incubations took place on a rocking platform. For development, the membranes were submerged in Enhanced Chemiluminescence reagent (ECL) (Pierce, Illinois U.S.A.) for approximately 3 min and placed in between 2 sheets of acetate before being exposed to X-ray film which was manually developed.

Table 2.4 Primary antibody dilutions

Protein	Primary Antibody Dilution
Actin	1:4000
APP-CT	1:6000
sAPPα	1:4000
sAPPβ	1:4000
BACE	1:2000
ADAM10	1:1500
ADAM17	1:1500
Presenilin-1	1:1000
p53	1:2500
Jagged1 CT	1:1000
Jagged1 NT	1:1500
E-cadherin	1:500

Table 2.5 Secondary antibody dilutions

Secondary Antibody	Secondary Antibody Dilution
RαM	1:4000
RαG	1:10000
GαR	1:4000

2.2.9 Immunoblot quantification

X-ray films were scanned using a flatbed scanner at 600 dpi and saved as tiff files before being converted to greyscale using the software package, 'Paint.Net'. Files were imported into 'ImageJ' quantification software and densitometric analysis carried out.

2.2.10 Amido black staining

PVDF membranes were submerged in amido black stain (0.1% (w/v) amido black, 1% (v/v) acetic acid, 40% (v/v) methanol) for 2 minutes before rinsing with tap water for approximately 30 seconds to destain.

2.2.11 Trypan Blue Assay

Cells were harvested by trypsinisation as described in section 2.1.1. An aliquot from the resultant resuspended cell pellet was then mixed with an equal volume of 0.4% Trypan Blue solution and loaded onto a haemocytometer. Cell counts of live cells were obtained and an average of four squares taken.

2.2.12 MTS (3-(4,5-dimethylthiazol-2-yl)-5-(3-carboxymethoxyphenyl)-2-(4-sulfophenyl)-2H-tetrazolium) assay

Cells for MTS assays were grown in 96-well plates. At the relevant time point, the growth medium was removed and the cells were washed *in situ* three times with 150 µl aliquots of UltraMem. A final 100 µl aliquot of UltraMem was then added to the cells followed by the addition of 20 µl CellTiter 96®Aqueous One Cell Proliferation Assay solution (MTS reagent) (Promega, Wisconsin, U.S.A.). Blanks consisting of UltraMem and MTS solution were also included in the plate. After gentle mixing, the plate was covered in foil and incubated at 37°C until a suitable colour development had been achieved. Absorbance (490 nm) was then read in a Victor2 1420 microplate reader.

2.2.13 Cell Imaging

Images were captured at 10X objective in the absence of stains using a CMEX-5 camera and ImageFocus4 software (Euromex, Holland).

2.2.14 Statistical Analysis

Statistical analysis was conducted via an unpaired, two-tailed homoscedastic Student's *t* test using Microsoft Excel 2016. Each error bar represents standard deviation unless stated otherwise. Statistical significance levels used are: *, $p \leq 0.05$, **, $p \leq 0.01$, ***, $p \leq 0.001$ ****, $p \leq 0.0001$.

Chapter 3: Results; The effects of DCA on untransfected SH-SY5Y cells

3.1 The effects of dichloroacetate incubation during growth on untransfected SH-SY5Y cells

Dichloroacetate (DCA) has previously been shown to cause morphological changes in the human prostate cancer cell line PC3 (Parkin, unpublished data), with treated cells producing increased numbers of neurite-like extensions. The development of neurite-like extensions is a process thought to be regulated by the amyloid precursor protein (APP)(Young-Pearse *et al*., 2008). Therefore, it was possible that DCA may be regulating changes in cell morphology via altered APP metabolism. In the current study, SH-SY5Y neuroblastoma cells were treated with DCA in order to characterise any effects of the drug on cell morphology, proliferation and APP metabolism. SH-SY5Y cells were used as they have been used historically as neuronal models when looking at Alzheimer's Disease (Harris *et al*., 2009) and Parkinson's Disease(Lopes *et al*., 2010). SH-SY5Y cells offer several benefits over primary neuronal cultures such as continuous proliferation, ease of maintenance, the ability to undergo transfection, the ability to grow on large scales, the expression of human proteins and isoforms not present in primary rodent cells and lastly, they do not have the same ethical issues associated with primary human neuronal culture (Kovalevich and Langford, 2013).

3.1.1 DCA-induced morphological changes in SH-SY5Y cells

SH-SY5Y cells were seeded in growth medium containing 0, 10 or 20 mM DCA and examined under a light microscope after 3 and 6 days growth. The results (Fig. 3.1.1) showed an increase in the number of neurite-like extensions at 10 mM (Fig. 3.1.1D) and at 20 mM DCA (Fig 3.1.1F) at both 3 and 6 day time points. The zoomed inset in Fig. 3.1.1F highlights the presence of these extensions in DCA-treated cells.

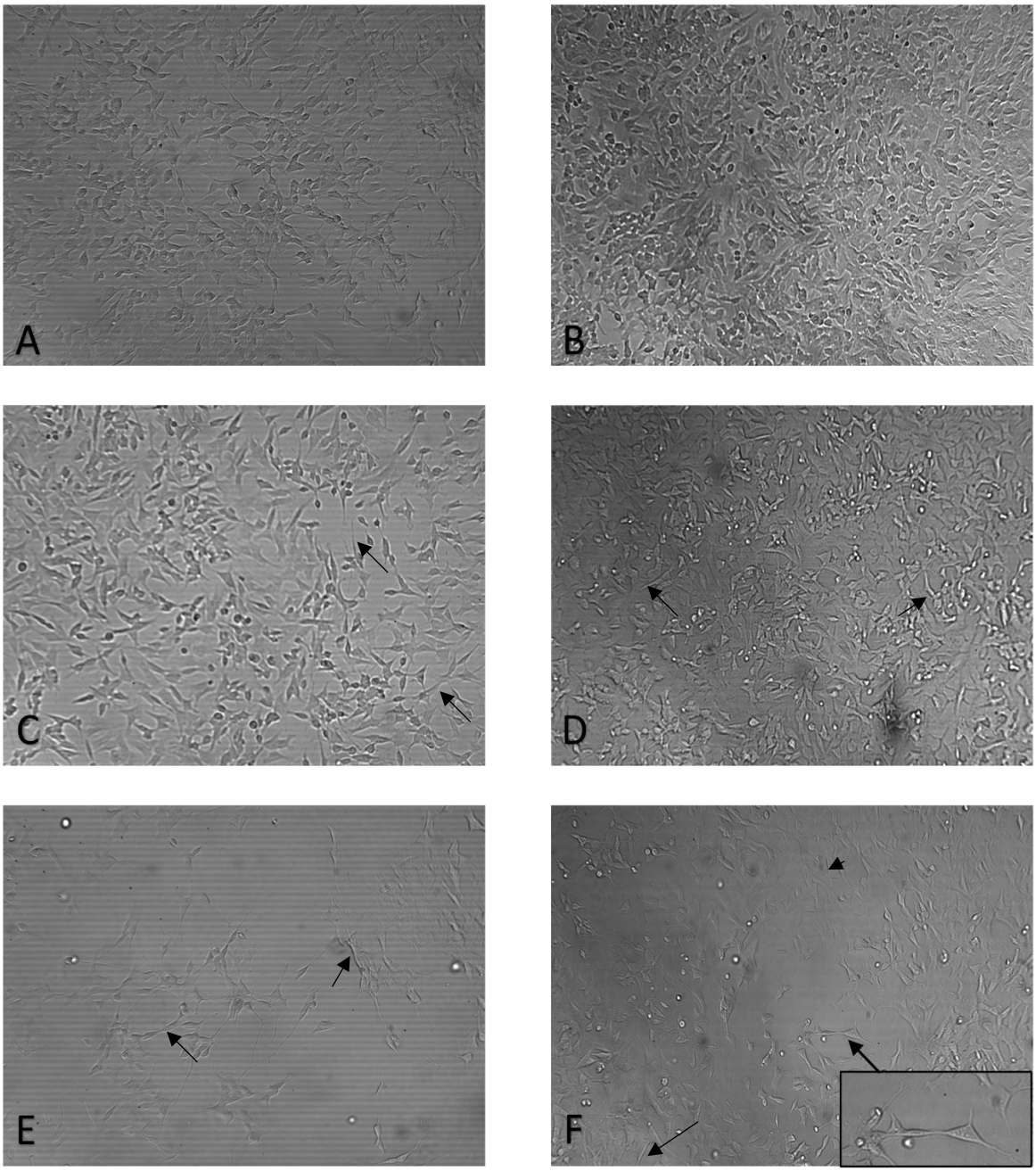

Figure 3.1.1. Morphology of DCA-treated SH-SY5Y cells. SH-SY5Y cells were treated with 0 **(A&B),** 10 mM **(C&D)** and 20 mM **(E&F)** DCA for a total period of 6 days. Cells were imaged after 3 days **(A, C, E)** or 6 days **(B, D, F)**. Images were captured at 10X objective in the absence of stains. Arrows indicate neurite-like extensions.

3.1.2 The effect of DCA on SH-SY5Y cell proliferation

When capturing images of DCA-treated cells to examine morphology, it was evident that fewer cells were present in DCA treated flasks at the endpoint of the treatment. Therefore, in order to determine whether DCA negatively impacted on cell viability, SH-SY5Y cells were treated with 10 mM and 20 mM DCA for 6 days and cell viability was assessed via trypan blue exclusion assay (see Materials and Methods). The results (Fig. 3.1.2.) showed a significant decrease in the viable cell count at 20 mM DCA. However, there was no decrease at the 10 mM drug concentration. It is important to note that very few non-viable cells were observed at any of the DCA concentrations employed indicating that the compound was growth inhibitory rather than cytotoxic.

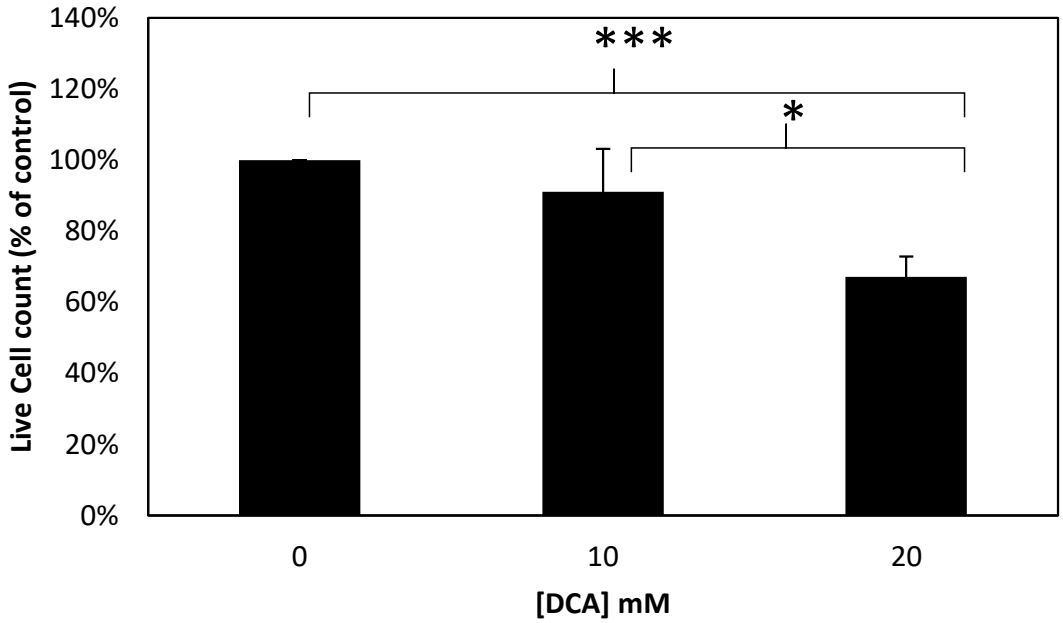

Figure 3.1.2. DCA decreases SH-SY5Y cell proliferation. SH-SY5Y cells were treated with 0, 10 and 20 mM DCA for 6 days (see Materials and Methods) and then trypsinised and counted via trypan blue exclusion assay. Counts reflect live cells. Results are means ± S.D. (n=3). Unless indicated otherwise, results were not significantly different; * P≤ 0.05 & *** P≤ 0.001.

3.1.3 The effect of DCA on cell metabolism

As DCA stimulates mitochondrial metabolism via inhibition of PDK, the effects of the drug on SH-SY5Y were also investigated using the MTS assay. This assay reflects mitochondrial metabolism and is used as an approximation for cell viability (Berridge *et al*., 2005) The results (Fig. 3.1.3) showed an increased MTS reduction at both 10 and 20 mM DCA. The increase

observed at 20 mM DCA was probably counteracted to a degree by the decreased cell number observed (see Fig. 3.1.2).

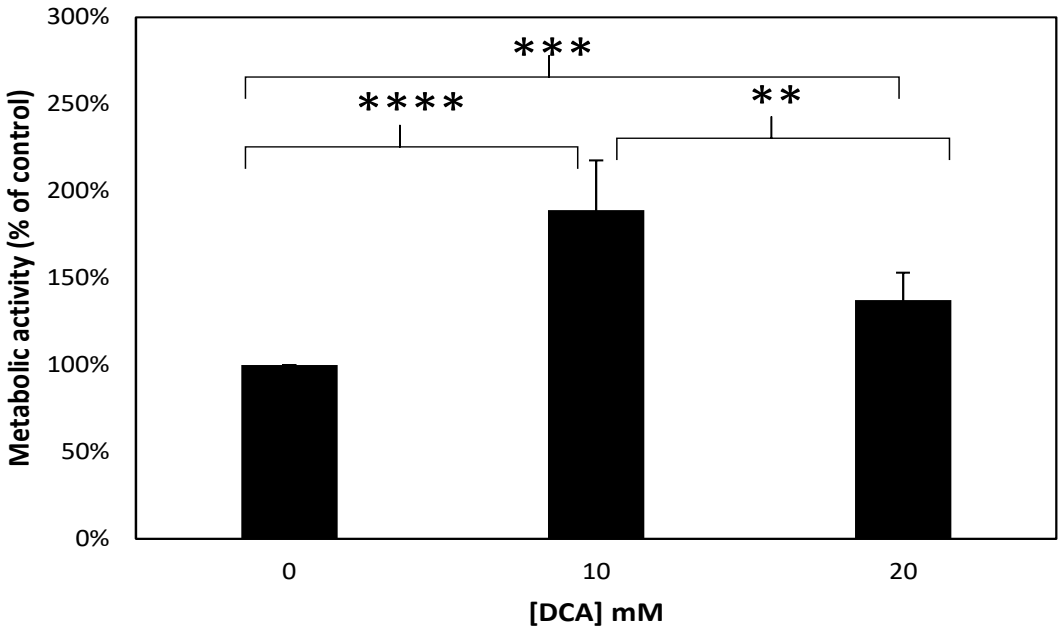

Figure 3.1.3. DCA increases the metabolic activity of SH-SY5Y cells. SH-SY5Y cells were treated with 0, 10 and 20 mM DCA for 7 days (see Materials and Methods) and then subjected to a MTS assay (see Materials and Methods). Results are means ± S.D. (n=6). Unless indicated otherwise, results were not significantly different; ** P≤ 0.01, *** P≤ 0.001 & **** P≤ 0.0001.

3.1.4 DCA alters expression of endogenous APP in SH-SY5Y cells

In order to determine any effects of DCA on APP expression/proteolysis the cells imaged in Fig. 3.1.1 were, at day 6, washed *in situ* with 10 ml UltraMem before adding a fresh 10 ml of the same medium (with the corresponding DCA stocks added) and incubated for a further 24 h. Cell lysates and conditioned medium samples were then prepared as described in the Materials and Methods section. Initially, the lysates were immunoblotted with an anti-APP C-terminal antibody and the results (Fig. 3.1.4) showed that, in response to DCA treatment, APP holoprotein levels decreased by 7% with 10 mM DCA and increased by 9% with 20 mM, relative to the control.

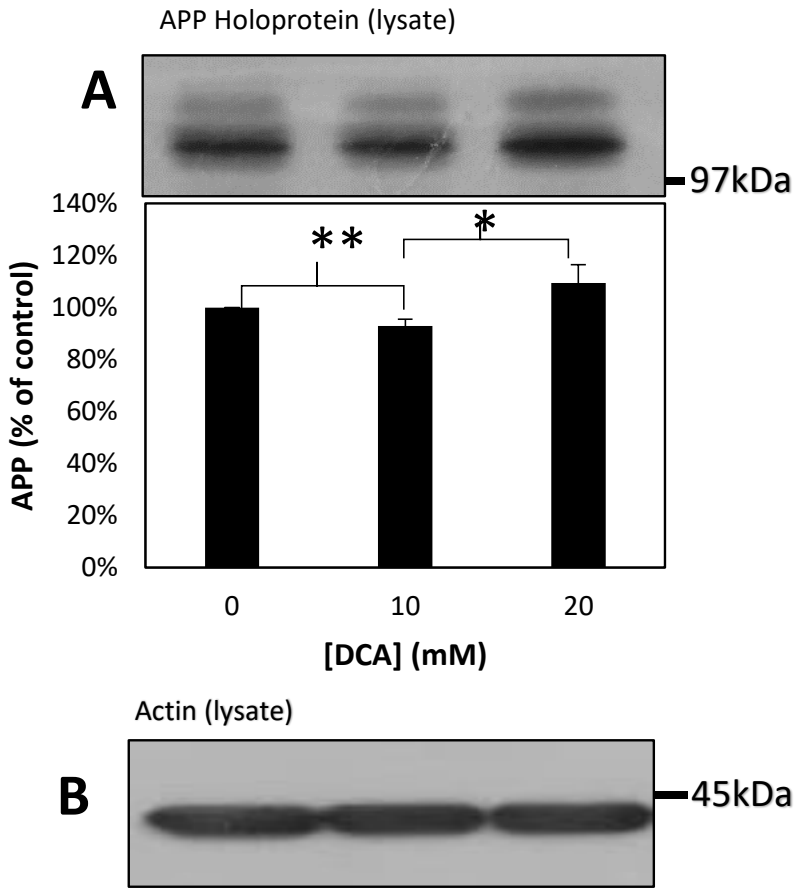

Figure 3.1.4. DCA alters expression of endogenous APP in SH-SY5Y cells. SH-SY5Y cells were treated with 0, 10 and 20 mM DCA for 6 days, with lysates prepared as per the Materials and Methods section. Immunoblot analysis of equal amounts of lysate proteins was carried out with anti-APP C-terminal **(A)** and anti-actin **(B)** antibodies. The results from the APP blot were quantified by densitometric analysis. Values are means ± S.D. (n=3). Unless indicated otherwise, results were not significantly different; * P≤ 0.05 and ** P≤0.01.

3.1.5 The effect of DCA on APP Proteolysis

In order to determine whether DCA affected APP proteolysis, immunoblot analyses of sAPPα and sAPPβ in conditioned media were conducted. Following immunoblotting with the anti-sAPPα antibody 6E10, the results (Fig. 3.1.5A) showed two distinct bands corresponding to sAPP$\alpha_{751}/_{770}$ (upper band) and sAPPα_{695} (lower band). The intensities of both bands were enhanced in the 10 mM DCA samples but not at the 20 mM concentration of the compound. However, it should be noted that these samples were resolved in gels on an equal volume basis i.e. they were not assayed for and equalized in terms of protein. Consequently, the levels of any shed proteins in conditioned medium would be impacted by cell number. In order to mitigate the changes in cell number (see Fig. 3.1.2) the shedding results in Fig. 3.1.5A were adjusted according to the cell number results obtained in the trypan blue assays. The resultant

data (Fig. 3.1.5B) then clearly showed enhanced sAPPα shedding from both 10 and 20 mM-treated cells.

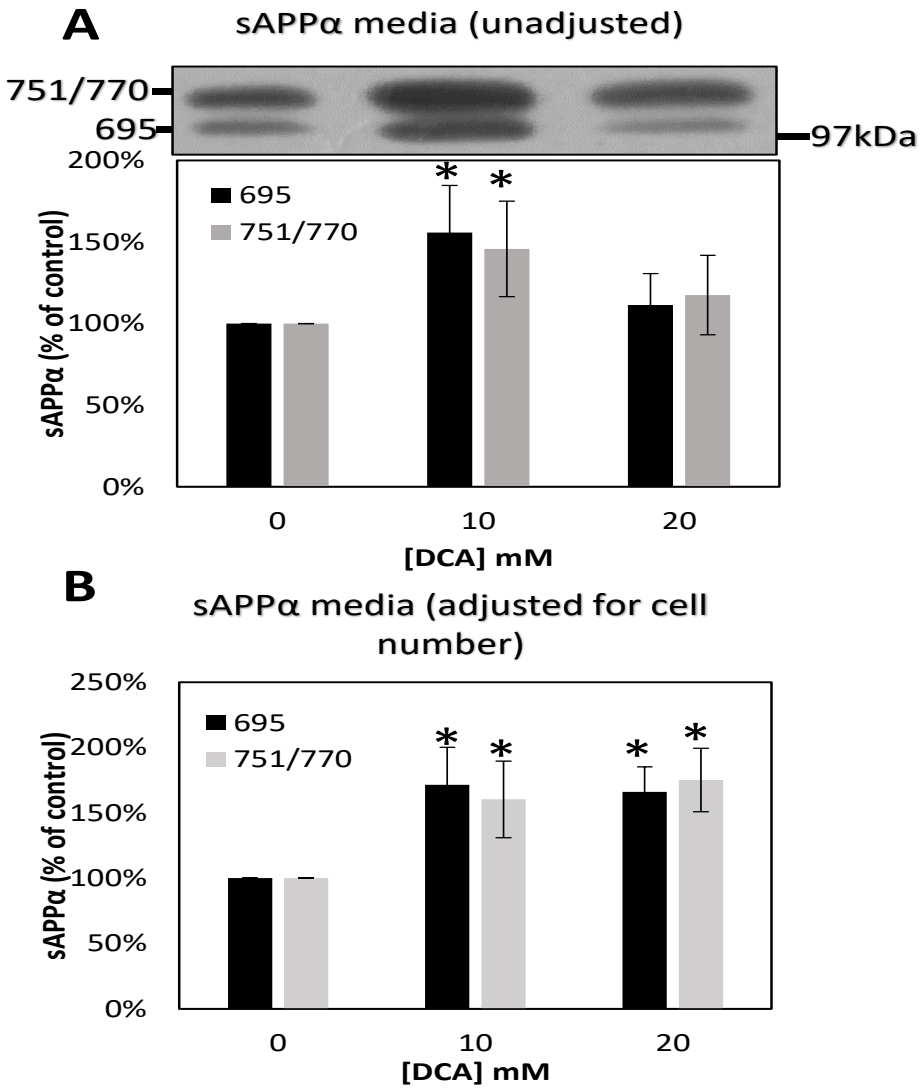

Figure 3.1.5. DCA increases sAPPα shedding from untransfected SH-SY5Y cells. SH-SY5Y cells were treated with 0, 10 and 20 mM DCA for 6 days, with conditioned media processed as per the Materials and Methods section. Immunoblot analysis of conditioned medium was carried out with anti-sAPPα antibody 6E10. The results from the immunoblot were quantified by densitometric analysis **(A)**. Data was also adjusted for cell number determined by trypan blue assay **(B)**. Values are means ± S.D. (n=3). Unless indicated otherwise, results were not significantly different; * P≤ 0.05.

In order to investigate whether the changes to APP proteolysis also extended to another product of APP, immunoblot analysis was performed on conditioned media for sAPPβ. Following immunoblotting with anti-sAPPβ antibody, two distinct bands were observed corresponding to $sAPP\beta_{751/770}$ (upper band) and $sAPP\beta_{695}$ (lower band) (Fig. 3.1.6A). The intensity of the $sAPP\beta_{751/770}$ band decreased at both 10 and 20 mM DCA treatment. The $sAPP\beta_{695}$ band was only detected in the control sample, denoting ablation of $sAPP\beta_{695}$

following DCA treatment at 10 and 20 mM of the compound. As with the alpha results, the beta results were adjusted to account for cell number as determined by trypan blue assay (see Fig. 3.1.2). Following adjustment for cell number (Fig 3.1.6B), the decrease in sAPP$\beta_{751/770}$ was only significant following 20 mM DCA treatment. The adjusted results (Fig 3.1.6B) show decreased sAPPβ_{695} shedding from both the 10 and 20 mM-treated cells along with a significant decrease in sAPP$\beta_{751/770}$ shedding from 20 mM-treated cells.

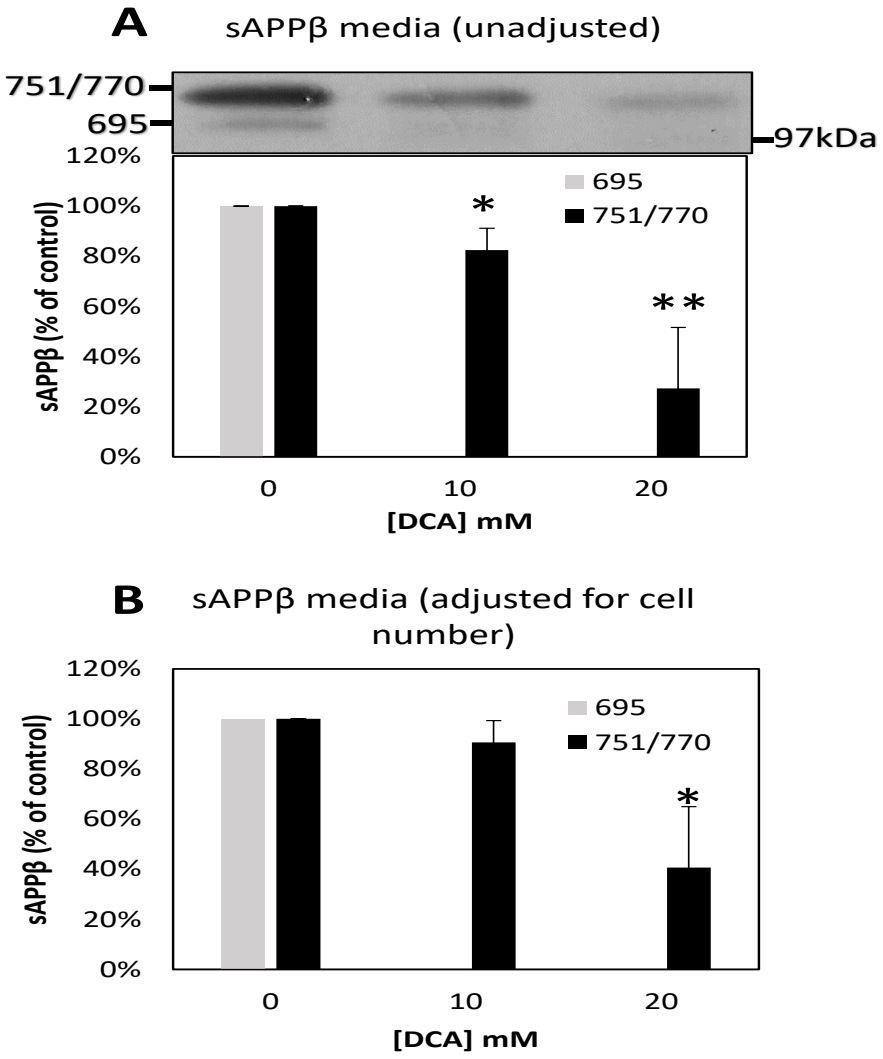

Figure 3.1.6. DCA decreases sAPPβ shedding from untransfected SH-SY5Y cells. SH-SY5Y cells were treated with 0, 10 and 20 mM DCA for 6 days, with conditioned media processed as per the Materials and Methods section. Immunoblot analysis of conditioned medium was carried out with anti-sAPPβ antibody. The results from the immunoblot were quantified by densitometric analysis **(A)**. Data was also adjusted for cell number determined by trypan blue assay **(B)**. Values are means ± S.D. (n=3). Unless indicated otherwise, results were not significantly different; * P≤ 0.05 and ** P≤ 0.01.

3.1.6 The effect of DCA on p53 expression in SH-SY5Y cells

DCA has previously been shown to alter the expression of the tumour suppressor p53 in B-chronic lymphocytic leukaemia cells (Agnoletto *et al*., 2014) and the protein is known to

be a regulator of APP expression (Cuesta *et al*., 2009). Therefore, in the current study, an immunoblot for p53 was conducted on lysates from the DCA-treated SH-SY5Y cells. The results (Fig. 3.1.7) showed a general increase in p53 expression; 18% with 10 mM and 71% with 20 mM DCA. Interestingly, two bands were also observed at ~53 kDa and ~50 kDa with the lower band decreasing following treatment. It was not possible to carry out densitometric analysis on the bands separately so the results reflect both bands quantified together.

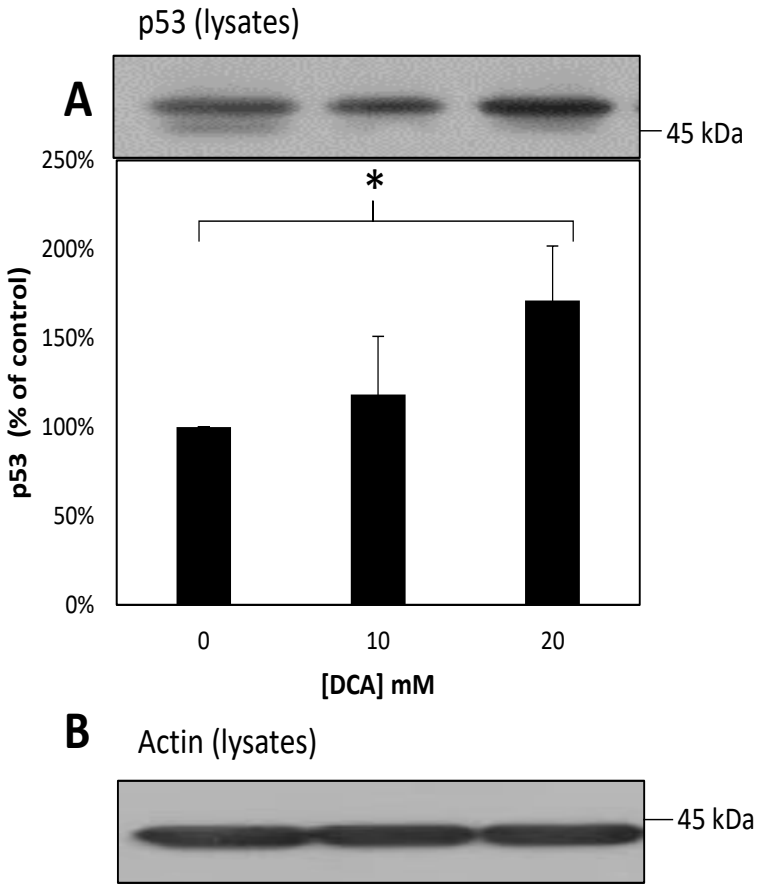

Figure 3.1.7. DCA increases expression of p53 in SH-SY5Y cells. SH-SY5Y cells were treated with 0, 10 and 20 mM DCA for 6 days, with lysates prepared as per the Materials and Methods section. Immunoblot analysis of equal amounts of lysate proteins was carried out with anti-p53 **(A)** and anti-actin **(B)** antibodies. The results from the p53 blot were quantified by densitometric analysis. Values are means ± S.D. (n=3). Unless indicated otherwise, results were not significantly different; * P≤ 0.05.

3.1.7 The effect of DCA on ADAM and presenilin-1 expression

As DCA enhanced sAPPα shedding from SH-SY5Y cells (Fig. 3.1.5), it was postulated that the compound might alter the expression of the α-secretases, ADAM10 and/or ADAM17. Therefore, the cell lysates were also immunoblotted for these proteins. The results (Fig. 3.1.8) were inconclusive as it was not possible to determine which band(s) correspond to the ADAM proteins as the specificity of the antibodies was low. Arrows indicate the suspected bands for the mature and immature forms of both proteins, which would suggest levels of ADAM10 (Fig. 3.1.8A) perhaps increase with DCA treatment whilst ADAM17 levels (Fig. 3.1.8B) remain constant however this is not quantifiable from the data obtained.

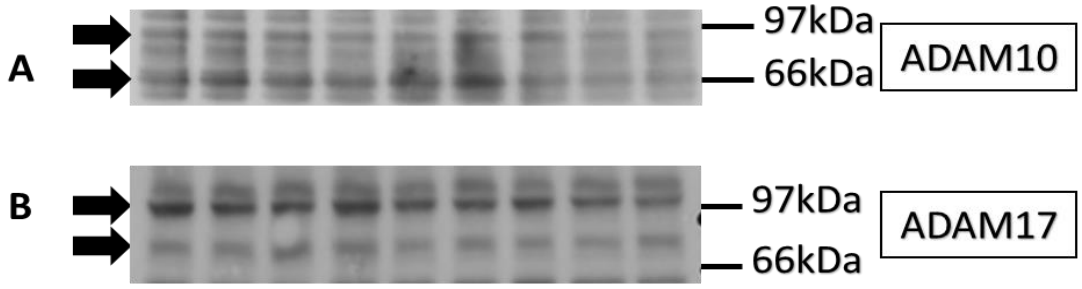

Figure 3.1.8. Alpha secretases in DCA treated SH-SY5Y cells. SH-SY5Y cells were treated in triplicate with 0, 10 and 20 mM DCA for 6 days, with lysates prepared as per the Materials and Methods section. Immunoblot analysis of equal amounts of lysate proteins was carried out with anti-ADAM10 **(A)** and anti-ADAM17 **(B)** antibodies. Lanes from left to right are 0,10, and 20 mM repeated 3 times. Arrows indicate suspected bands of interest with the immature form at around 100 kDa and the mature form of each secretase at around 66 kDa.

The lysates were also immunoblotted for presenilin-1 (Fig. 3.1.9). However, the antibody employed was also non-specific.

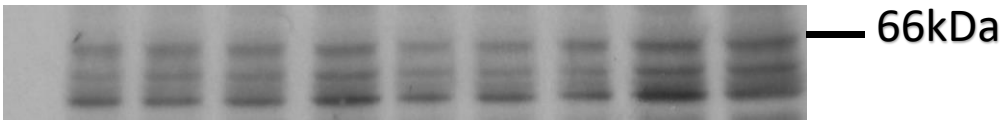

Figure 3.1.9. Preseinilin-1 in DCA treated SH-SY5Y cells. SH-SY5Y cells were treated in triplicate with 0, 10 and 20 mM DCA for 6 days, with lysates prepared as per the Materials and Methods section. Immunoblot analysis of equal amounts of lysate proteins was carried out with anti-presenilin-1 antibody. Lanes from left to right are 0,10, and 20 mM repeated 3 times. The expected molecular weight of presenilin-1 is approximately 50 kDa.

Due to the poor specificity of the anti-ADAM10, anti-ADAM17 and anti-presenilin-1 antibodies, further immunoblots on other cell lines using these antibodies were not carried out as the initial results were poor.

3.2 24-hour treatment of confluent SH-SY5Y cells with DCA

3.2.1 Introduction

Data from the DCA-treated SH-SY5Y cells indicated that DCA treatment impacts on cell proliferation, without being cytotoxic (Fig. 3.1.2). In order to further probe into the relationship between DCA, metabolism and toxicity, a 24 hour DCA experiment was devised. Confluent SH-SY5Y cells were used as they are less likely to be undergoing proliferation, and so any changes in cell count would be attributed to dead cells as opposed to altered growth rate. The same cohort of experiments were performed on the 24h treated cells, with cells being confluent prior to the addition of DCA.

3.2.2 DCA-induced morphological changes in confluent SH-SY5Y cells after 24 hours

SH-SY5Y cells were grown to confluence and then treated with UltraMem containing 0,10 or 20 mM DCA for 24 h and examined under a light microscope before starting treatment and 24 hours later at the end of the treatment. The results (Fig 3.2.1) show an increase in extensions at 10 and 20 mM DCA treatments (Fig. 3.2.1D & F). Due to the sheer number and proximity of cells in the flask, it is more difficult identify individual neurite-like extensions, however arrows highlight some neurite-like extensions present in the treated flasks.

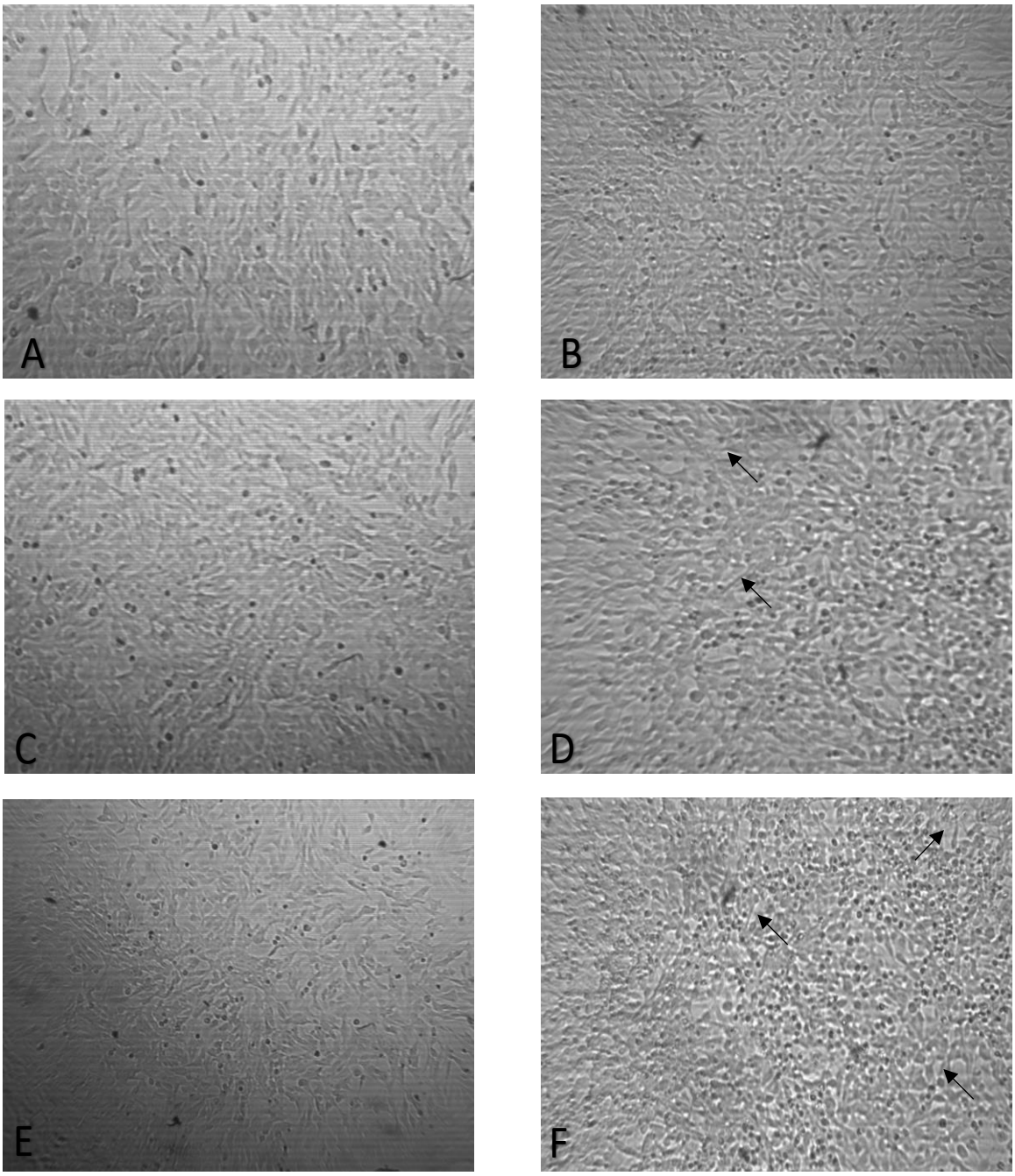

Figure 3.2.1. Morphology of 24-hour DCA-treated SH-SY5Y cells. Confluent SH-SY5Y cells were treated with 0 **(A&B),** 10 mM **(C&D)** and 20 mM **(E&F)** DCA for a total period of 24 hours. Cells were imaged prior to treatment **(A, C, E)** and 24 hours later **(B, D, F)**. Images were captured at 10X objective in the absence of stains. Arrows indicate neurite-like extensions.

3.2.3 The effect of DCA on cell proliferation of confluent SH-SY5Y cells after 24 hours

In order to confirm that DCA altered cell proliferation rather than impacting cell viability, confluent SH-SY5Y cells were treated with 10 mM and 20 mM DCA for 24 hours and cell viability assessed using the trypan blue exclusion assay (see Materials and Methods). The results (Fig. 3.2.2) show no change in viability of confluent SH-SY5Y cells after 24 hour DCA treatment.

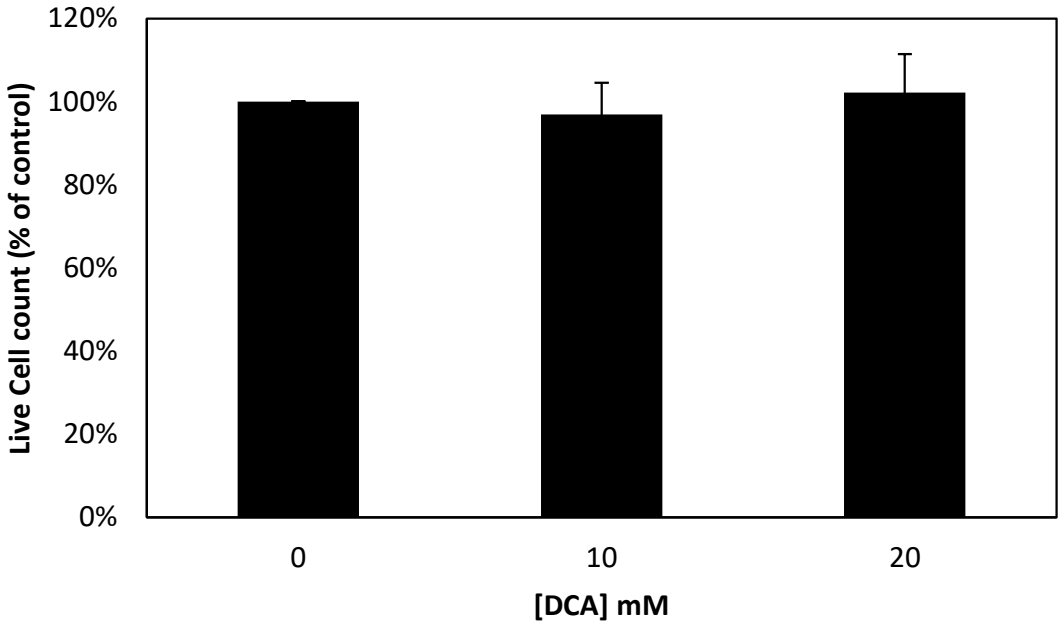

Figure 3.2.2 The viability of confluent SH-SY5Y cells is unaffected by DCA after 24 hours. SH-SY5Y cells were grown to confluence and treated with 0, 10 or 20 mM DCA for 24 hours (see Materials and Methods) and then trypsinised and counted via trypan blue exclusion assay. Counts reflect live cells. Results are means ± S.D. (n=3). Unless indicated otherwise, results were not significantly different.

3.2.4 The effect of DCA on the metabolism of confluent SH-SY5Y cells after 24 hours

The results from the trypan blue viability assay showed no change in viability after 24-hour treatment with DCA and a MTS assay was carried out to see whether the same was true of metabolic activity assessed via MTS. SH-SY5Y cells were seeded in 96-well plates and grown to confluence before the addition of 0, 10 or 20 mM DCA for 24 hours. A MTS assay was performed (see Materials and Methods). The results (Fig 3.2.3) show an increase in metabolic activity after both DCA treatments, and the 8% increase with 20 mM treatment relative to the control was significant.

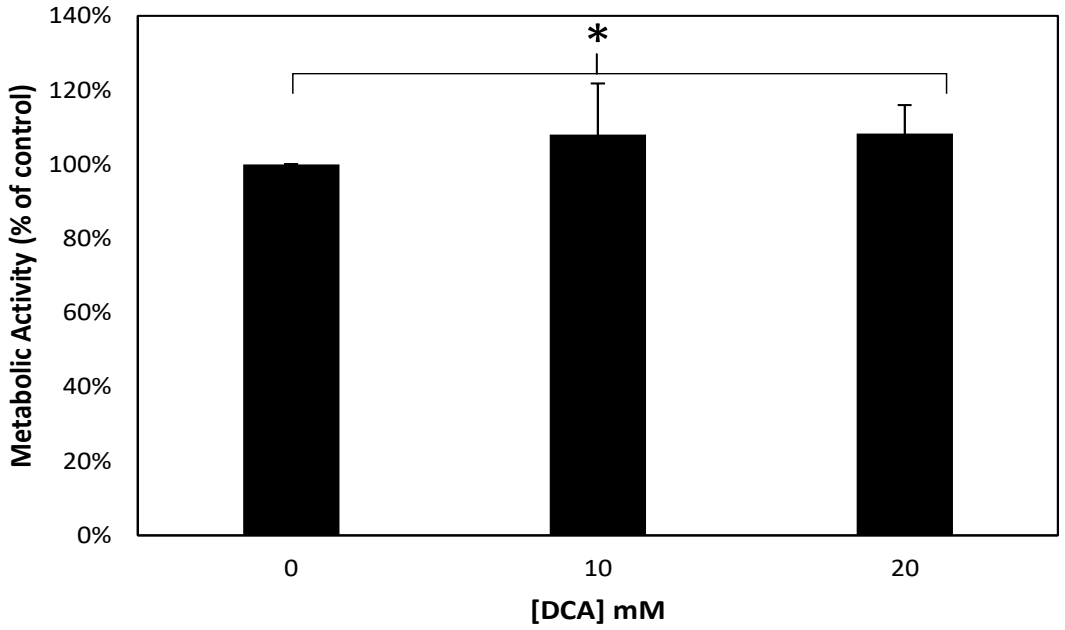

Figure 3.2.3. DCA increases the metabolic activity of confluent SH-SY5Y cells after 24 hours. SH-SY5Y cells were grown to confluence and treated with 0, 10 and 20 mM DCA for 24 hours (see Materials and Methods) and then subjected to a MTS assay (see Materials and Methods). Results are means ± S.D. (n=6). Unless indicated otherwise, results were not significantly different; * P≤ 0.05.

3.2.5 DCA alters expression of APP in confluent SH-SY5Y cells after 24 hours

To determine any effects of DCA on APP expression after 24 hours, the SH-SY5Y cells imaged in Fig.3.2.1 were harvested after 24 hour DCA treatment. Cell lysates and conditioned medium samples were then prepared as described in the Materials and Methods section. Lysates were immunoblotted with an anti-APP C-terminal antibody and the results (Fig. 3.2.4) showed that, in response to DCA treatment, APP holoprotein levels increased by 25% with 10 mM DCA and increased by 29% with 20 mM relative to the control. It is worth noting that in the extended treatment, a decrease in APP holoprotein was seen with 10 mM treatment.

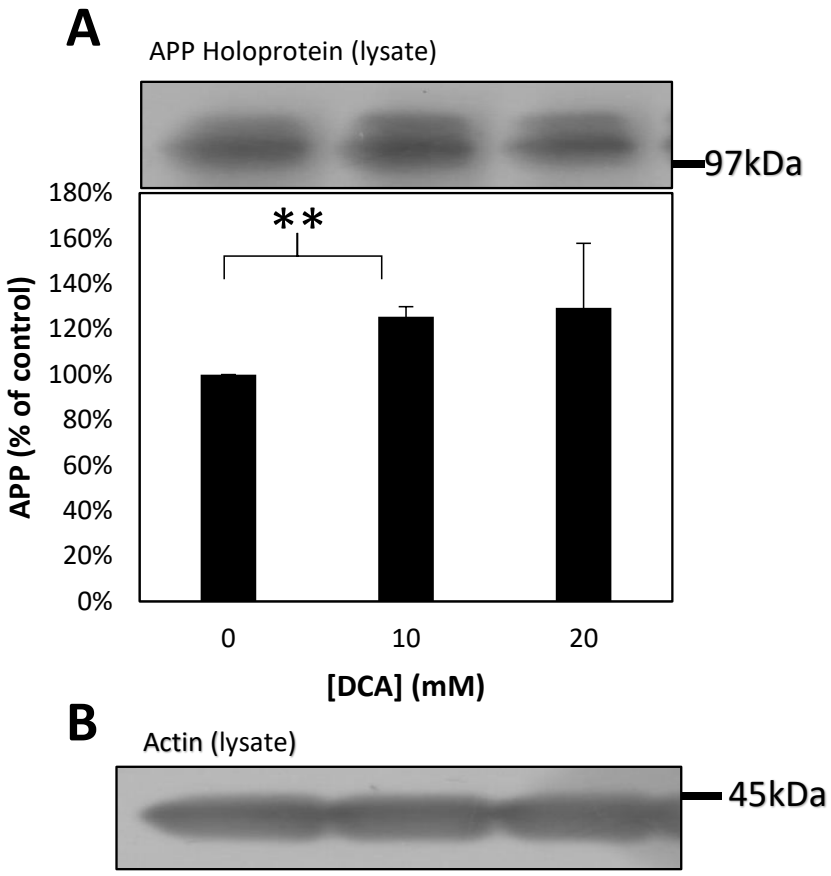

Figure 3.2.4. DCA alters expression of endogenous APP in SH-SY5Y cells after 24 hours. SH-SY5Y cells were grown to confluence and treated with 0, 10 and 20 mM DCA for 24 hours, with lysates prepared as per the Materials and Methods section. Immunoblot analysis of equal amounts of lysate proteins was carried out with anti-APP C-terminal **(A)** and anti-actin **(B)** antibodies. The results from the APP blot were quantified by densitometric analysis. Values are means ± S.D. (n=3). Unless indicated otherwise, results were not significantly different; ** P≤0.01.

3.2.6 The effect of DCA on APP proteolysis in confluent SH-SY5Y cells after 24 hours

As changes to APP proteolysis was observed with the extended treatment (Figs. 3.1.5 & 3.1.6), immunoblot analyses of sAPPα and sAPPβ levels in conditioned media from 24h DCA treated SH-SY5Y cells were performed. The results from the sAPPα immunoblots showed a 2% decrease in sAPPα levels with 10 mM DCA and a 29% increase with 20 mM DCA (Fig. 3.2.5A). When adjusted for cell number obtained via trypan blue assay (see Fig. 3.2.2), the results (Fig. 3.2.5B) showed sAPPα levels increased by 1% at 10 mM and 26% with 20 mM DCA. It was not possible to quantify bands for the different isoforms separately.

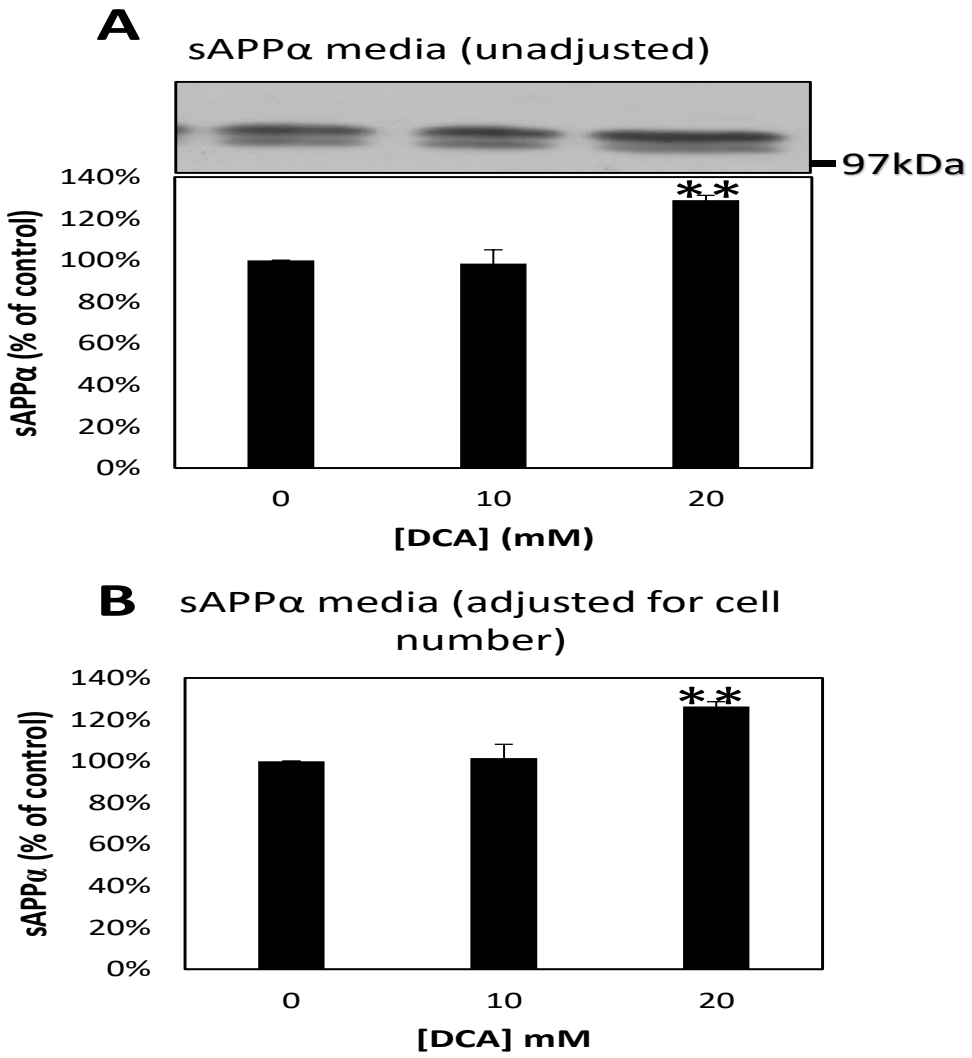

Figure 3.2.5. DCA increases sAPPα shedding from untransfected SH-SY5Y cells after 24 hours. SH-SY5Y cells were grown to confluence and treated with 0, 10 and 20 mM DCA for 24 hours, with conditioned media processed as per the Materials and Methods section. Immunoblot analysis of conditioned medium was carried out with anti-sAPPα antibody 6E10. The results from the immunoblot were quantified by densitometric analysis **(A)**. Data was also adjusted for cell number determined by trypan blue assay **(B)**. Values are means ± S.D. (n=3). Unless indicated otherwise, results were not significantly different; ** P≤ 0.01.

Investigation of sAPPβ levels in conditioned media from 24H treated cells was performed by immunoblot analysis. Although two bands were observed, it was not possible to quantify them separately so the results in Fig 3.2.6 reflect both bands quantified together. The results show a significant decrease in sAPPβ levels, dropping to 36% with 10 mM DCA and 32% with 20 mM DCA (Fig. 3.2.6A). When adjusted for cell number obtained via trypan blue assay (see Fig. 3.2.2), sAPPβ levels decreased to 37% with 10 mM DCA and 31% with 20 mM

DCA (Fig. 3.2.6B). This aligns with the general trend from the extended treatment results (Fig.3.1.6).

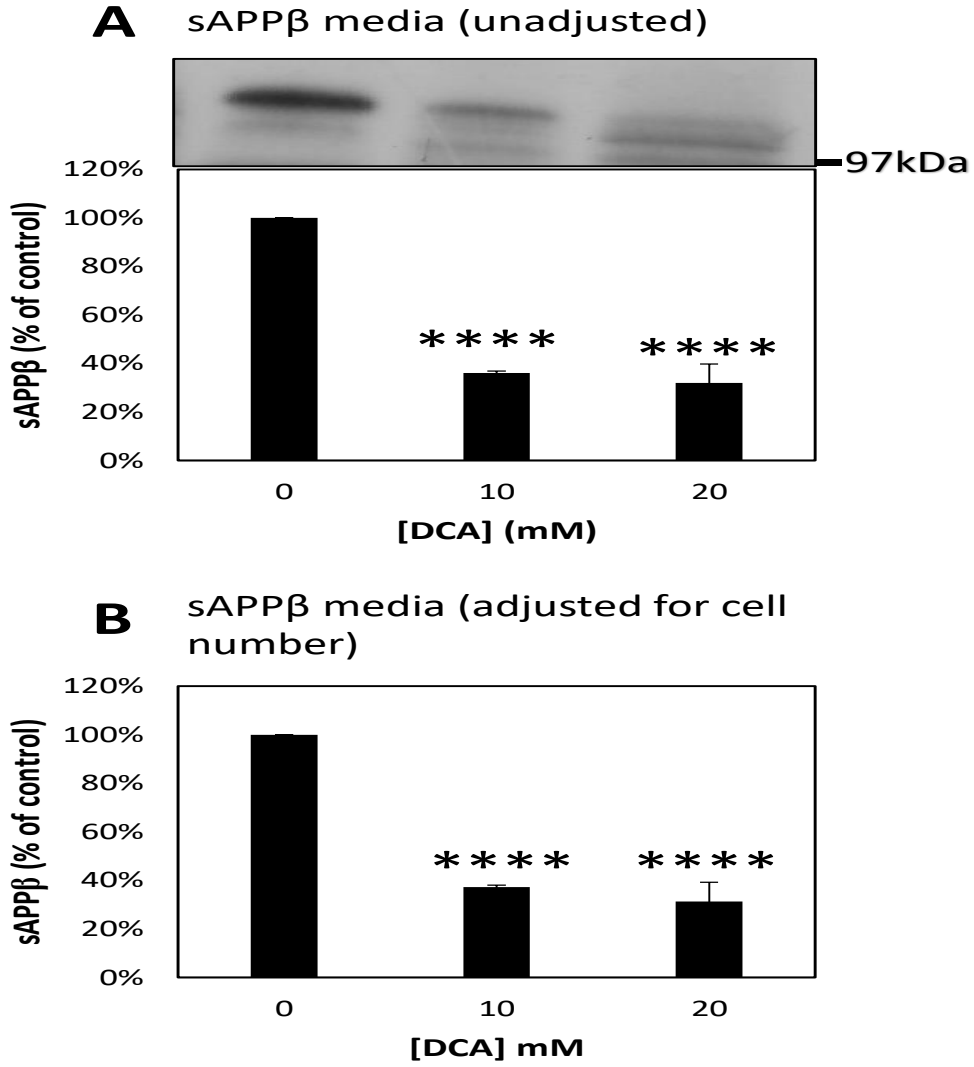

Figure 3.2.6. DCA decreases sAPPβ shedding from untransfected SH-SY5Y cells. SH-SY5Y cells were treated with 0, 10 and 20 mM DCA for 6 days, with conditioned media processed as per the Materials and Methods section. Immunoblot analysis of conditioned medium was carried out with anti-sAPPβ antibody. The results from the immunoblot were quantified by densitometric analysis **(A)**. Data was also adjusted for cell number determined by trypan blue assay **(B)**. Values are means ± S.D. (n=3). Unless indicated otherwise, results were not significantly different; **** P≤ 0.0001.

3.2.7 The effect of DCA on p53 expression in confluent SH-SY5Y cells after 24 hours

The results from the extended treatment (Fig 3.1.7) indicated that p53 expression increases in response to DCA. Cell lysates from the 24h treatment were immunoblotted for

p53 to see whether this trend occurs after 24 h treatment. The results (Fig. 3.2.7) show that after 24 h DCA treatment, p53 levels increased by 62% with 10 mM and 50% with 20 mM DCA.

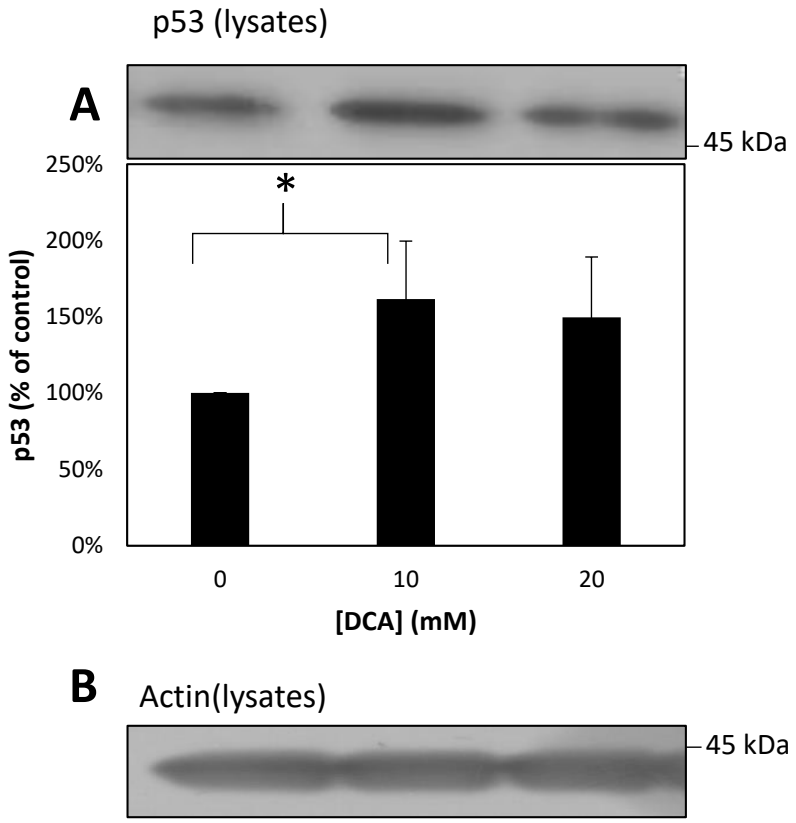

Figure 3.2.7. DCA increases expression of p53 in confluent SH-SY5Y cells after 24 hours. SH-SY5Y cells were grown to confluence and treated with 0, 10 and 20 mM DCA for 24 hours, with lysates prepared as per the Materials and Methods section. Immunoblot analysis of equal amounts of lysate proteins was carried out with anti-p53 **(A)** and anti-actin **(B)** antibodies. The results from the p53 blot were quantified by densitometric analysis. Values are means ± S.D. (n=3). Unless indicated otherwise, results were not significantly different; * P≤ 0.05.

3.3 Summary

As with the initial experiments with PC3 cells conducted by our research group, a morphological change was seen in SH-SY5Y cells exposed to DCA; specifically, an increase in neurite-like extensions. Cell viability assays indicated that DCA treatment increased metabolic activity in cells and impacted on cell growth as fewer cells were present in DCA-treated flasks. The 24h DCA treatment confirmed this as no significant change in cell viability was observed. Protein analysis showed altered APP expression, with APP holoprotein levels increasing and a change in APP proteolysis was observed; increased sAPPα levels and decreased sAPPβ levels The changes in APP proteolysis in 24 h treated SH-SY5Y cells mirrored those observed across the extended treatment, whilst APP expression increased at both 10 and 20 mM DCA in the

24H treated cells. Interestingly an increase in p53 levels, a known regulator of APP expression, was also seen in both treatments (extended and 24h). Western blot analysis of enzymes that are involved in the proteolytic cleavage of APP showed inconclusive results as the antibodies used showed poor specificity.

Chapter 4: Results; The effects of DCA on APP-over-expressing SH-SY5Y cells

4.1 Introduction

The analysis of changes to APP expression and proteolysis following DCA treatment is the salient focus of these experiments. To develop on from the changes seen in untransfected SH-SY5Y cells, experiments were repeated using SH-SY5Y cells that overexpress APP_{695}. This isoform of APP is highly expressed in neurons and most relevant to the situation in Alzheimer's disease (Beyreuther *et al*., 1993). Overexpression of APP also allows for investigation into the effect of DCA on APP expression and proteolysis when there is an abundance of APP. The overexpressing cells express around 50X the level of APP_{695} compared to untransfected SH-SY5Y cells and were also chosen as a model as previously it had not been possible to detect endogenous sAPPβ in SH-SY5Y cells. As with the untransfected SH-SY5Y cells, SH-SY5Y APP_{695} cells were treated with DCA to investigate how overexpression of APP alters the effects of DCA on cell morphology, proliferation and APP proteolysis.

4.2 DCA-induced morphological changes in SH-SY5Y APP_{695} cells

As there is an abundance of APP expressed by the SH-SY5Y APP_{695}, morphological differences can be observed when comparing SH-SY5Y APP_{695} and untransfected SH-SY5Y cells, with the overexpressing cells having a wealth of neurite-like extensions. SH-SY5Y APP_{695} cells were seeded in growth medium containing 0, 10 or 20 mM DCA and examined under a light microscope after 3 and 6 days growth. The results (Fig. 4.1) showed an increase in the number of neurite-like extensions at 10 mM (Fig. 4.1D) and at 20 mM DCA (Fig 4.1F) at both 3 and 6 day time points. The existing neurite-like extensions were also altered with extensions increasing in length. These changes were similar to the observations seen with untransfected SH-SY5Y cells but were more pronounced.

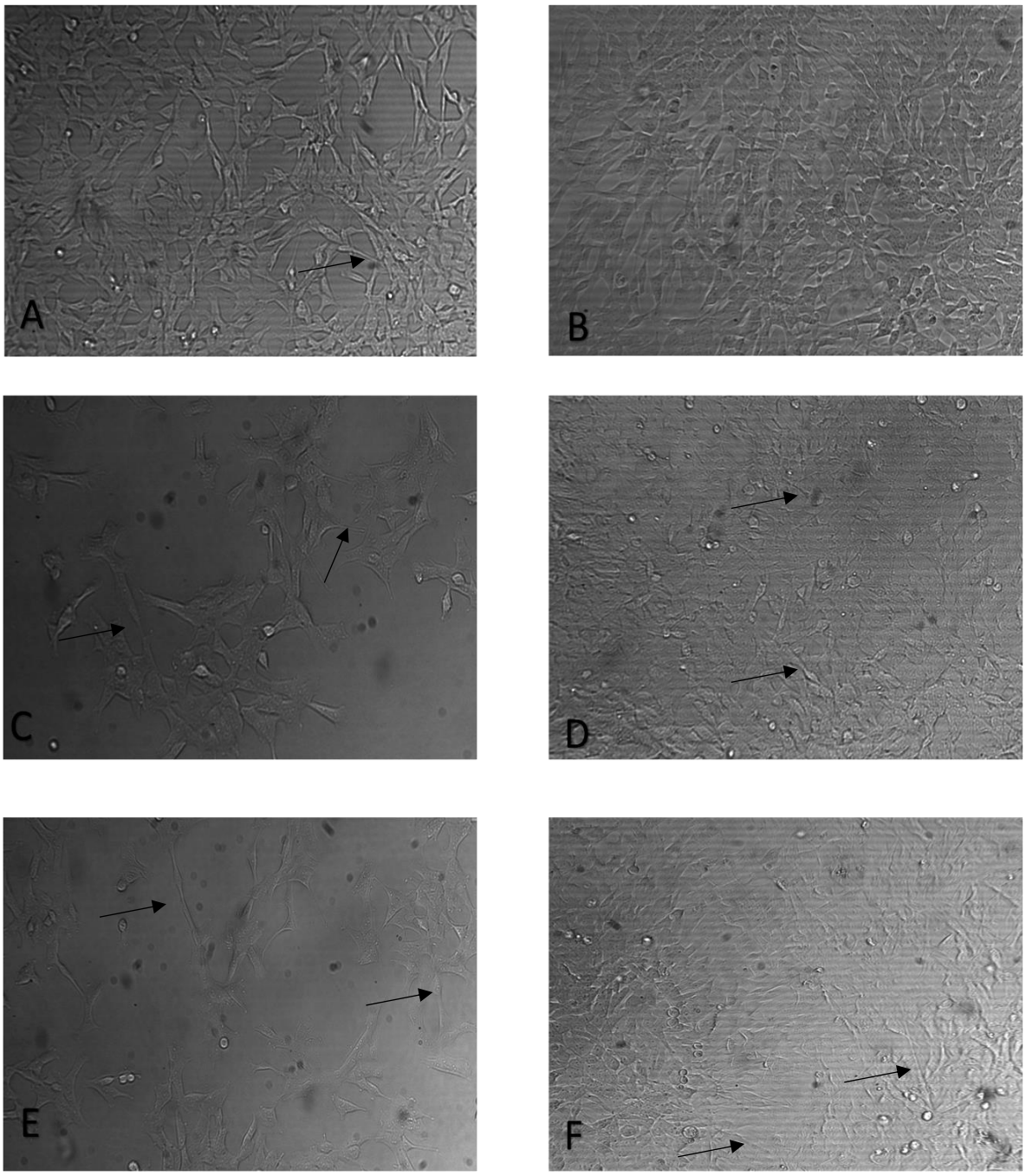

Figure 4.1. Morphology of DCA-treated SH-SY5Y APP_{695} cells. SH-SY5Y APP_{695} cells were treated with 0 **(A&B),** 10 mM **(C&D)** and 20 mM **(E&F)** DCA for a total period of 6 days. Cells were imaged after 3 days **(A, C, E)** or 6 days **(B, D, F)**. Images were captured at 10X objective in the absence of stains. Arrows indicate neurite-like extensions.

4.3 The effect of DCA on SH-SY5Y APP_{695} cell proliferation

Similar to the trend seen with untransfected SH-SY5Y cells, it was evident that fewer cells were present in DCA treated flasks at the endpoint of the treatment. These visual observations were quantified by a trypan blue assay. SH-SY5Y APP_{695} cells were treated for 6 days with 10 mM and 20 mM DCA before the assay was performed. The results (Fig. 4.2) showed a similar trend to the untransfected SH-SY5Y cells; a general decrease in viable cell count. The viable cell count decreased to 97% with 10 mM DCA and to 68% with 20 mM DCA. As with the untransfected SH-SY5Y cells, few dead cells were observed when conducting the trypan blue assay.

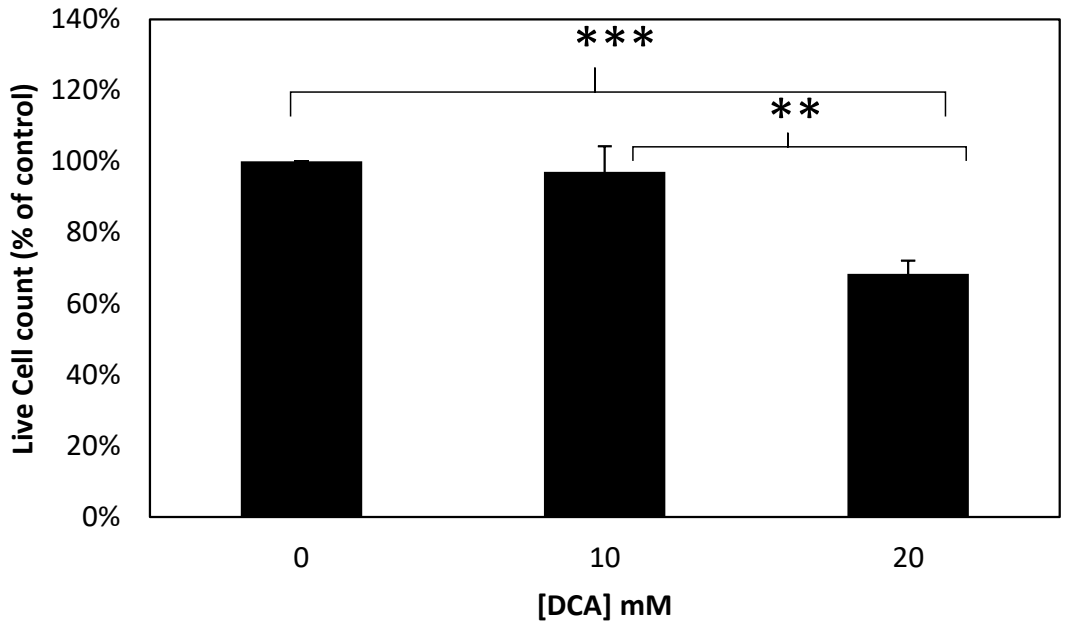

Figure 4.2. DCA decreases SH-SY5Y APP_{695} cell proliferation. SH-SY5Y APP_{695} cells were treated with 0, 10 and 20 mM DCA for 6 days (see Materials and Methods) and then trypsinised and counted via trypan blue exclusion assay. Counts reflect live cells. Results are means ± S.D. (n=3). Unless indicated otherwise, results were not significantly different; ** P≤ 0.01 & *** P≤ 0.001.

4.4 The effect of DCA on SH-SY5Y APP_{695} cell metabolism

DCA increased metabolism in SH-SY5Y cells and is known to promote mitochondrial metabolism via inhibition of PDK. A MTS assay was performed on SH-SY5Y APP_{695} cells in the same manner as the one conducted on untransfected SH-SY5Y cells. The results (Fig. 4.3) showed metabolic activity increased by 128% with 10 mM treatment and increased by 27% with 20 mM DCA. These significant increases are similar to the results observed with untransfected SH-SY5Y cells (Fig 3.1.3), however the increase at 20 mM was larger in the untransfected SH-SY5Y cells.

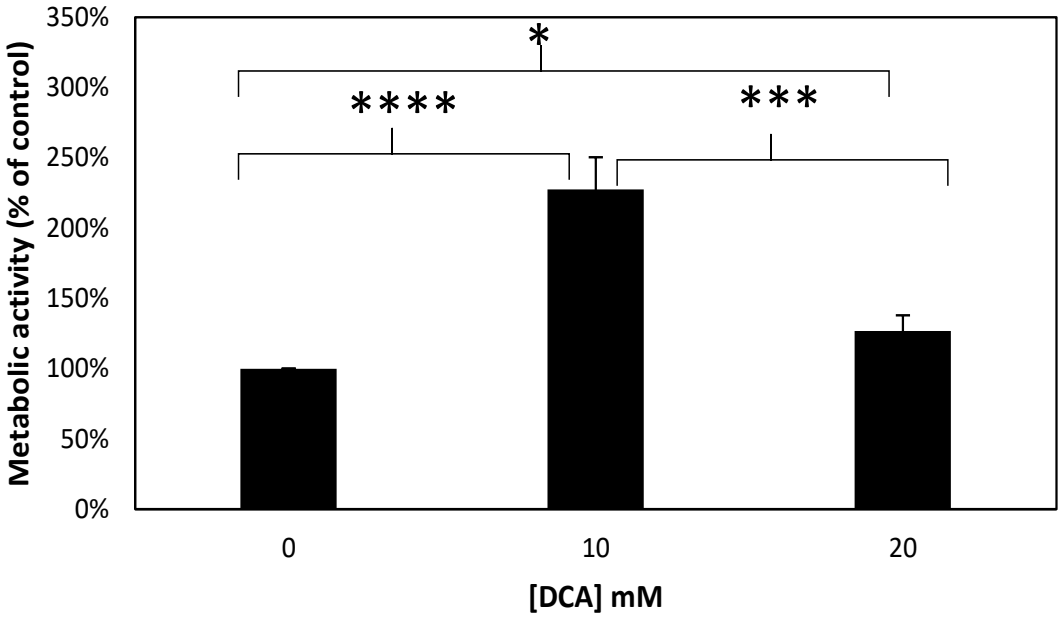

Figure 4.3. DCA increases the metabolic activity of SH-SY5Y APP_{695} cells. SH-SY5Y APP_{695} cells were treated with 0, 10 and 20 mM DCA for 7 days (see Materials and Methods) and then subjected to a MTS assay (see Materials and Methods). Results are means ± S.D. (n=6). Unless indicated otherwise, results were not significantly different; * P≤ 0.05, *** P≤ 0.001 & **** P≤ 0.0001.

4.5 DCA alters expression of overexpressed APP in SH-SY5Y APP_{695} cells

As alterations were seen with APP holoprotein levels in SH-SY5Y cells treated with DCA, it was of interest to see what happened when there was an abundance of APP within the system. Cell lysates were produced from the cells imaged in Fig. 4.1 as described in the Materials and Methods section. Immunoblot analysis of cell lysates using anti-APP C-terminal antibody showed that APP holoprotein levels increased by 57% with 10 mM DCA and increased by 107% with 20 mM DCA treatment (Fig. 4.4A). Due to the abundance of APP, it was also possible to detect the C-terminal fragment of APP via immunoblot analysis using the same antibody (Fig. 4.4B). The results showed that the CTF increased by 42% at 10 mM DCA

and 166% at 20 mM DCA mirroring the increase in APP holoprotein levels. The CTF is a product of APP proteolysis, which indicated that along with a change to APP expression, there was an increase in APP proteolysis compared to the control. This increase may be due to the increased APP available for cleavage. To examine specific changes to APP proteolysis, additional immunoblots were carried out (see section 4.6).

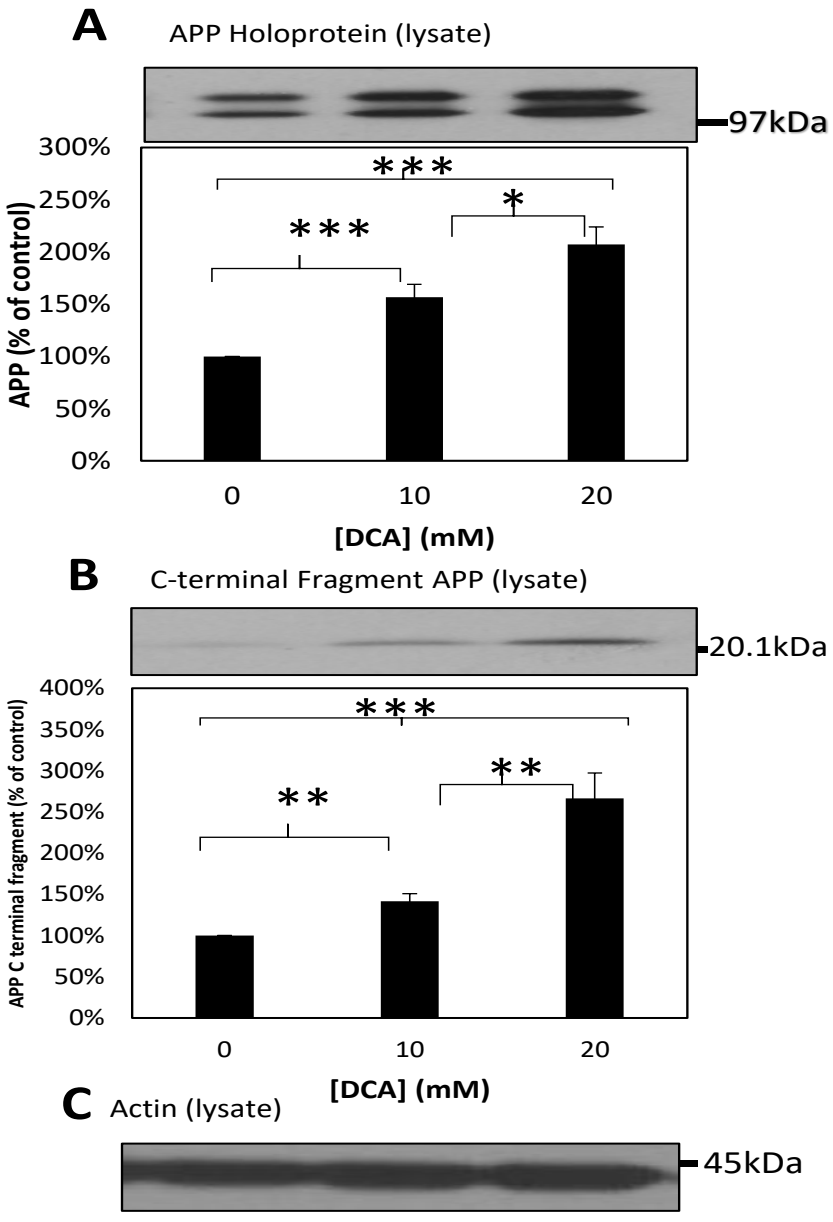

Figure 4.4. DCA alters expression of overexpressed APP in SH-SY5Y APP_{695} cells. SH-SY5Y APP_{695} cells were treated with 0, 10 and 20 mM DCA for 6 days, with lysates prepared as per the Materials and Methods section. Immunoblot analysis of equal amounts of lysate proteins was carried out with anti-APP C-terminal **(A)** and anti-actin **(B)** antibodies. The results from the APP blot were quantified by densitometric analysis. Values are means ± S.D. (n=3). Unless indicated otherwise, results were not significantly different; * P≤ 0.05, ** P≤ 0.01 & *** P≤0.001.

4.6 The effect of DCA on APP proteolysis in SH-SY5Y APP_{695} cells

A marked increase in the CTF of APP was observed, suggesting an increase in proteolysis (Fig. 4.4A). This was also matched by an increase in APP holoprotein levels (Fig. 4.4B). To see whether there were any changes to the proteolysis of APP, conditioned media from DCA treated SH-SY5Y APP_{695} cells was subject to immunoblot for sAPPα (Fig. 4.5) and sAPPβ (Fig. 4.6). Following immunoblotting with the anti-sAPPα antibody 6E10, the results (Fig. 4.6) showed one band corresponding to all three sAPPα isoforms. The results (Fig. 4.5A) showed no statistical difference in sAPPα but a small increase with 10 and 20 mM treatments. However, when adjusting for cell number as determined by trypan blue assay (see Fig. 4.2), the results (Fig. 4.5B) showed an increase of 8% with 10 mM treatment and a significant increase of 69% with 20 mM DCA. This showed increased shedding of sAPPα from 20 mM-treated cells.

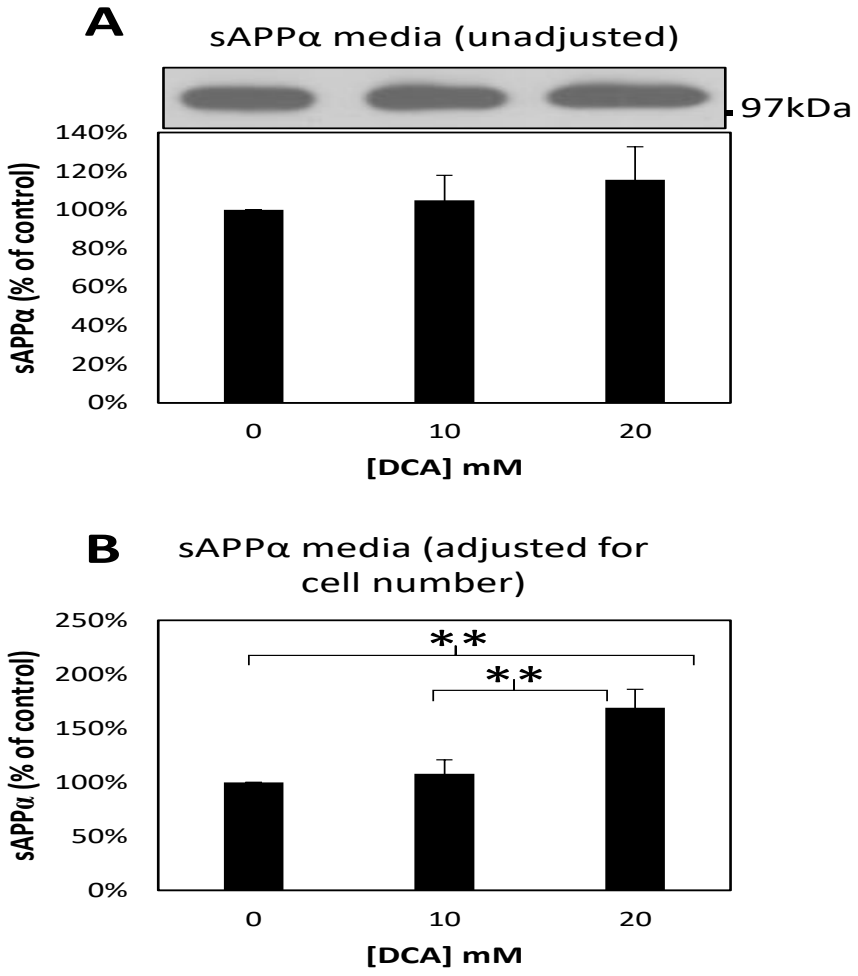

Figure 4.5. DCA increases sAPPα shedding from SH-SY5Y APP_{695} cells. SH-SY5Y APP_{695} cells were treated with 0, 10 and 20 mM DCA for 6 days, with conditioned media processed as per the Materials and Methods section. Immunoblot analysis of conditioned medium was carried out with anti-sAPPα antibody 6E10. The results from the immunoblot were quantified by densitometric analysis **(A)**. Data was also adjusted for cell number determined by trypan blue assay **(B)**. Values are means ± S.D. (n=3). Unless indicated otherwise, results were not significantly different; ** P≤ 0.01.

In addition to analysing levels of sAPPα, sAPPβ levels were examined to look for changes in APP proteolysis induced by DCA in SH-SY5Y APP_{695} cells. It was thought that overexpression of APP would alter the effects of DCA. In contrast to the sAPPα blots, it was possible to distinguish different isoforms; two distinct bands were observed corresponding to $sAPP\beta_{751/770}$ (upper band) and $sAPP\beta_{695}$ (lower band) (Fig. 4.6A). The intensity of the $sAPP\beta_{751/770}$ band decreased at both 10 and 20 mM DCA treatment, as did the intensity of the $sAPP\beta_{695}$ band (Fig. 4.6A). The adjusted results (Fig. 4.6B) show decreased $sAPP\beta_{751/770}$ with 10 and 20 mM DCA treatment, the level of $sAPP\beta_{695}$ however increased by 24% with 20 mM DCA. This is in contrast to the untransfected SH-SY5Y cells where endogenous levels of APP were present and a complete ablation of the 695 isoform was seen as well as a decrease in the levels of 751/770 isoforms (Fig. 3.1.6). This data suggests that overexpression of APP negates the impact DCA has on the levels of sAPPβ.

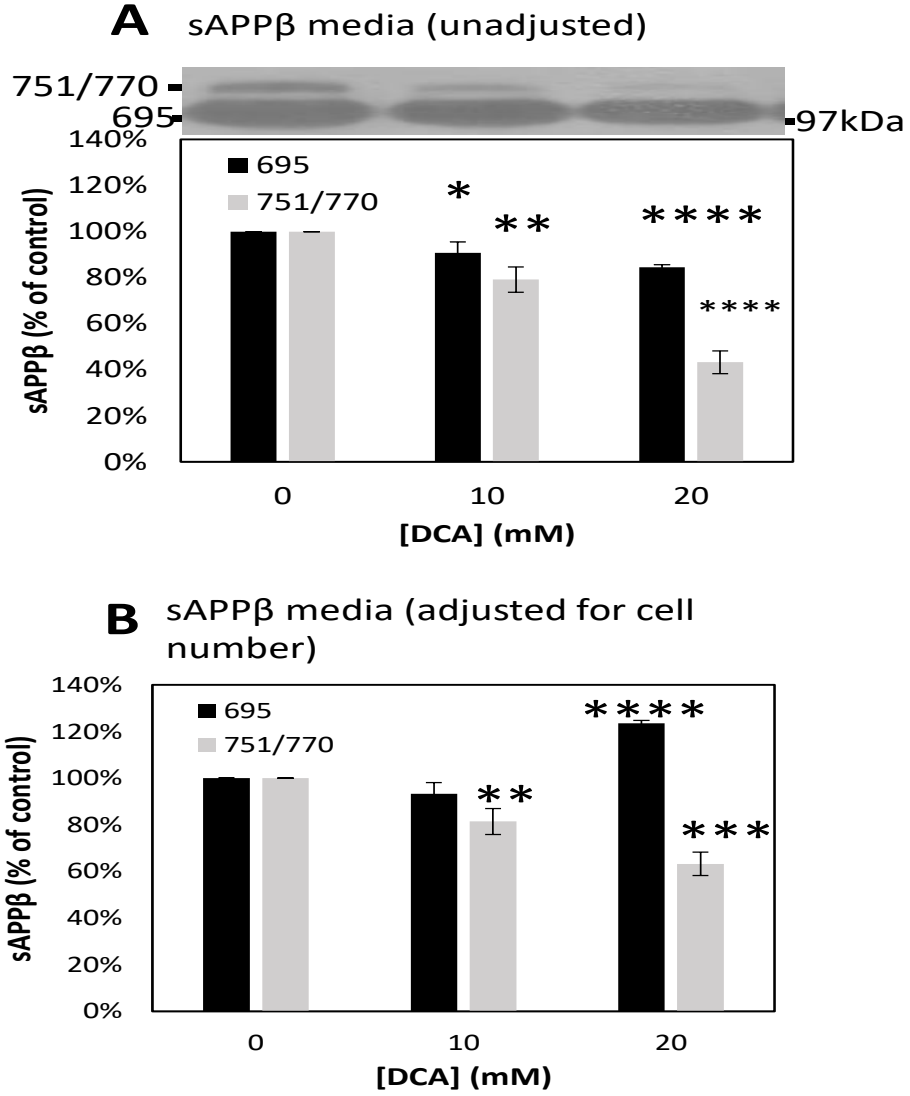

Figure 4.6. Overexpression of APP negates the effects of DCA on sAPPβ levels in SH-SY5Y APP$_{695}$ cells. SH-SY5Y APP$_{695}$ cells were treated with 0, 10 and 20 mM DCA for 6 days, with conditioned media processed as per the Materials and Methods section. Immunoblot analysis of conditioned medium was carried out with anti-sAPPβ antibody. The results from the immunoblot were quantified by densitometric analysis **(A)**. Data was also adjusted for cell number determined by trypan blue assay **(B)**. Values are means ± S.D. (n=3). Unless indicated otherwise, results were not significantly different; * P≤ 0.05, ** P≤ 0.01, *** P≤ 0.001 and **** P≤ 0.0001.

4.7 The effect of DCA on p53 expression in SH-SY5Y APP$_{695}$ cells

Data from the untransfected SH-SY5Y cells demonstrated that p53 increased in response to DCA treatment (Figs. 3.1.7 & 3.2.7). APP and p53 levels are closely linked, so it was of interest to see whether an overexpression of APP and subsequent increase in levels following DCA treatment resulted in an increase in p53 levels. The results (Fig. 4.7) confirm that p53 levels increase in response to DCA. In contrast to the results from the untransfected

SH-SY5Y cells, only a single band was observed in p53 immunoblots from SH-SY5Y APP_{695} lysates. Unlike the untransfected cells, APP levels increased dramatically following DCA treatment in SH-SY5Y APP_{695} cells yet the levels of p53, a regulator of APP expression, still followed the same trend.

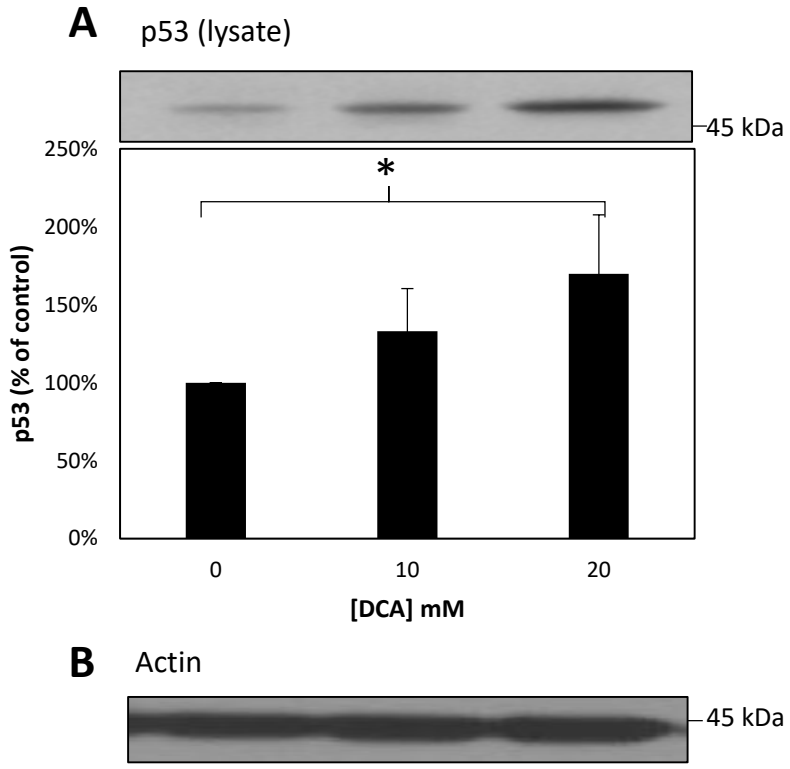

Figure 4.7. DCA increases expression of p53 in SH-SY5Y APP_{695} cells. SH-SY5Y APP_{695} cells were treated with 0, 10 and 20 mM DCA for 6 days, with lysates prepared as per the Materials and Methods section. Immunoblot analysis of equal amounts of lysate proteins was carried out with anti-p53 **(A)** and anti-actin **(B)** antibodies. The results from the p53 blot were quantified by densitometric analysis. Values are means ± S.D. (n=3). Unless indicated otherwise, results were not significantly different; * P≤ 0.05.

4.8 Summary

In general, similar trends were observed with SH-SY5Y APP_{695} cells and untransfected SH-SY5Y cells with some notable differences. Morphological changes following DCA treatment were in line with the untransfected cells but with extensions being a lot longer in APP_{695} overexpressing cells. Cell viability data revealed a small decline in viability at 10 mM and a larger decline at 20 mM, along with an increase in metabolic activity. This further supports the idea that DCA alters growth rate. Protein analysis revealed a large increase in APP levels and a corresponding increase in CTF and sAPPα levels in response to DCA treatment. It is of note

that a decrease in levels of sAPPβ 751/770 was observed despite a large increase in APP levels. This suggests that overexpression of APP negated the effects of DCA on APP proteolysis; there was not a vast reduction in sAPPβ levels. The increase in p53 levels mirrors that seen in untransfected SH-SY5Y cells.

Chapter 5: Results; The effects of DCA on BACE1-over-expressing SH-SY5Y cells

5.1 Introduction

The key finding from experiments with untransfected SH-SY5Y cells was the decrease in sAPPβ levels with DCA treatment and the overexpression of APP negating that effect. BACE1 is the enzyme responsible for the cleavage of APP that generates sAPPβ in the amyloidogenic pathway, however it is not possible to detect endogenous protein levels of BACE1 in SH-SY5Y cells. To examine the relationship between BACE1, sAPPβ and DCA further, the cohort of experiments was repeated on SH-SY5Y cells overexpressing BACE1. As with APP_{695} in the APP_{695} overexpressing cells, levels of BACE1 are about 50X that of untransfected SH-SY5Y cells.

5.2 DCA-induced morphological changes in SH-SY5Y BACE1 cells

SH-SY5Y BACE1 cells were seeded in growth medium containing 0, 10 or 20 mM DCA and examined under a light microscope after 3 and 6 days growth. The results (Fig. 5.1) showed an increase in the number of neurite-like extensions was at 10 mM (Fig. 5.1D) and at 20 mM DCA (Fig 5.1F) at both 3 and 6 day time points. This pattern was the same as that of the untransfected and APP overexpressing SH-SY5Y cells.

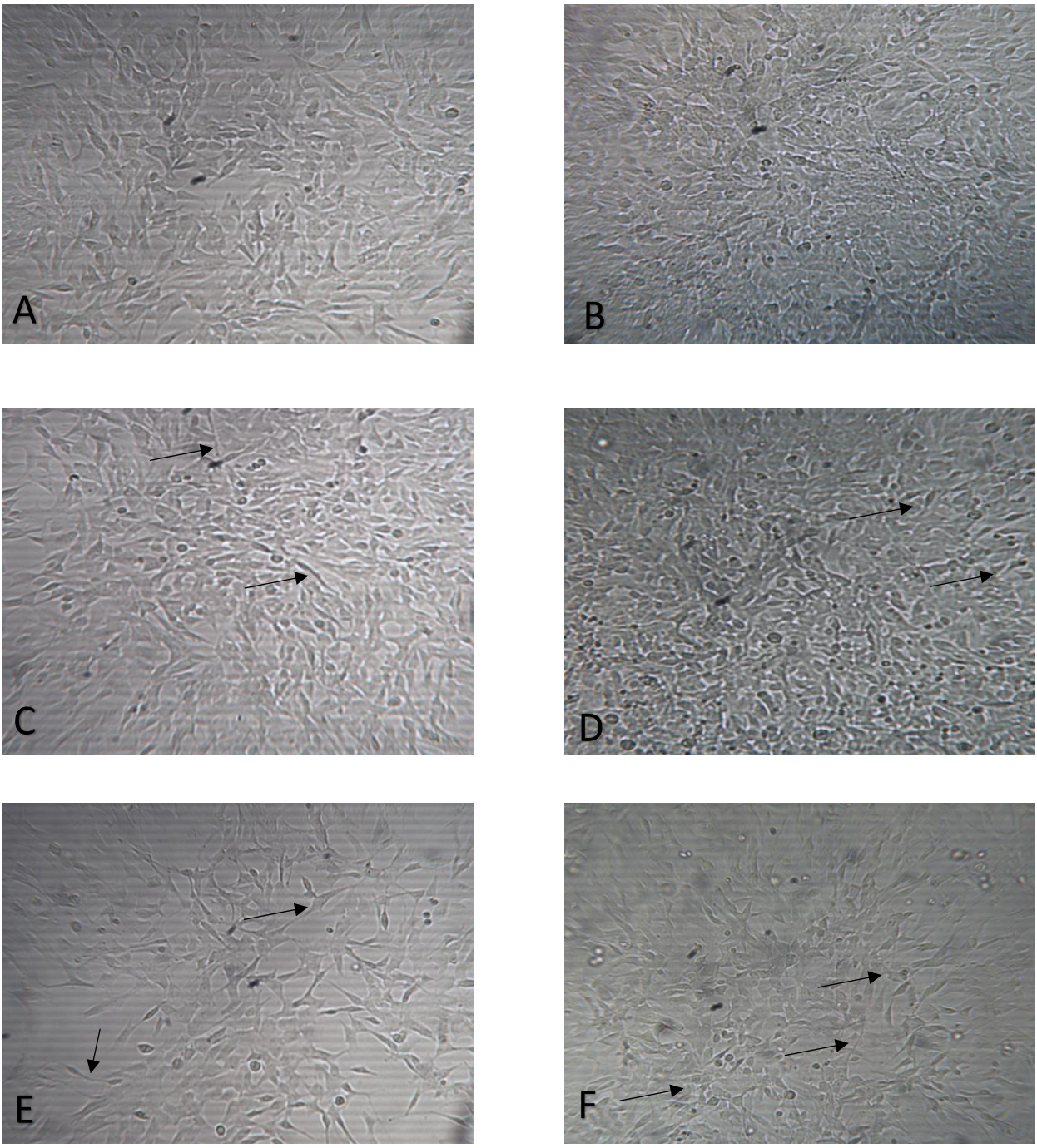

Figure 5.1. Morphology of DCA-treated SH-SY5Y BACE1 cells. SH-SY5Y BACE1 cells were treated with 0 **(A&B),** 10 mM **(C&D)** and 20 mM **(E&F)** DCA for a total period of 6 days. Cells were imaged after 3 days **(A, C, E)** or 6 days **(B, D, F)**. Images were captured at 10X objective in the absence of stains. Arrows indicate neurite-like extensions.

5.3 The effect of DCA on SH-SY5Y BACE1 cell proliferation

A decrease in cell number was seen following DCA treatment of both the APP_{695} overexpressing and untransfected SH-SY5Y cells. It was predicted that a similar trend would be observed with BACE1 overexpressing cells following DCA treatment. In order to investigate whether DCA negatively impacted on SH-SY5Y BACE1 cell proliferation, SH-SY5Y BACE1 cells were treated with 10 mM and 20 mM DCA for 6 days and cell viability was assessed via trypan blue exclusion assay (see Materials and Methods). The results (Fig. 5.2.) showed a significant decrease in the viable cell count at 20 mM DCA. Very few non-viable cells were observed at any of the DCA concentrations employed, again indicating that cell growth is inhibited rather than induction of apoptosis.

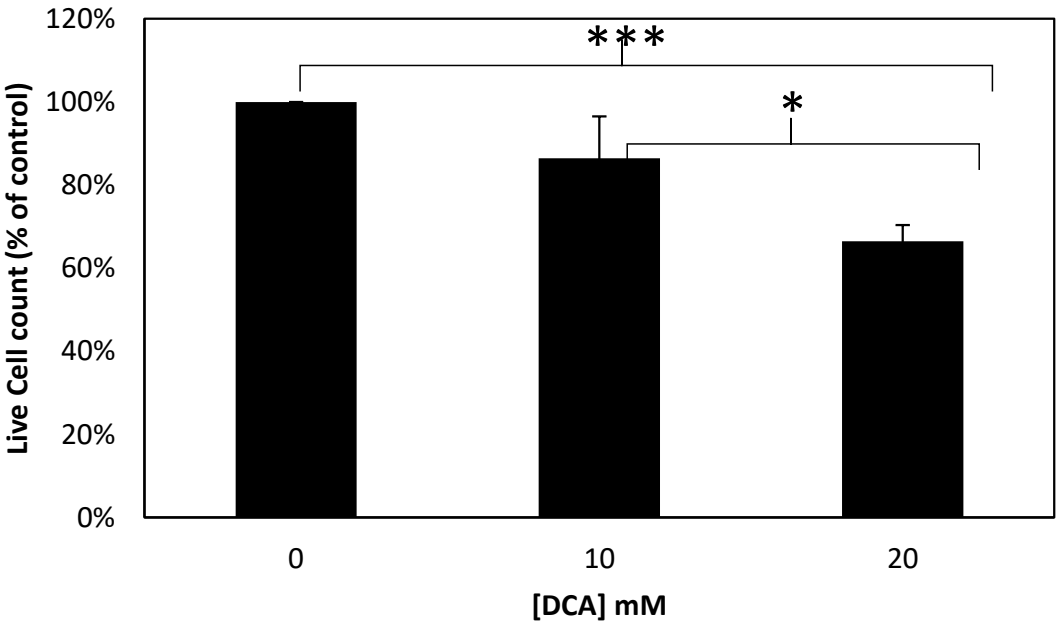

Figure 5.2. DCA decreases SH-SY5Y BACE1 cell proliferation. SH-SY5Y BACE1 cells were treated with 0, 10 and 20 mM DCA for 6 days (see Materials and Methods) and then trypsinised and counted via trypan blue exclusion assay. Counts reflect live cells. Results are means ± S.D. (n=3). Unless indicated otherwise, results were not significantly different; * P≤ 0.05 & *** P≤ 0.001.

5.4 The effect of DCA on SH-SY5Y BACE1 cell metabolism

To investigate whether BACE1 overexpression alters the impact of DCA on cell metabolism, a MTS assay was carried out on DCA-treated SH-SY5Y BACE1 cells. Tracing the trend of earlier experiments, metabolic activity of SH-SY5Y BACE1 cells (Fig. 5.3) increased at

10 mM and at 20 mM relevant to the control. Again, the increase at 20 mM was thought to be counteracted by the number of cells present in the flask (see Fig. 5.2).

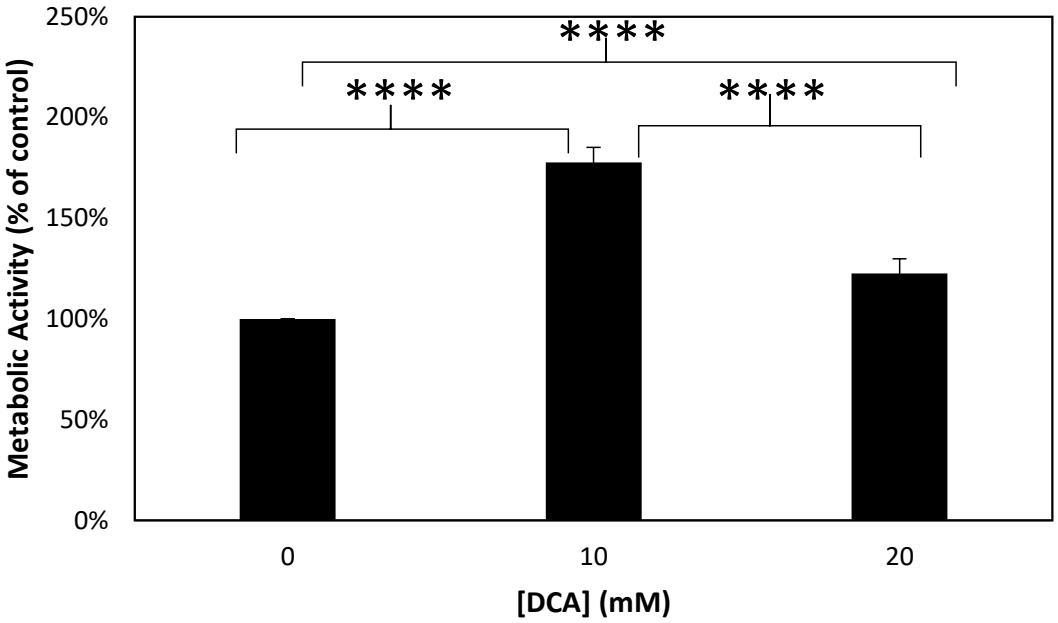

Figure 5.3. DCA increases the metabolic activity of SH-SY5Y BACE1 cells. SH-SY5Y BACE1 cells were treated with 0, 10 and 20 mM DCA for 7 days (see Materials and Methods) and then subjected to a MTS assay (see Materials and Methods). Results are means ± S.D. (n=6). Unless indicated otherwise, results were not significantly different; **** P≤ 0.0001.

5.5 The effect of DCA on endogenous APP expression in SH-SY5Y BACE1 cells

Experiments with untransfected SH-SY5Y showed that endogenous APP expression is altered following DCA treatment (Fig. 3.1.4). BACE1 overexpressing SH-SY5Y cells were treated with DCA and lysates produced as per the Materials and Methods. The lysates were immunoblotted with anti-APP C-terminal antibody and the results (Fig. 5.4) showed a 7% decrease with 10 mM DCA and a 4% increased with 20 mM DCA. These changes were not significant and align with those seen in the untransfected SH-SY5Y cells.

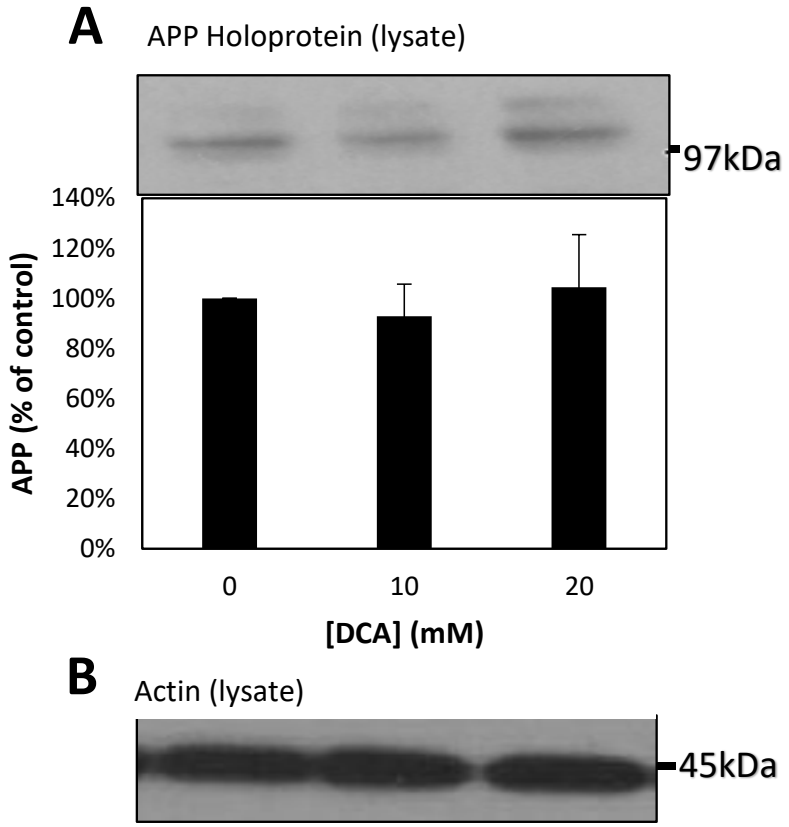

Figure 5.4. APP expression is unaltered by DCA in SH-SY5Y BACE1 cells. SH-SY5Y BACE1 cells were treated with 0, 10 and 20 mM DCA for 6 days, with lysates prepared as per the Materials and Methods section. Immunoblot analysis of equal amounts of lysate proteins was carried out with anti-APP C-terminal **(A)** and anti-actin **(B)** antibodies. The results from the APP blot were quantified by densitometric analysis. Values are means ± S.D. (n=3). Unless indicated otherwise, results were not significantly different.

5.6 The effect of DCA on APP proteolysis in SH-SY5Y BACE1 cells

BACE1 is responsible for cleaving APP to produce sAPPβ via the amyloidogenic pathway. It was expected that overexpression of BACE1 would yield more sAPPβ than generated by untransfected cells. Previously, DCA decreased levels of sAPPβ in SH-SY5Y APP_{695} cells and completely removed $sAPP\beta_{695}$ levels in untransfected cells. It was therefore of interest to see whether the overexpression of BACE1 negated the effects of DCA on sAPPβ levels. In order to determine whether DCA affected APP proteolysis, immunoblot analyses of sAPPα and sAPPβ in conditioned media were conducted. Following immunoblotting with the anti-sAPPα antibody 6E10, the results (Fig. 5.5A) showed two distinct bands corresponding to $sAPP\alpha_{751/770}$ (upper band) and $sAPP\alpha_{695}$ (lower band). The intensity of the upper band was enhanced at both concentrations whilst the intensity of the lower band was enhanced in the 10 mM DCA samples but not at the 20 mM concentration of the compound. When adjusting for cell number, the results (Fig. 5.5B) showed increased $sAPP\alpha_{751/770}$ shedding and increased

sAPPα$_{695}$, but to a lesser extent. Only the increase in sAPPα$_{751/770}$ with 20 mM DCA, relative to the control, was significant. These data show that DCA still enhances sAPPα shedding in the presence of elevated BACE1 levels.

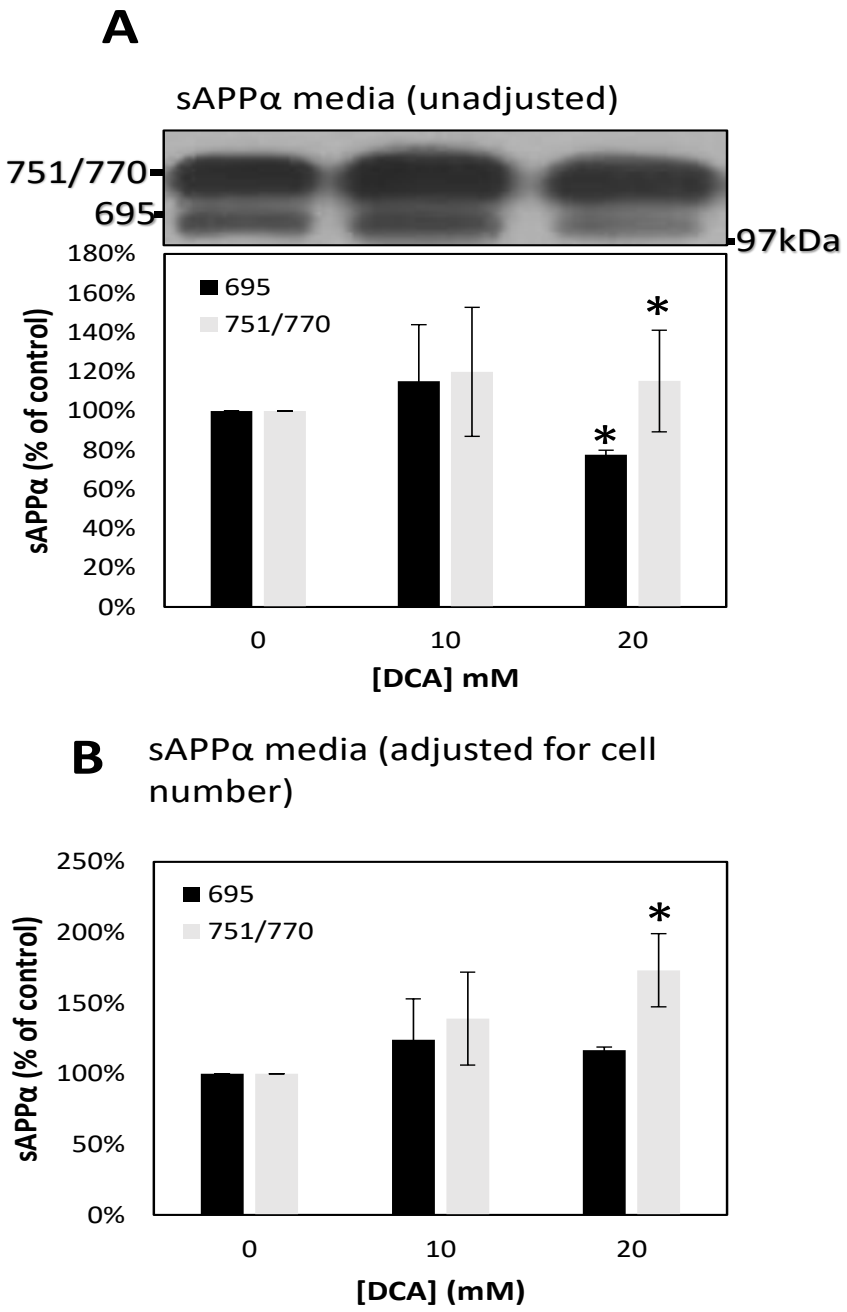

Figure 5.5. DCA alters sAPPα shedding from SH-SY5Y BACE1 cells. SH-SY5Y BACE1 cells were treated with 0, 10 and 20 mM DCA for 6 days, with conditioned media processed as per the Materials and Methods section. Immunoblot analysis of conditioned medium was carried out with anti-sAPPα antibody 6E10. The results from the immunoblot were quantified by densitometric analysis **(A)**. Data was also adjusted for cell number determined by trypan blue assay **(B)**. Values are means ± S.D. (n=3). Unless indicated otherwise, results were not significantly different; * P≤ 0.05.

Conditioned media was also immunoblotted for sAPPβ. Following immunoblotting with anti-sAPPβ antibody, two distinct bands were observed corresponding to $sAPP\beta_{751/770}$ (upper band) and $sAPP\beta_{695}$ (lower band) (Fig. 5.6A). The intensity of the $sAPP\beta_{751/770}$ band was unaltered at both 10 and 20 mM DCA treatment. The $sAPP\beta_{695}$ band was only detected in the control sample, denoting ablation of $sAPP\beta_{695}$ following DCA treatment at 10 and 20 mM of the compound. Following adjustment for cell number (Fig 5.6B) $sAPP\beta_{751/770}$ levels increased significant following 10 and 20 mM DCA treatment. As no $sAPP\beta_{695}$ was detected, it cannot be adjusted for cell number.

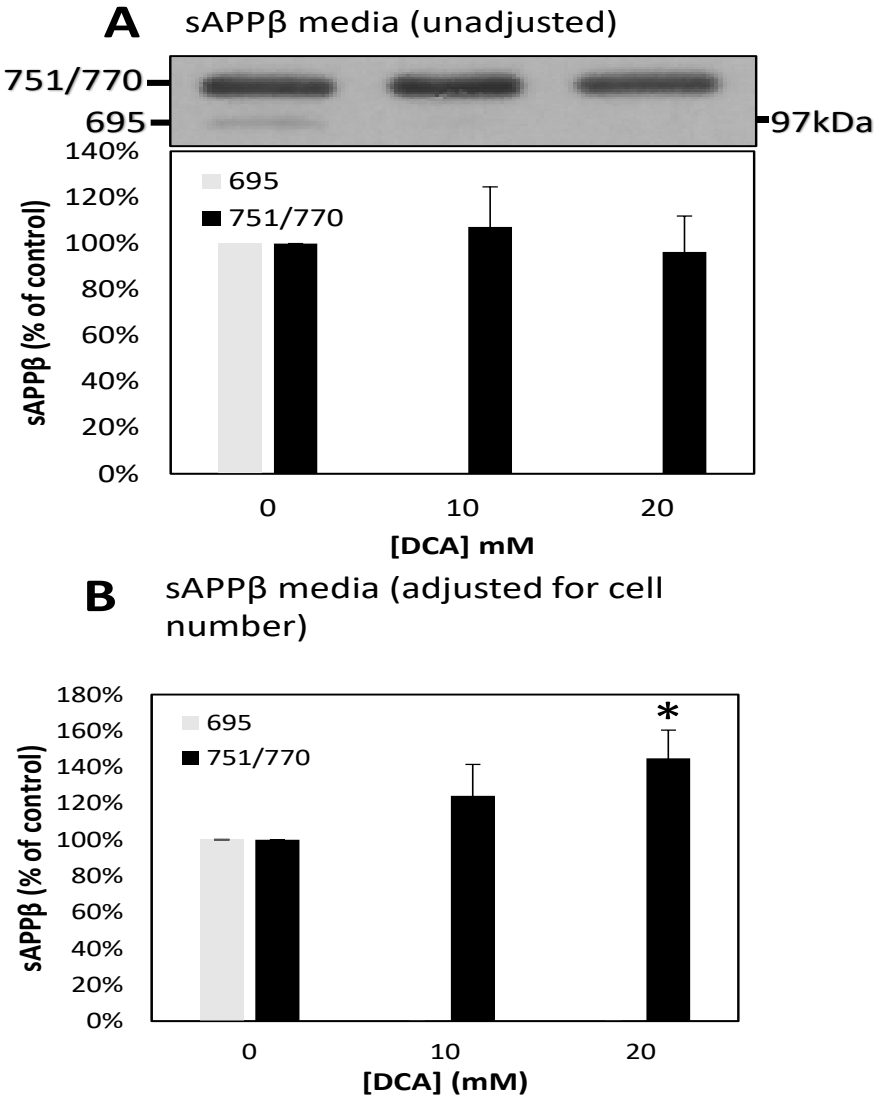

Figure 5.6. DCA alters sAPPβ shedding from SH-SY5Y BACE1 cells. SH-SY5Y BACE1 cells were treated with 0, 10 and 20 mM DCA for 6 days, with conditioned media processed as per the Materials and Methods section. Immunoblot analysis of conditioned medium was carried out with anti-sAPPβ antibody. The results from the immunoblot were quantified by densitometric analysis **(A)**. Data was also adjusted for cell number determined by trypan blue assay **(B)**. Values are means ± S.D. (n=3). Unless indicated otherwise, results were not significantly different; * P≤ 0.05.

5.7 The effect of DCA on BACE1 expression in SH-SY5Y BACE1 cells

Immunoblots for ADAM10,17 and presenilin-1 were not carried out due to the poor specificity of the antibodies. However, it was possible to analyse the effects of DCA on BACE1 in the overexpressing cells. Part of the reasoning behind using BACE1 overexpressing cells was to be able to detect levels of BACE1 protein in cells treated with DCA. The results from the APP proteolysis immunoblots (Fig. 5.5) also rely on a wider context of changes to the enzymes involved to assist in making a judgement as to how these changes to APP proteolysis are driven by DCA at a molecular level. Lysates from DCA-treated SH-SY5Y BACE1 cells were immunoblotted with anti-BACE1 antibody. The results (Fig. 5.7) showed an increase in BACE1 expression in response to DCA treatment with a 12% increase at 10 mM and 35% increase at 20 mM DCA.

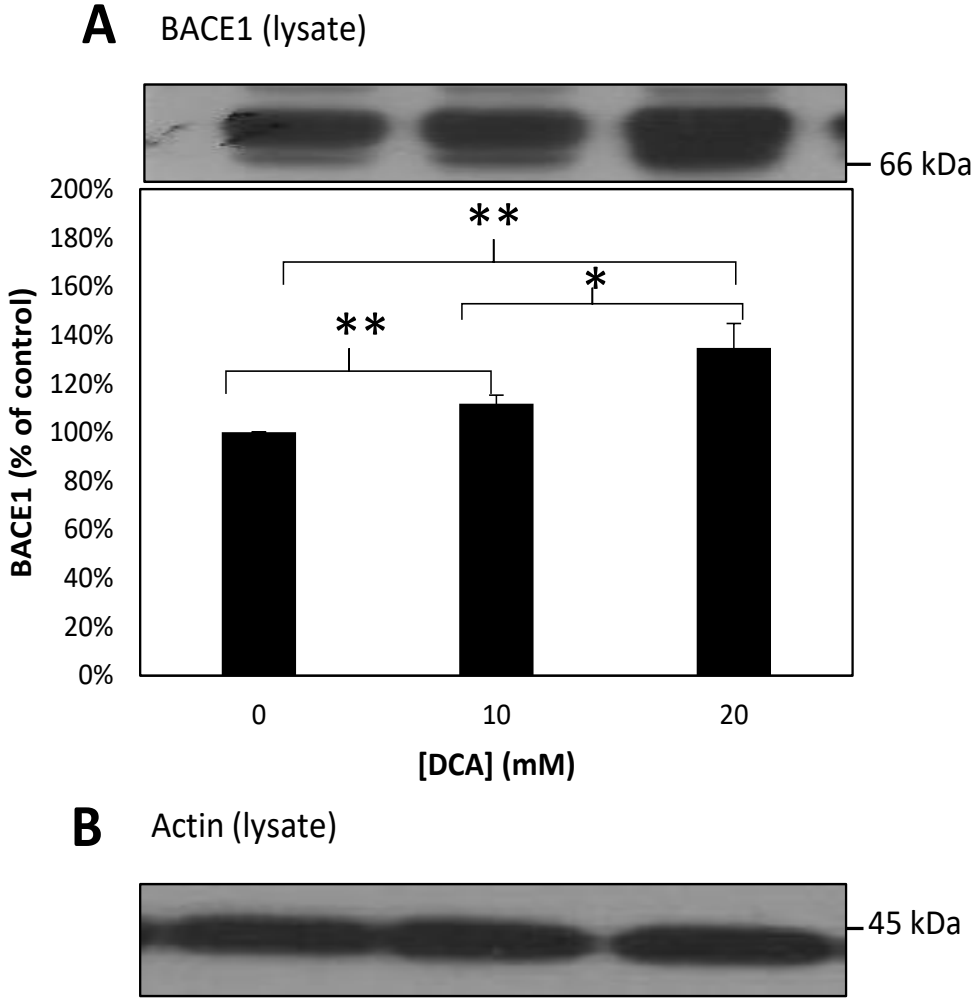

Figure 5.7. DCA increases expression of BACE1 in SH-SY5Y BACE1 cells. SH-SY5Y BACE1 cells were treated with 0, 10 and 20 mM DCA for 6 days, with lysates prepared as per the Materials and Methods section. Immunoblot analysis of equal amounts of lysate proteins was carried out with anti-BACE1 **(A)** and anti-actin **(B)** antibodies. The results from the p53 blot were quantified by densitometric analysis. Values are means ± S.D. (n=3). Unless indicated otherwise, results were not significantly different; * P≤ 0.05 & ** P≤ 0.01.

5.8 The effect of DCA on p53 expression in SH-SY5Y BACE1 cells

An immunoblot for p53 was conducted on lysates from DCA-treated SH-SY5Y BACE1 cells. The results (Fig. 5.8) showed an increase in p53 levels in response to DCA, however the increases at 10 and 20 mM DCA were not significant. Increased p53 expression was also observed in the other two SH-SY5Y cell lines in response to DCA.

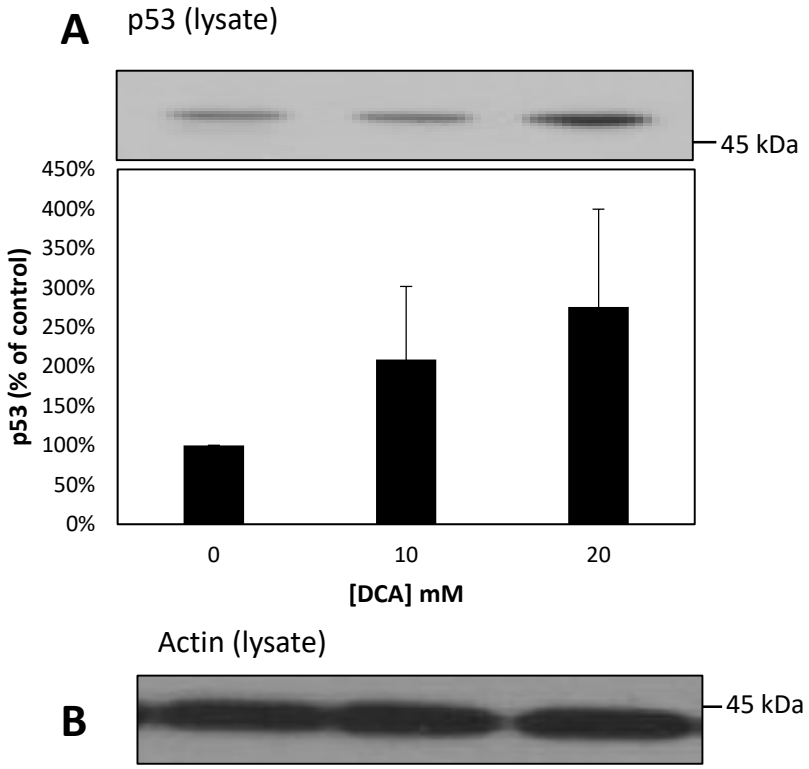

Figure 5.8. DCA increases expression of p53 in SH-SY5Y BACE1 cells. SH-SY5Y BACE1 cells were treated with 0, 10 and 20 mM DCA for 6 days, with lysates prepared as per the Materials and Methods section. Immunoblot analysis of equal amounts of lysate proteins was carried out with anti-p53 **(A)** and anti-actin **(B)** antibodies. The results from the p53 blot were quantified by densitometric analysis. Values are means ± S.D. (n=3). Unless indicated otherwise, results were not significantly different.

5.9 Summary

Overexpression of BACE1 didn't alter the effect of DCA on cell morphology, proliferation and metabolism. APP expression and p53 expression mirrored the results in the untransfected SH-SY5Y cells; no significant change in APP holoprotein and an increase in p53 levels.The effect of DCA on APP proteolysis however was altered to some extent with BACE1 overexpression; sAPPβ_{695} levels were ablated as they were in the untransfected SH-SY5Y cells, however sAPP$\beta_{751/770}$levels increased in response to DCA. There was still an increase in sAPPα

shedding from SH-SY5Y BACE1 cells, despite increasing levels of BACE1 expression in response to DCA. These data suggest DCA treatment can overcome BACE1 overexpression with regards to levels of sAPPβ_{695}, but not sAPP$\beta_{751/770}$.

Chapter 6: Results; The effects of DCA on the shedding of ADAM substrates in alternative cell lines

6.1 SW480 Cells

6.1.1 Introduction

The results from DCA treatment of the different SH-SY5Y cell lines indicated that DCA increased alpha shedding. To investigate whether this was due to increased ADAM activity and therefore to see whether DCA affected other ADAM substrates, Dukes type B colorectal cancer cells – SW480, were treated with DCA. SW480 cells have endogenous levels of Jagged1 and E-cadherin (both ADAM substrates) which can be detected via immunoblotting, whereas SH-SY5Y cells do not. It is also possible to detect APP in SW480 cells via immunoblotting (Venkataramani *et al*., 2010). The same experiments were conducted as those conducted on all 3 SH-SY5Y cell lines. In addition to looking at APP expression and proteolysis, the expression and proteolysis of Jagged1 and E-cadherin were examined.

6.1.2 DCA-induced morphological changes in SW480 cells

SW480 cells have a spreading epithelial-type morphology and tend to form aggregates and grow in clumps (Hewitt *et al*., 2000). It was predicted that morphological changes in the form of neurite-like extensions and an increase in elongated cells would be observed. Previous experiments with SW480 cells and DCA showed a small change in morphology (Parkin, unpublished data). SW480 cells were seeded in growth medium containing 0, 10 or 20 mM DCA and examined under a light microscope after 3 and 6 days growth. The results (Fig. 6.1.1) showed an increase in the number of neurite-like extensions was at 10 mM (Fig. 6.1.1D) and at 20 mM DCA (Fig 6.1.1F) at both 3 and 6 day time points. The morphological changes seen in SW480 cells were not as pronounced as those seen in the 3 SH-SY5Y cell lines.

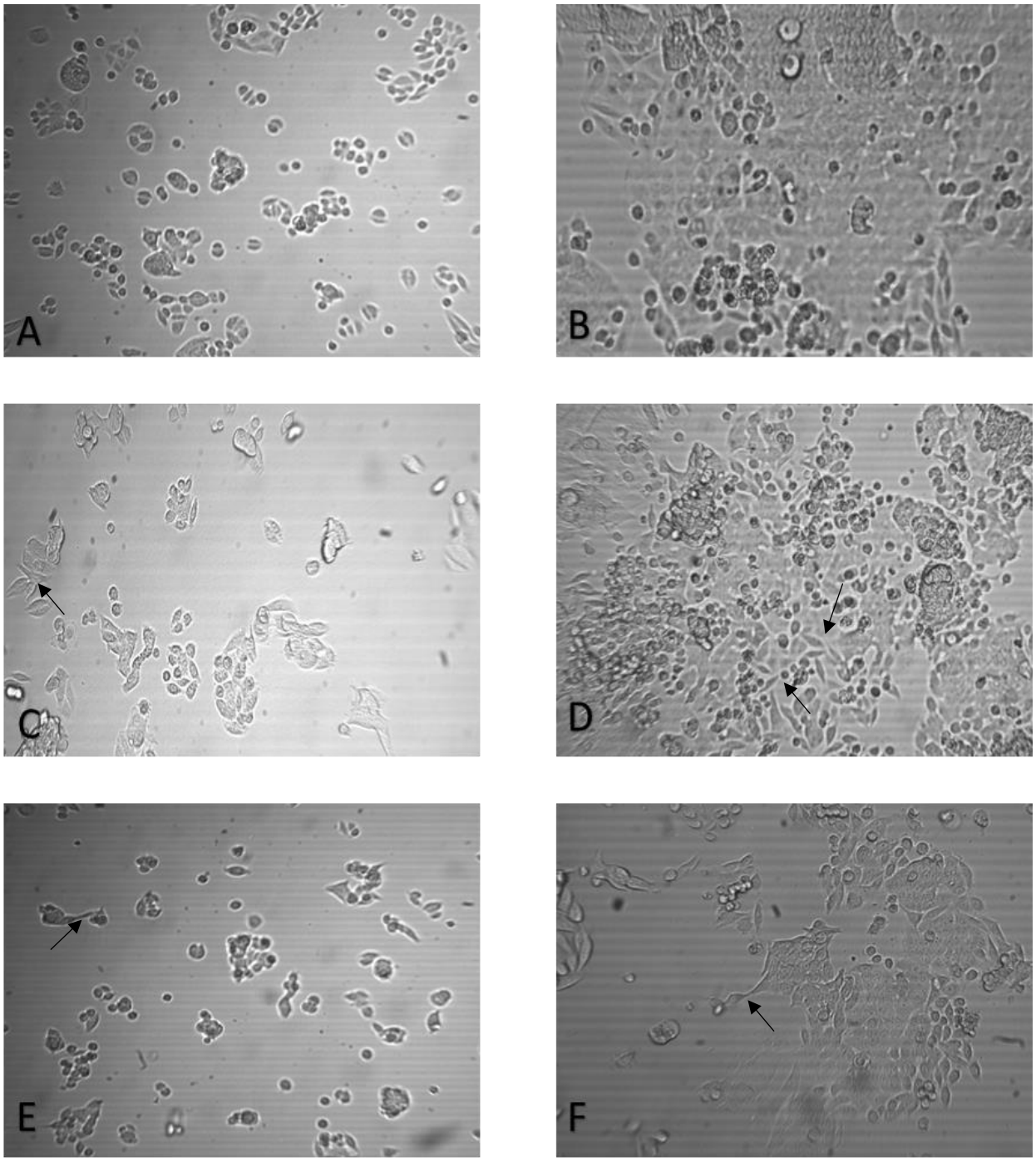

Figure 6.1.1 Morphology of DCA-treated SW480 cells. SW480 cells were treated with 0 **(A&B),** 10 mM **(C&D)** and 20 mM **(E&F)** DCA for a total period of 6 days. Cells were imaged after 3 days **(A, C, E)** or 6 days **(B, D, F)**. Images were captured at 10X objective in the absence of stains. Arrows indicate neurite-like extensions.

6.1.3 The effect of DCA on SW480 cell proliferation

As previously mentioned, DCA has been examined as a potential cancer treatment. SW480 cells have been shown to undergo apoptosis in response to DCA treatment (Shahrzad *et al*., 2010). It was predicted that DCA would have more of an impact on cell proliferation and viability on SW480 cells than the SH-SY5Y cell lines due to the more metastatic nature of SW480 cells. The results of the trypan blue assay (Fig. 6.1.2) show that in response to DCA, viable cell count decreased by 20% with 10 mM and 53% with 20 mM. The decrease to 47% with 20 mM was the greatest decline in viable cell count seen in all of the trypan blue assays conducted.

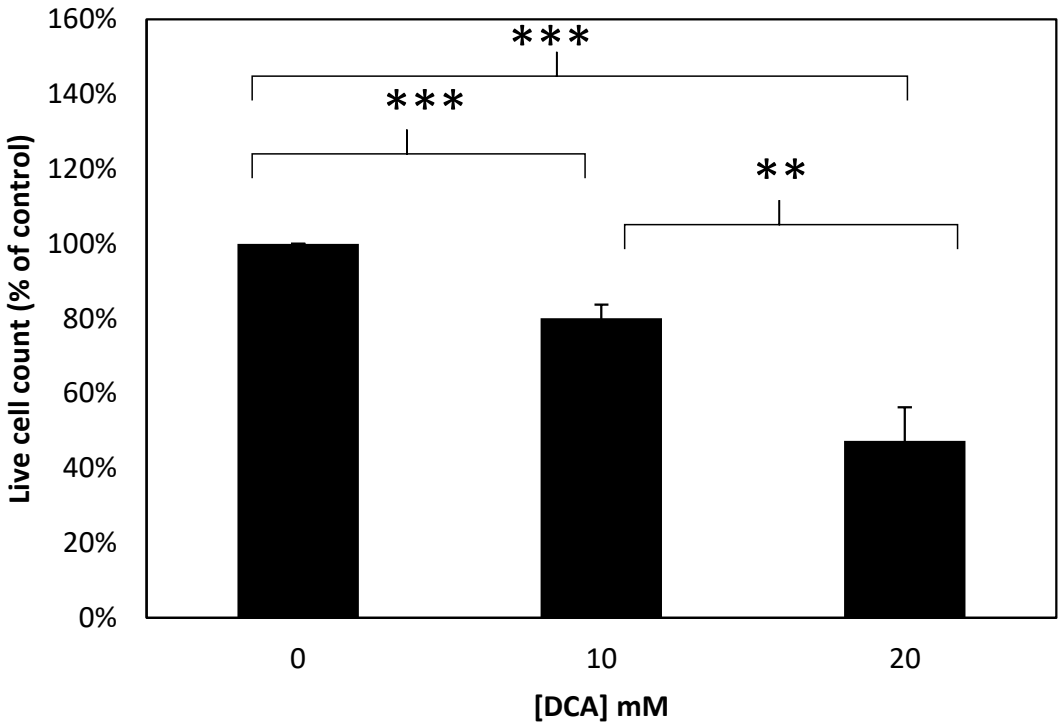

Figure 6.1.2. DCA decreases SW480 cell proliferation. SW480 cells were treated with 0, 10 and 20 mM DCA for 6 days (see Materials and Methods) and then trypsinised and counted via trypan blue exclusion assay. Counts reflect live cells. Results are means ± S.D. (n=3). Unless indicated otherwise, results were not significantly different; ** P≤ 0.01 & *** P≤ 0.001.

6.1.4 The effect of DCA on SW480 cell metabolism

The metabolic activity of SW480 cells following DCA treatment was assessed by means of a MTS assay. The results (Fig. 6.1.3) mirroring the trend seen in the SH-SY5Y cell lines; metabolic activity of SW480 cells increased at 10 and 20 mM DCA. The increase at 20 mM

was likely counteracted by the significant reduction in cell number (see Fig. 6.1.2). The data confirms that DCA alters metabolism.

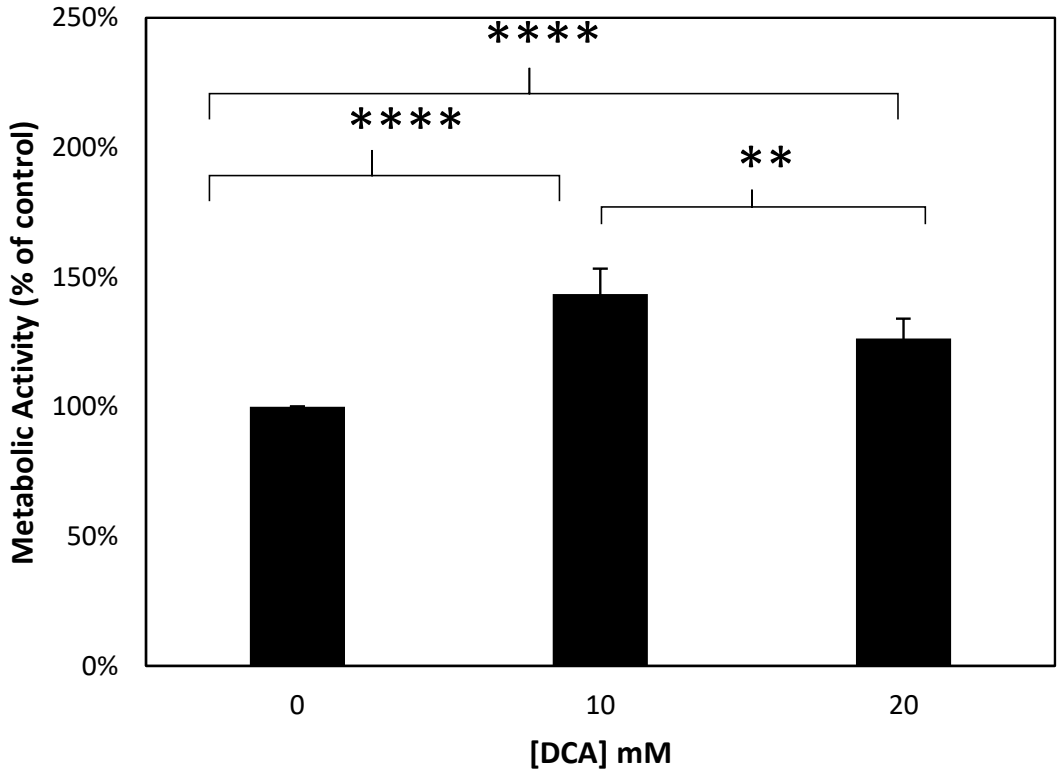

Figure 6.1.3. DCA increases the metabolic activity of SW480 cells. SW480 cells were treated with 0, 10 and 20 mM DCA for 7 days (see Materials and Methods) and then subjected to a MTS assay (see Materials and Methods). Results are means ± S.D. (n=6). Unless indicated otherwise, results were not significantly different; ** P≤ 0.01 & **** P≤ 0.0001.

6.1.5 DCA alters expression of APP in SW480 cells

Fewer morphological changes (neurite-like extensions) were observed in SW480 cells than SH-SY5Y cell lines, a process thought to be controlled by APP. To assess any changes to APP expression induced by DCA, the cells imaged in Fig. 6.1.1 were harvested and cell lysates and conditioned media prepared as described in the Materials and Methods section. Cell lysates were immunoblotted with an anti-APP C-terminal antibody and the results (Fig. 6.1.4) showed that, in response to DCA treatment, APP holoprotein levels increased with both doses. APP holoprotein levels increased by 23% with 10 mM DCA and by 68% with 20 mM DCA, relative to the control.

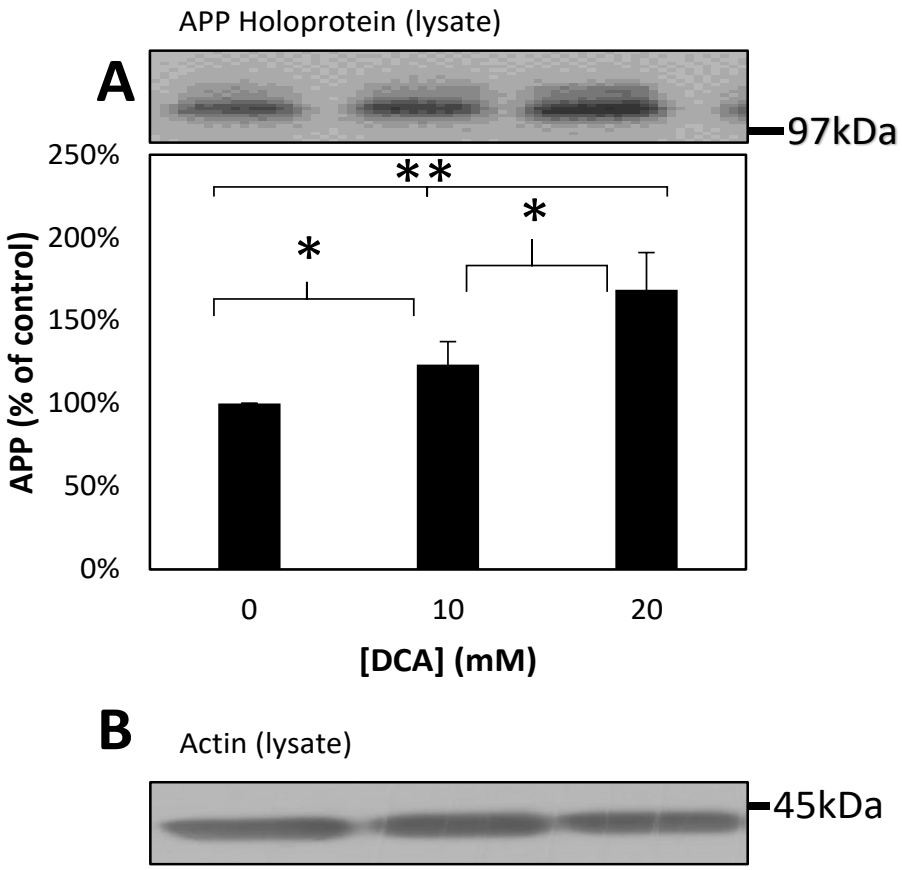

Figure 6.1.4. DCA increases expression of endogenous APP in SW480 cells. SW480 cells were treated with 0, 10 and 20 mM DCA for 6 days, with lysates prepared as per the Materials and Methods section. Immunoblot analysis of equal amounts of lysate proteins was carried out with anti-APP C-terminal **(A)** and anti-actin **(B)** antibodies. The results from the APP blot were quantified by densitometric analysis. Values are means ± S.D. (n=3). Unless indicated otherwise, results were not significantly different; * P≤ 0.05 and ** P≤0.01.

6.1.6 The effect of DCA on APP proteolysis in SW480 cells

To investigate any changes to APP proteolysis following DCA treatment, conditioned media was immunoblotted for sAPPα and sAPPβ. The results from the sAPPα immunoblot showed no significant change in sAPPα levels (Fig. 6.1.5A). When adjusting for cell number, the resultant data (Fig. 6.1.5B) showed enhanced sAPPα shedding from both 10 and 20 mM treated cells; sAPPα levels increased by 30% at 10 mM and 136% at 20 mM DCA, relative to the control.

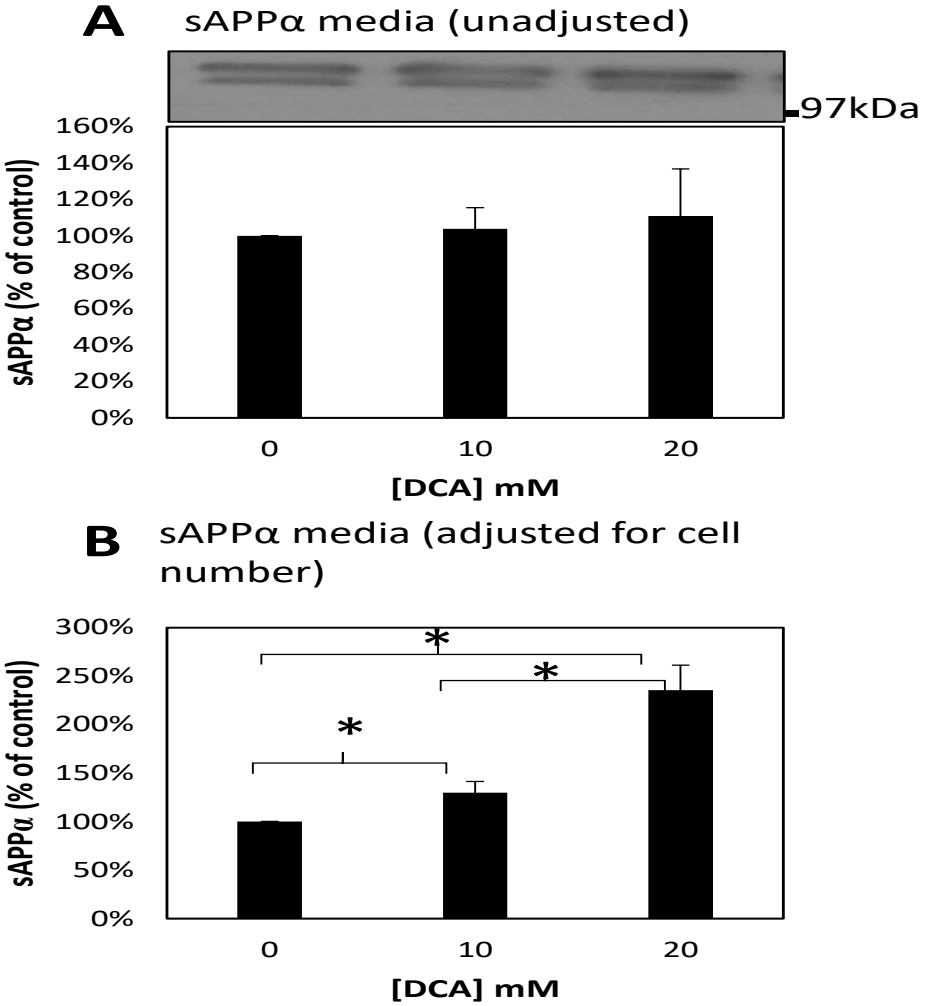

Figure 6.1.5. DCA increases sAPPα shedding from SW480 cells. SW480 cells were treated with 0, 10 and 20 mM DCA for 6 days, with conditioned media processed as per the Materials and Methods section. Immunoblot analysis of conditioned medium was carried out with anti-sAPPα antibody 6E10. The results from the immunoblot were quantified by densitometric analysis **(A)**. Data was also adjusted for cell number determined by trypan blue assay **(B)**. Values are means ± S.D. (n=3). Unless indicated otherwise, results were not significantly different; * P≤ 0.05.

Conditioned media was also immunoblot using anti-sAPPβ antibody. The results from the sAPPβ immunoblot showed no detectable sAPPβ in any of the samples (Fig. 6.1.6).

Figure 6.1.6 sAPPβ is undetectable in SW480 cells. SW480 cells were treated with 0, 10 and 20 mM DCA for 6 days, with conditioned media processed as per the Materials and Methods section. Immunoblot analysis of conditioned medium and a positive control was carried out with anti-sAPPβ antibody. No sAPPβ was detectable in the conditioned media.

6.1.7 The effect of DCA on p53 expression in SW480 cells

An immunoblot for p53 was performed on cell lysates from DCA-treated SW480 cells as described in the Materials and Methods. The results (Fig. 6.1.7) showed a general increase in p53 expression in response to DCA, compared to the control. However, these results were not of statistical significance. This data follows the trend in p53 expression in response to DCA, seen in the other cell lines tested.

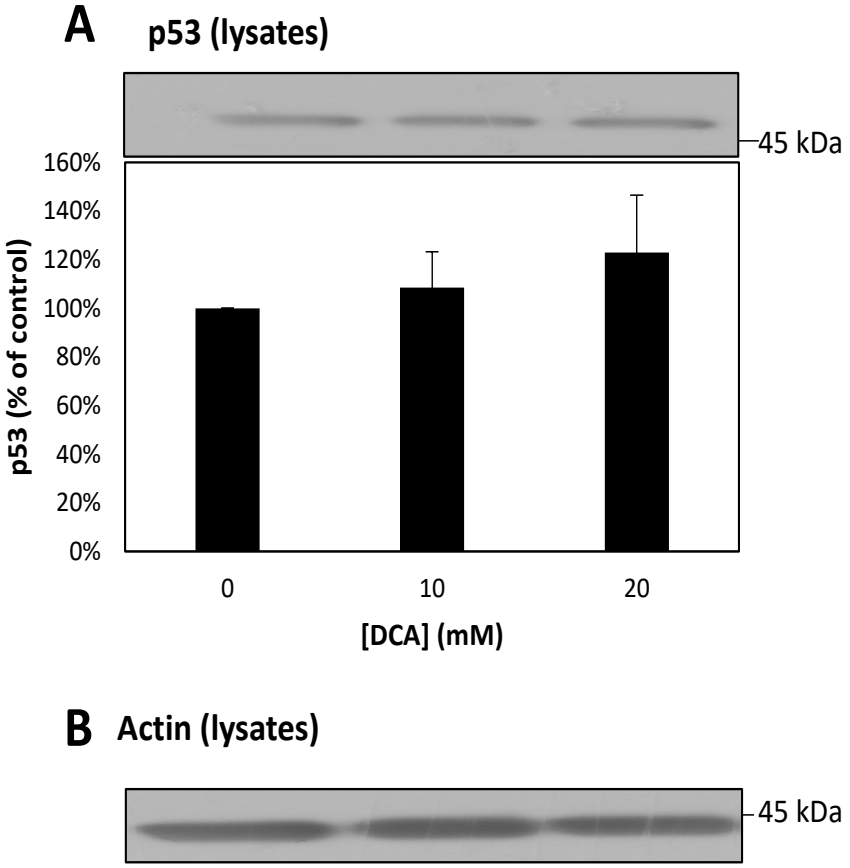

Figure 6.1.7. DCA increases expression of p53 in SW480 cells. SW480 cells were treated with 0, 10 and 20 mM DCA for 6 days, with lysates prepared as per the Materials and Methods section. Immunoblot analysis of equal amounts of lysate proteins was carried out with anti-p53 **(A)** and anti-actin **(B)** antibodies. The results from the p53 blot were quantified by densitometric analysis. Values are means ± S.D. (n=3). Unless indicated otherwise, results were not significantly different.

6.1.8 DCA alters expression of Jagged1 in SW480 cells

The alpha secretases ADAM10 and ADAM17 cleave other substrates aside from APP, one example being Jagged1. Jagged1 is one of five notch ligands in mammals for notch, playing a crucial role in the activation of the evolutionarily conserved notch signalling pathway (Grochowski *et al.*, 2016). The notch signalling pathway is the classical example of RIP and plays a vital role in controlling a number of processes from embryonic development and cell

differentiation to angiogenesis and cancer (Li *et al*., 2014). To see whether DCA affects other ADAM substrates, SW480 lysates were immunoblotted using anti-Jagged1 C-terminal antibody. The logic behind this was that if other ADAM substrates are affected by DCA, then ADAMs may be affected by DCA and be responsible for the changes in APP proteolysis. The results (Fig. 6.1.8A) showed an increase in Jagged1 holoprotein levels in response to DCA treatment. A significant increase in the Jagged1 CTF was also seen with 20 mM DCA (Fig. 6.1.8B). The CTF is produced following proteolysis of Jagged1 holoprotein and is embedded in the cell membrane just like the CTF of APP.

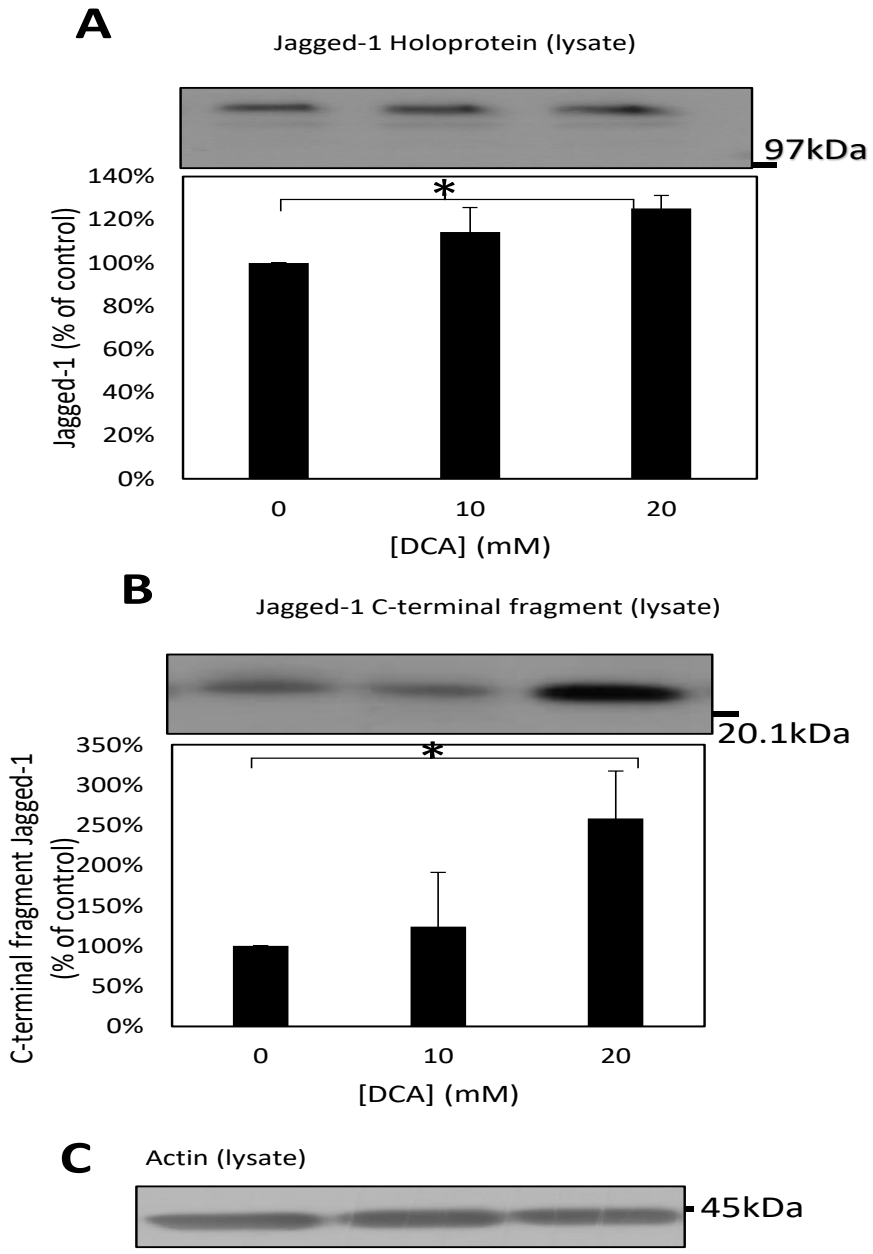

Figure 6.1.8. DCA alters expression of Jagged1 in SW480 cells. SW480 cells were treated with 0, 10 and 20 mM DCA for 6 days, with lysates prepared as per the Materials and Methods section. Immunoblot analysis of equal amounts of lysate proteins was carried out with anti-Jagged C-terminal **(A)** and anti-actin **(B)** antibodies. The results from the Jagged1 blot were quantified by densitometric analysis. Values are means ± S.D. (n=3). Unless indicated otherwise, results were not significantly different; * P≤ 0.05.

6.1.9 The effect of DCA on Jagged1 proteolysis in SW480 cells

Jagged1 proteolysis, which occurs through a combination of ADAM10 and 17 activity as well as BACE1, is necessary to generate the Jagged1 ICD (JICD) which is involved in nuclear signalling (He *et al*., 2014). The effect of Jagged1 (and its cleavage) on cell signalling is biphasic; both the soluble ectodomain which is shed from the cell surface and the cytosolic domain (from which JICD is generated) are involved in cell signalling (Parr-Sturgess *et al*., 2010). The product of Jagged1 proteolysis that is shed into the media is soluble N-terminal (NT) Jagged1. In order to determine whether DCA affected Jagged1 proteolysis, conditioned media was immunoblotted for the N-terminal fragment of Jagged1. The results (Fig. 6.1.9A) showed increased Jagged1 shedding in response to DCA treatment. When adjusted for cell number (see Fig. 6.1.2), the increase was even more dramatic; NT Jagged1 increased by 299% with 10 mM DCA and by 799% with 20 mM DCA (Fig. 6.1.9B). Along with the increased Jagged1 CTF levels, this data clearly shows that DCA enhances Jagged1 shedding in SW480 cells.

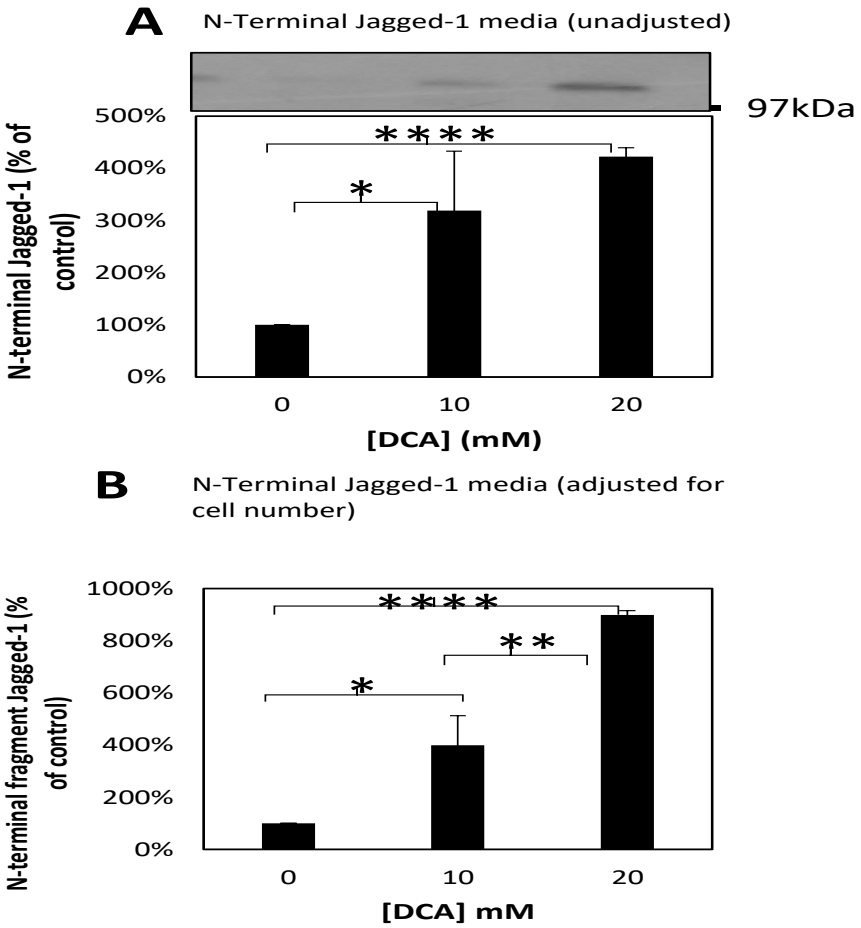

Figure 6.1.9. DCA increases Jagged1 ectodomain shedding from SW480 cells. SW480 cells were treated with 0, 10 and 20 mM DCA for 6 days, with conditioned media processed as per the Materials and Methods section. Immunoblot analysis of conditioned medium was carried out with anti-Jagged1 N-terminal antibody. The results from the immunoblot were quantified by densitometric analysis **(A)**. Data was also adjusted for cell number determined by trypan blue assay **(B)**. Values are means ± S.D. (n=3). Unless indicated otherwise, results were not significantly different; * P≤ 0.05, ** P≤ 0.01 & **** P≤ 0.0001.

6.1.10 DCA decreases E-cadherin expression in SW480 cells

E-cadherin is a transmembrane glycoprotein receptor involved in regulating cell-cell adhesion, playing an important role in proliferation and development (Arikkath and Reichardt, 2008, van Roy and Berx, 2008). E-cadherin expression is down-regulated by Jagged1 holoprotein and N-terminal Jagged1 whilst the JICD enhances E-cadherin expression (Delury *et al*., 2013). To further examine the relationship between ADAM substrates and DCA, the expression of E-cadherin (another ADAM substrate) was examined via immunoblot analysis. The results (Fig. 6.1.10) show that, in response to DCA, E-cadherin expression decreased. With 10 mM DCA, E-cadherin expression decreased by 16%, and decreased by 39% with 20 mM DCA. This is in contrast to the other two ADAM substrates, APP and Jagged1 whose expression levels both increased in response to DCA in SW480 cells.

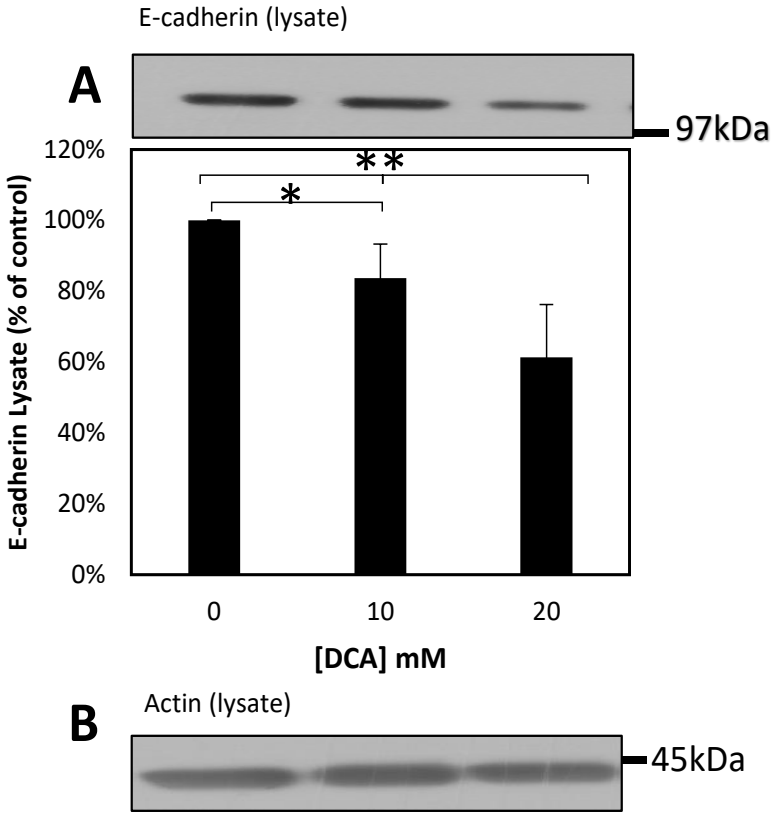

Figure 6.1.10. DCA decreases expression of E-cadherin in SW480 cells. SH-SY5Y cells were treated with 0, 10 and 20 mM DCA for 6 days, with lysates prepared as per the Materials and Methods section. Immunoblot analysis of equal amounts of lysate proteins was carried out with anti-E-cadherin **(A)** and anti-actin **(B)** antibodies. The results from the E-cadherin blot were quantified by densitometric analysis. Values are means ± S.D. (n=3). Unless indicated otherwise, results were not significantly different; * P≤ 0.05 and ** P≤0.01.

6.1.11 The effect of DCA on E-cadherin proteolysis in SW480 cells

E-cadherin is subject to ADAM mediated proteolysis, just like APP and Jagged1. Cleavage of E-cadherin by an α-secretase (in this case ADAM 10 or 15) yields a soluble ectodomain fragment (sE-cad) that is shed (Delury *et al*., 2013, Maretzky et al., 2005). To determine the impact of DCA on E-cadherin proteolysis, conditioned media from DCA-treated SW480 cells was subjected to immunoblot analysis for soluble E-cadherin. The results (Fig. 6.1.11A) showed a decrease in E-cadherin shedding from SW480 cells. When adjusting for cell number determined by trypan blue assay (see Fig. 6.1.2), a 20% decrease was seen with 10 mM DCA and a 34% increase with 20 mM DCA, compared to the control (Fig. 6.1.11B). The increase at 20 mM was not significant when compared to the control. These results suggest that E-cadherin shedding is either decreased or unaltered (when taking cell number into account).

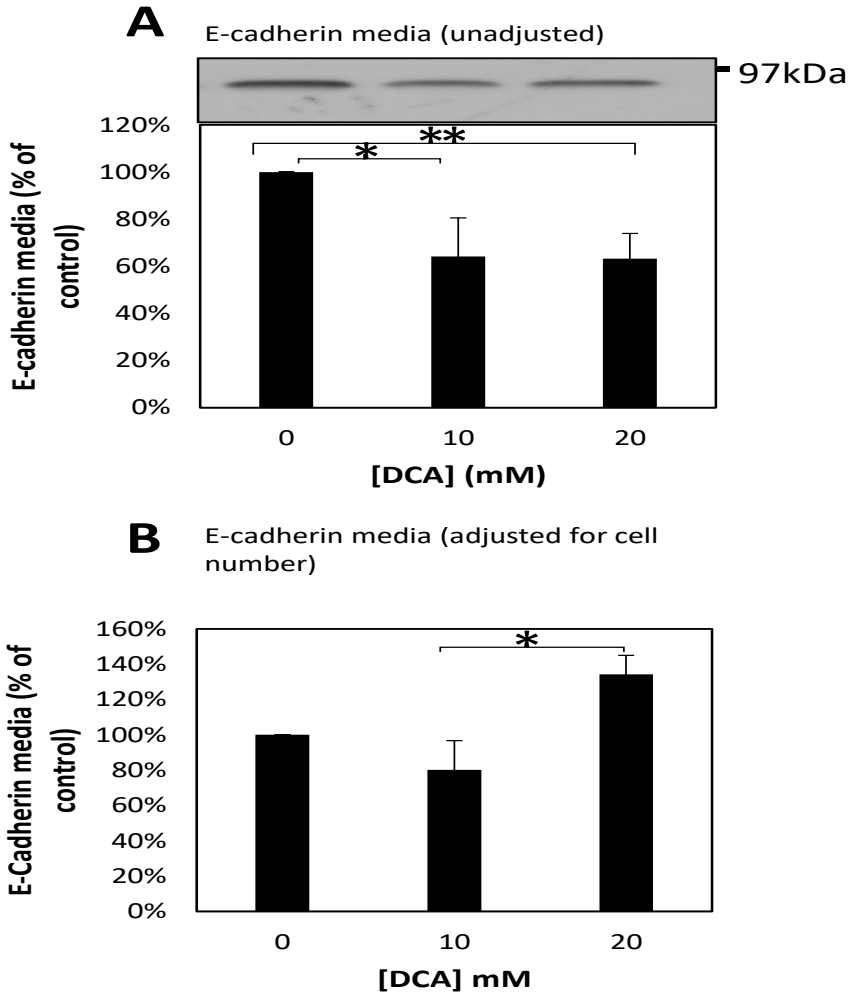

Figure 6.1.11. DCA alters E-cadherin shedding from SW480 cells. SW480 cells were treated with 0, 10 and 20 mM DCA for 6 days, with conditioned media processed as per the Materials and Methods section. Immunoblot analysis of conditioned medium was carried out with anti-E-cadherin antibody. The results from the immunoblot were quantified by densitometric analysis **(A)**. Data was also adjusted for cell number determined by trypan blue assay **(B)**. Values are means ± S.D. (n=3). Unless indicated otherwise, results were not significantly different; * P≤ 0.05 & ** P≤ 0.01.

6.2 HEK Jagged1 Cells

6.2.1 Introduction

The cell lines previously treated with DCA were all cancerous in origin. It is known that DCA has anti-neoplastic capabilities, so in order to compare changes specific to cancer cells, a somatic immortalized cell line was treated with DCA – Human Embryonic Kidney cells (HEK) overexpressing Jagged1. Data from immunoblot analysis of SW480 cells indicated that DCA exerted effects on Jagged1 and E-cadherin as well as APP, and HEK Jagged1 cells have previously been used for studying Jagged1 and E-cadherin pathway interactions (Delury *et al*., 2013). The same cohort of experiments was repeated on HEK Jagged1 cells; morphological analysis, cell proliferation & metabolism assays and protein analysis.

6.2.2 DCA-induced morphological changes in HEK Jagged1 cells

HEK Jagged1 cells were seeded in growth medium containing 0, 10 or 20 mM DCA and examined under a light microscope after 3 and 6 days growth. The results (Fig. 6.2.1) showed an increase in the number of neurite-like extensions was at 10 mM (Fig. 6.2.1D) and at 20 mM DCA (Fig 6.2.1F) at both 3 and 6 day time points. HEK 293 cells have an elongated epithelial morphology, but doubts have been raised as to what cell type they derive from with evidence supporting a more neuronal phenotype than previously thought (Shaw *et al*., 2002). It is worth noting that as HEK Jagged1 cells approached confluence, they grew more elongated as seen in the untreated cells (Fig. 6.2.1B). This elongation can be difficult to distinguish from changes in APP and neurite-like outgrowth, however several pronounced neurite-like extensions can be seen at the 20 mM level as indicated by the arrows.

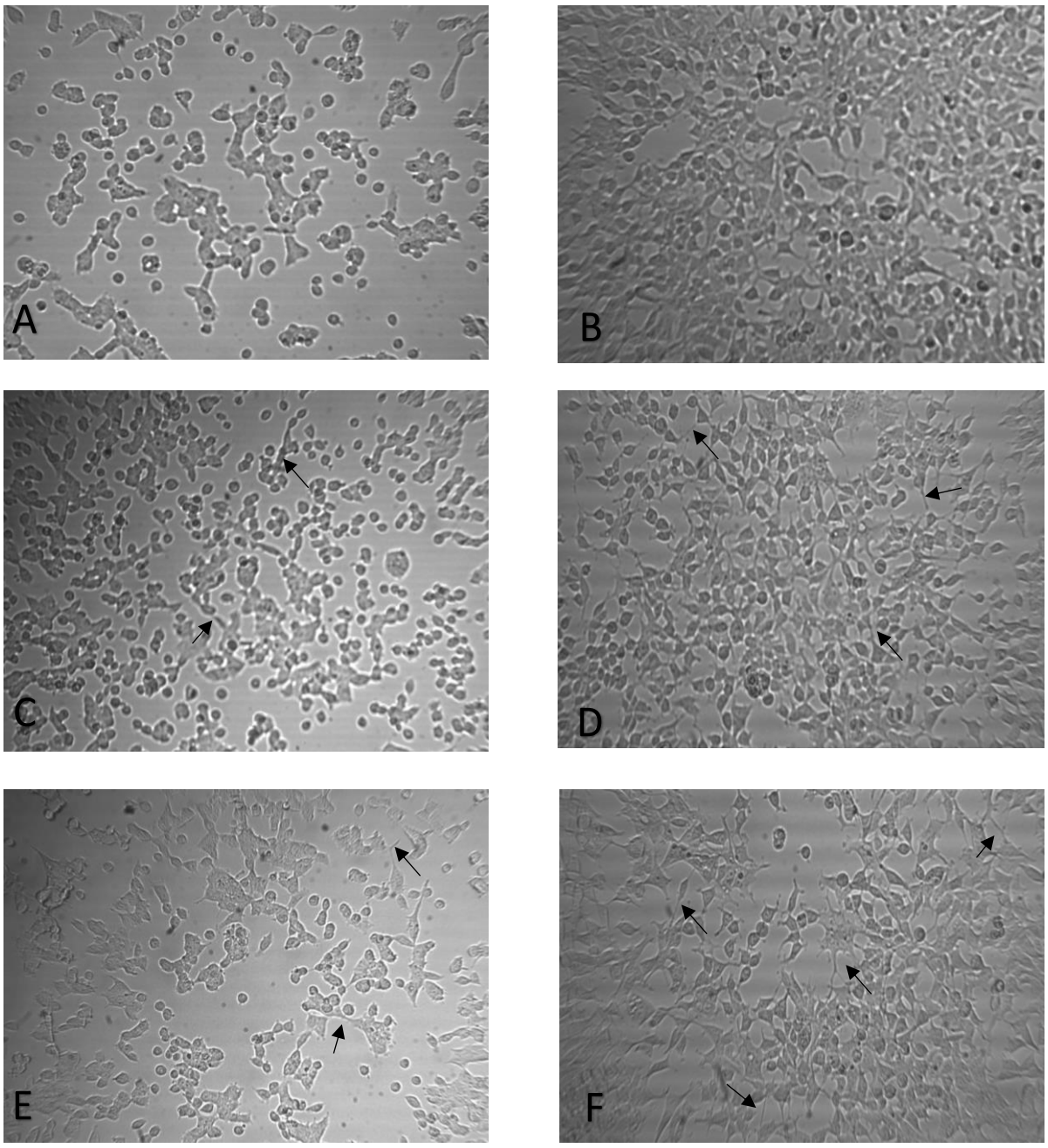

Figure 6.2.1 Morphology of DCA-treated HEK Jagged1 cells. HEK Jagged1 cells were treated with 0 **(A&B),** 10 mM **(C&D)** and 20 mM **(E&F)** DCA for a total period of 6 days. Cells were imaged after 3 days **(A, C, E)** or 6 days **(B, D, F)**. Images were captured at 10X objective in the absence of stains. Arrows indicate neurite-like extensions.

6.2.3 The effect of DCA on HEK Jagged1 cell proliferation

HEK Jagged1 cells are a non-cancerous cell line whereas the previous cell lines used have been cancerous in origin. When capturing images of DCA-treated cells in Fig. 6.2.1, it was evident that there was still a decrease in cell number in DCA treated flasks at the end of the treatment. A trypan blue assay was conducted and the results (Fig. 6.2.2) showed a decrease in viable cell count at both the 10 and 20 mM levels. There were few dead cells present during trypan blue analysis as per previous trypan blue assays for other cell lines.

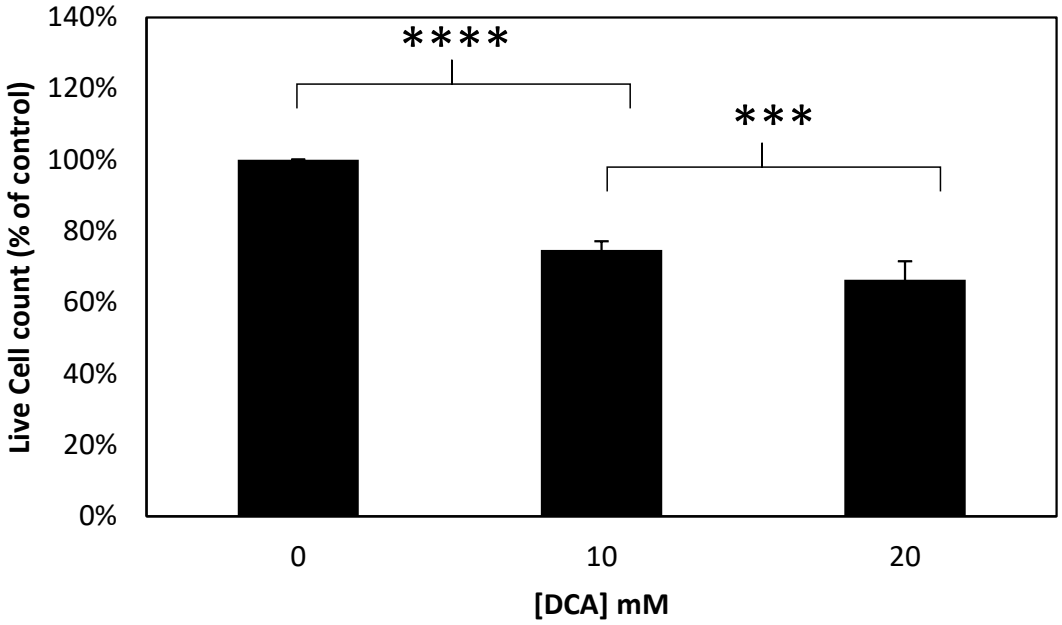

Figure 6.2.2. DCA decreases HEK Jagged1 cell proliferation. HEK Jagged1 cells were treated with 0, 10 and 20 mM DCA for 6 days (see Materials and Methods) and then trypsinised and counted via trypan blue exclusion assay. Counts reflect live cells. Results are means ± S.D. (n=3). Unless indicated otherwise, results were not significantly different; *** P≤ 0.001 & **** P≤ 0.0001.

6.2.4 The effect of DCA on HEK Jagged1 cell metabolism

The metabolic activity of DCA-treated HEK Jagged1 cells was investigated by means of a MTS assay. The results (Fig. 6.2.3) showed an increase in metabolic activity at both 10 and 20 mM DCA. As with the other metabolic activity assay results, the increase at 20 mM was less than the increase at 10 mM, thought to be due to the decreased cell number at 20 mM (see Fig. 6.2.2)

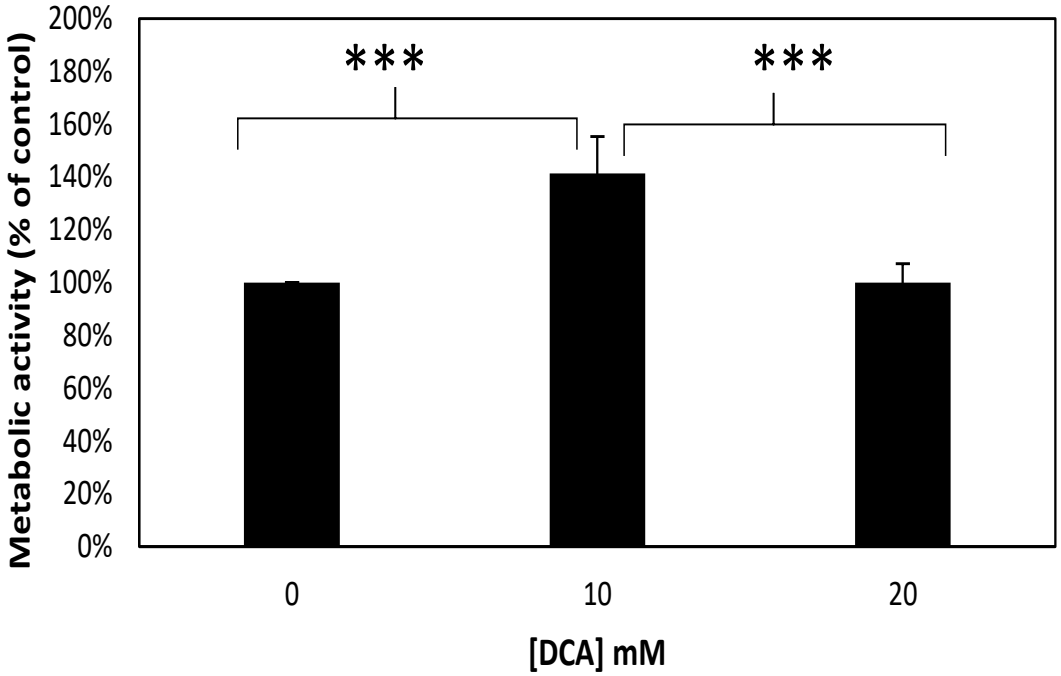

Figure 6.2.3. DCA increases the metabolic activity of HEK Jagged1 cells. HEK Jagged1 cells were treated with 0, 10 and 20 mM DCA for 7 days (see Materials and Methods) and then subjected to a MTS assay (see Materials and Methods). Results are means ± S.D. (n=6). Unless indicated otherwise, results were not significantly different; *** P≤ 0.001.

6.2.5 DCA alters expression of APP in HEK Jagged1 cells

HEK cells have sufficient APP present to be detected via immunoblot analysis and so lysates from DCA-treated HEK Jagged1 cells were prepared as per the Materials and Methods and immunoblotted using anti-APP C-terminal antibody. Both APP holoprotein and APP CTF were detected and the results (Fig. 6.2.4) showed an increase in APP holoprotein and CTF in response to DCA.

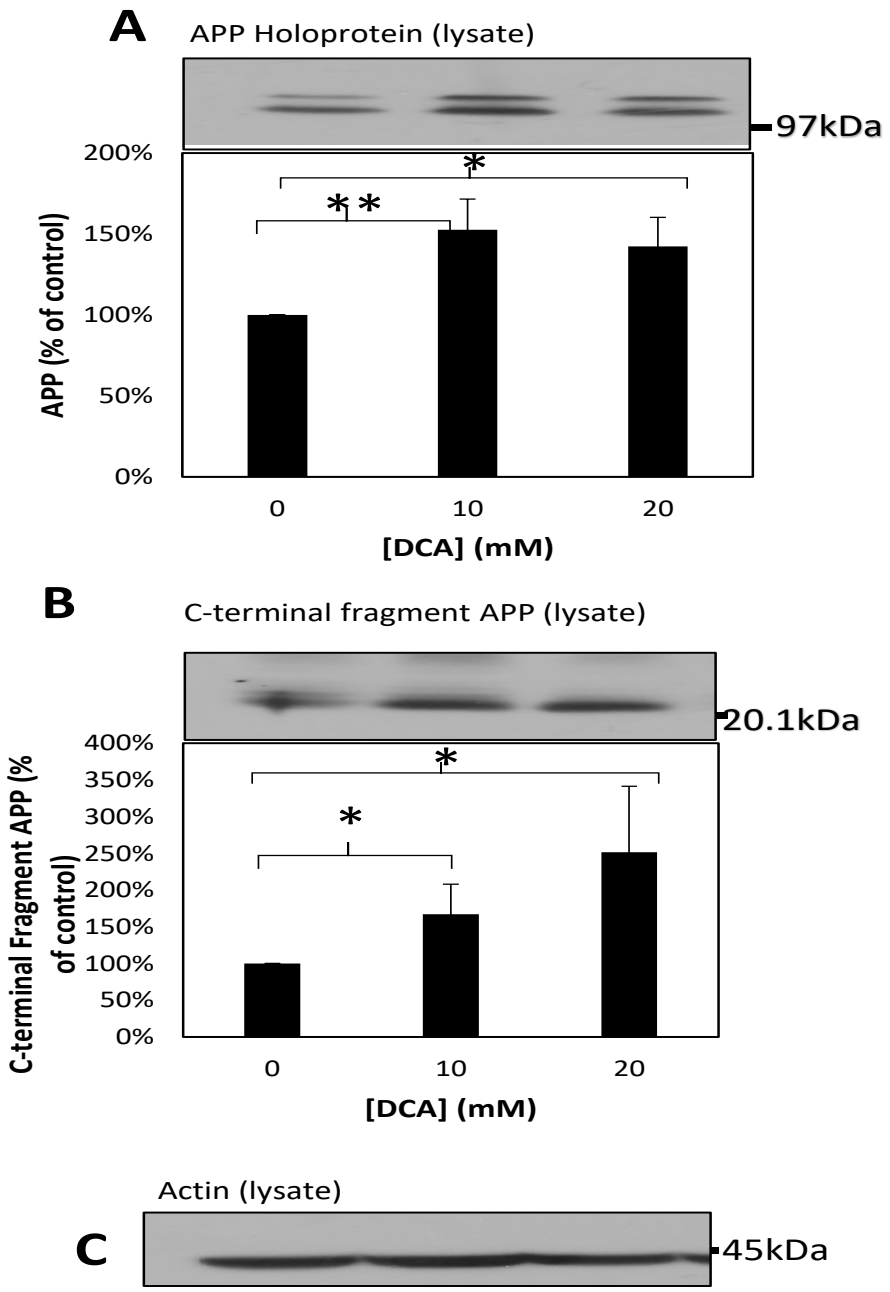

Figure 6.2.4. DCA alters expression of APP in HEK Jagged1 cells. HEK Jagged1 cells were treated with 0, 10 and 20 mM DCA for 6 days, with lysates prepared as per the Materials and Methods section. Immunoblot analysis of equal amounts of lysate proteins was carried out with anti-APP C-terminal **(A)** and anti-actin **(B)** antibodies. The results from the Jagged1 blot were quantified by densitometric analysis. Values are means ± S.D. (n=3). Unless indicated otherwise, results were not significantly different; * P≤ 0.05 and ** P≤0.01.

6.2.6 The effect of DCA on APP Proteolysis in HEK Jagged1 cells

To investigate any changes to APP proteolysis following DCA treatment, conditioned media from DCA-treated HEK Jagged1 cells was immunoblotted for sAPPα and sAPPβ. A single

band was detected, corresponding to all three APP isoforms. The results from the sAPPα immunoblot showed an increase with 10 mM DCA and a slight decrease with 20 mM DCA, relative to the control (Fig. 6.2.5A). When adjusting for cell number, the resultant data showed (Fig. 6.2.5B) enhanced sAPPα shedding from both 10 and 20-mM treated cells; sAPPα levels increased by 82% at 10 mM and 43% at 20 mM DCA, relative to the control.

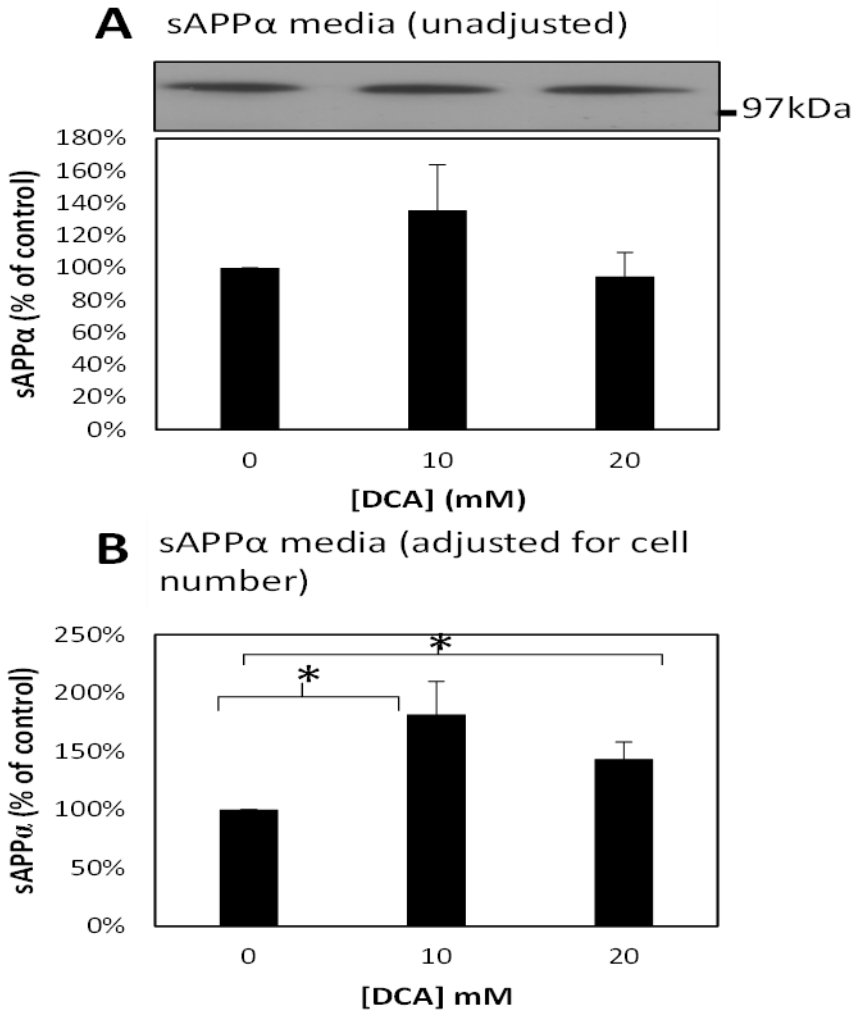

Figure 6.2.5. DCA increases sAPPα shedding from HEK Jagged1 cells. HEK Jagged1 cells were treated with 0, 10 and 20 mM DCA for 6 days, with conditioned media processed as per the Materials and Methods section. Immunoblot analysis of conditioned medium was carried out with anti-sAPPα antibody 6E10. The results from the immunoblot were quantified by densitometric analysis **(A)**. Data was also adjusted for cell number determined by trypan blue assay **(B)**. Values are means ± S.D. (n=3). Unless indicated otherwise, results were not significantly different; * P≤ 0.05.

Conditioned media was also immunoblot using anti-sAPPβ antibody. The results from the sAPPβ immunoblot showed no detectable sAPPβ in any of the samples (Fig. 6.2.6).

Figure 6.2.6 sAPPβ is undetectable in HEK Jagged1 cells. HEK Jagged1 cells were treated with 0, 10 and 20 mM DCA for 6 days, with conditioned media processed as per the Materials and Methods section. Immunoblot analysis of conditioned medium and a positive control was carried out with anti-sAPPβ antibody. No sAPPβ was detectable in the conditioned media.

6.2.7 The effect of DCA on p53 expression in HEK Jagged1 cells

Lysates produced from DCA-treated HEK Jagged1 cells were immunoblotted with anti-p53 antibody (see Materials and Methods). The results (Fig. 6.2.7) showed an increase in p53 levels, with a 16% increase at 10 mM DCA and a 52% increase at 20 mM DCA. This data confirms the trend seen in the other cell lines treated with DCA; p53 levels increase following DCA treatment. This also demonstrates the process occurs in non-cancerous cells as well as cancerous cells.

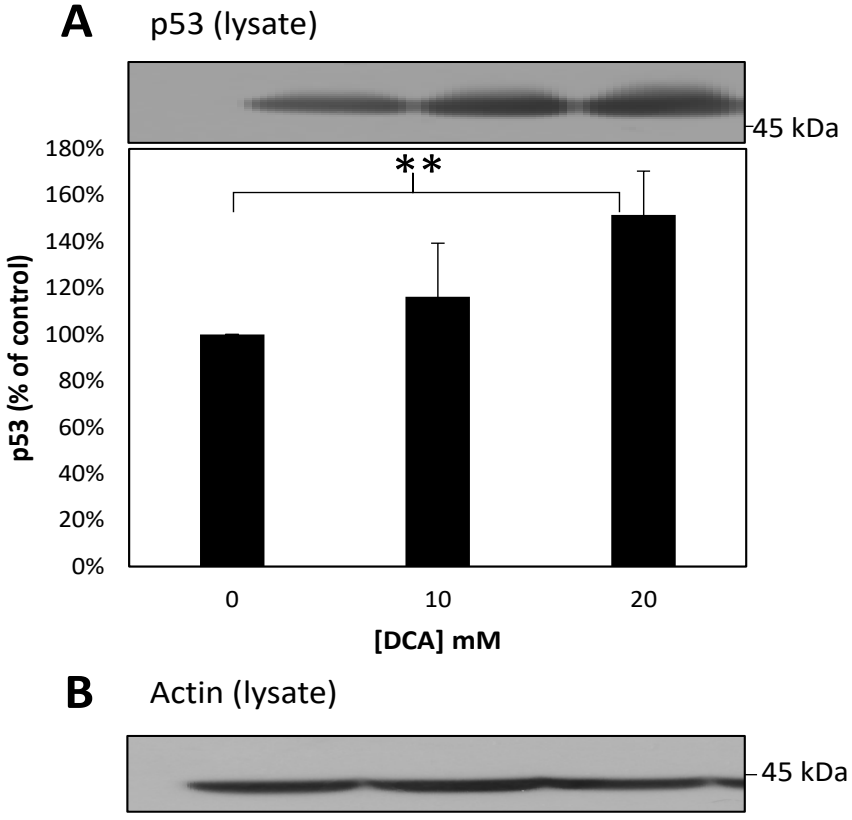

Figure 6.2.7. DCA increases expression of p53 in HEK Jagged1 cells. HEK Jagged1 cells were treated with 0, 10 and 20 mM DCA for 6 days, with lysates prepared as per the Materials and Methods section. Immunoblot analysis of equal amounts of lysate proteins was carried out with anti-p53 **(A)** and anti-actin **(B)** antibodies. The results from the p53 blot were quantified by densitometric analysis. Values are means ± S.D. (n=3). Unless indicated otherwise, results were not significantly different; ** P≤ 0.01.

6.2.8 The effect of DCA on Jagged1 Expression in HEK Jagged1 cells

To look at the effect of DCA when there is an abundance of Jagged1, HEK Jagged1 cells were treated with DCA and lysates produced as per the Materials and Methods. Lysates were immunoblotted with anti-Jagged1 C-terminal antibody. The results (Fig. 6.2.8A) showed an increase in Jagged1 holoprotein levels in response to DCA treatment, although this was not significant. Jagged1 CTF levels increased (Fig. 6.2.8B) in response to DCA, with a 219% increase at 10 mM DCA and a 323% increase at 20 mM DCA relative to the control. The increase in CTF is indicative of increased Jagged1 shedding.

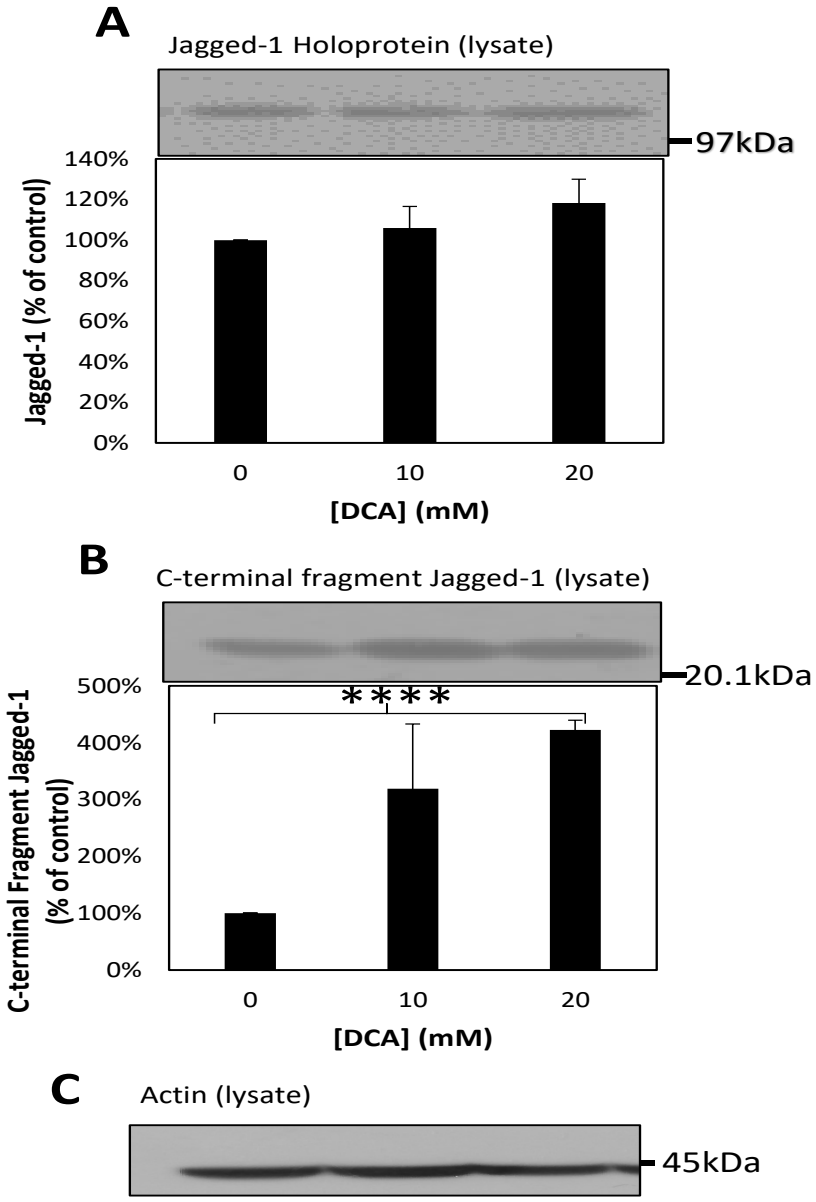

Figure 6.2.8. Overexpressed Jagged1 levels are unaffected by DCA in HEK Jagged1 cells. HEK Jagged1 cells were treated with 0, 10 and 20 mM DCA for 6 days, with lysates prepared as per the Materials and Methods section. Immunoblot analysis of equal amounts of lysate proteins was carried out with anti-Jagged1 C-terminal **(A)** and anti-actin **(B)** antibodies. The results from the APP blot were quantified by densitometric analysis. Values are means ± S.D. (n=3). Unless indicated otherwise, results were not significantly different; **** P≤ 0.0001.

6.2.9 The effect of DCA on Jagged1 proteolysis in HEK Jagged1 cells

Jagged1 proteolysis was investigated alongside changes to Jagged1 expression. In order to determine whether DCA affected Jagged1 proteolysis, conditioned media was immunoblotted for the N-terminal fragment of Jagged1. The results (Fig. 6.2.9A) showed decreased Jagged1 shedding in response to DCA treatment. When adjusted for cell number (see Fig. 6.2.2), there was no significant change in Jagged1 shedding (Fig. 6.1.9B).

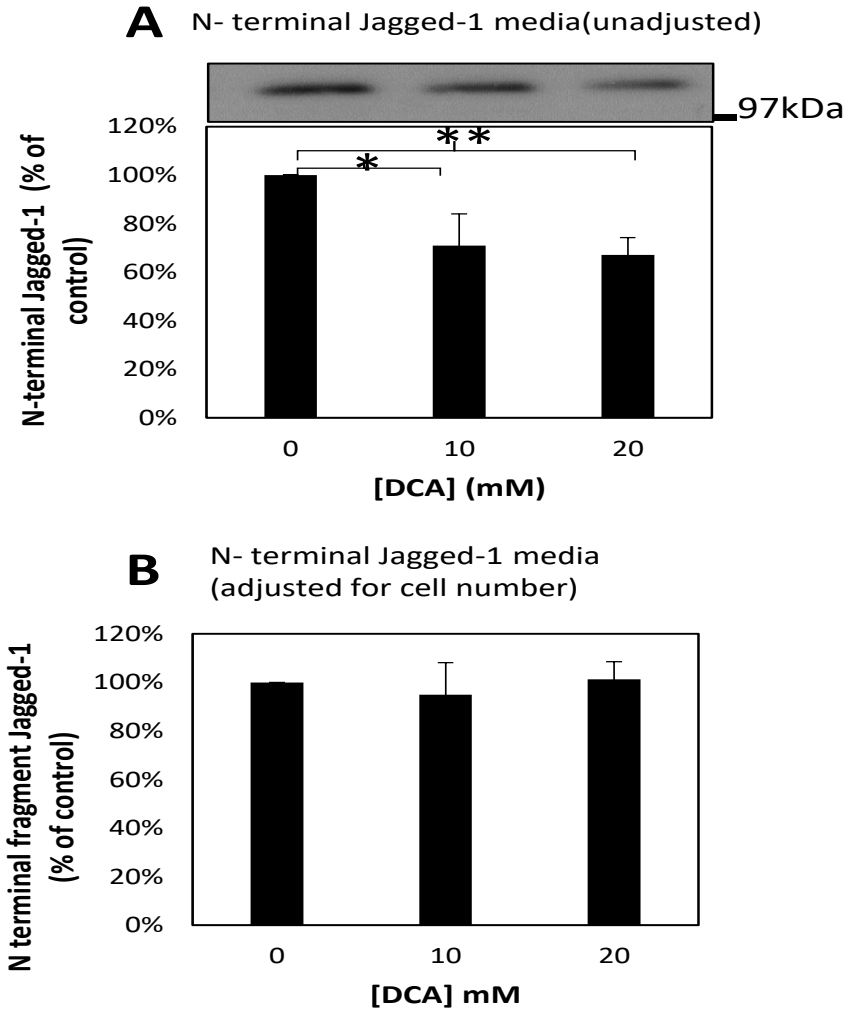

Figure 6.2.9. Jagged1 ectodomain shedding from HEK Jagged1 cells is unaltered by DCA. HEK Jagged1 cells were treated with 0, 10 and 20 mM DCA for 6 days, with conditioned media processed as per the Materials and Methods section. Immunoblot analysis of conditioned medium was carried out with anti-Jagged1 N-terminal antibody. The results from the immunoblot were quantified by densitometric analysis **(A)**. Data was also adjusted for cell number determined by trypan blue assay **(B)**. Values are means ± S.D. (n=3). Unless indicated otherwise, results were not significantly different; * P≤ 0.05 & ** P≤ 0.01.

6.2.10 The effect of DCA on E-cadherin expression in HEK Jagged1 cells

To examine changes to E-cadherin expression, cell lysates from DCA-treated HEK Jagged 1 cells were immunoblot with anti-E-cadherin antibody. The results (Fig. 6.2.10) show

that, in response to DCA, E-cadherin expression decreased. With 10 mM DCA, E-cadherin expression decreased by 13%, and decreased by 27% with 20 mM DCA. This is in contrast to the other two ADAM substrates, APP and Jagged1 as APP expression increased whilst there was no change in Jagged1 expression in response to DCA.

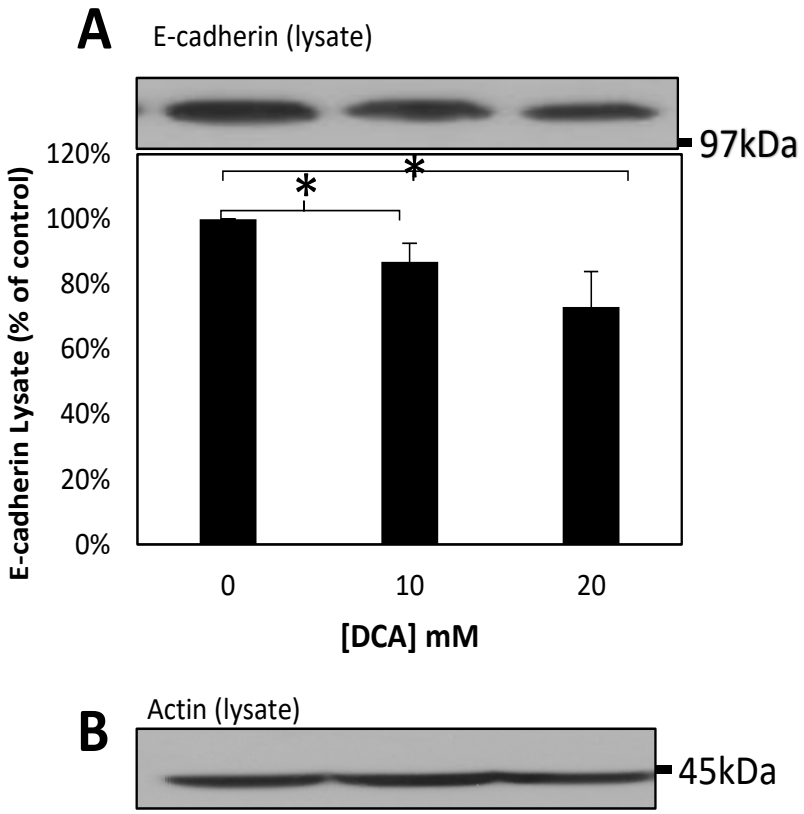

Figure 6.2.10. DCA decreases expression of E-cadherin in HEK Jagged1 cells. HEK Jagged1 cells were treated with 0, 10 and 20 mM DCA for 6 days, with lysates prepared as per the Materials and Methods section. Immunoblot analysis of equal amounts of lysate proteins was carried out with anti-E-cadherin **(A)** and anti-actin **(B)** antibodies. The results from the E-cadherin blot were quantified by densitometric analysis. Values are means ± S.D. (n=3). Unless indicated otherwise, results were not significantly different; * P≤ 0.05.

6.2.11 The effect of DCA on E-cadherin proteolysis in HEK Jagged1 Cells

To determine whether E-cadherin proteolysis was affected by DCA, conditioned media from DCA-treated HEK Jagged1 cells was subjected to immunoblot analysis for soluble E-cadherin. The results (Fig. 6.2.11A) showed a decrease in E-cadherin shedding from HEK Jagged1 cells. When adjusting for cell number determined by trypan blue assay (see Fig. 6.1.2), a 18% decrease was seen with 10 mM DCA and a 53% decrease with 20 mM DCA, compared to the control (Fig. 6.2.11B). The increase at 20 mM was not significant when compared to the

control. These results illustrate that E-cadherin shedding is decreased in DCA-treated HEK Jagged1 cells.

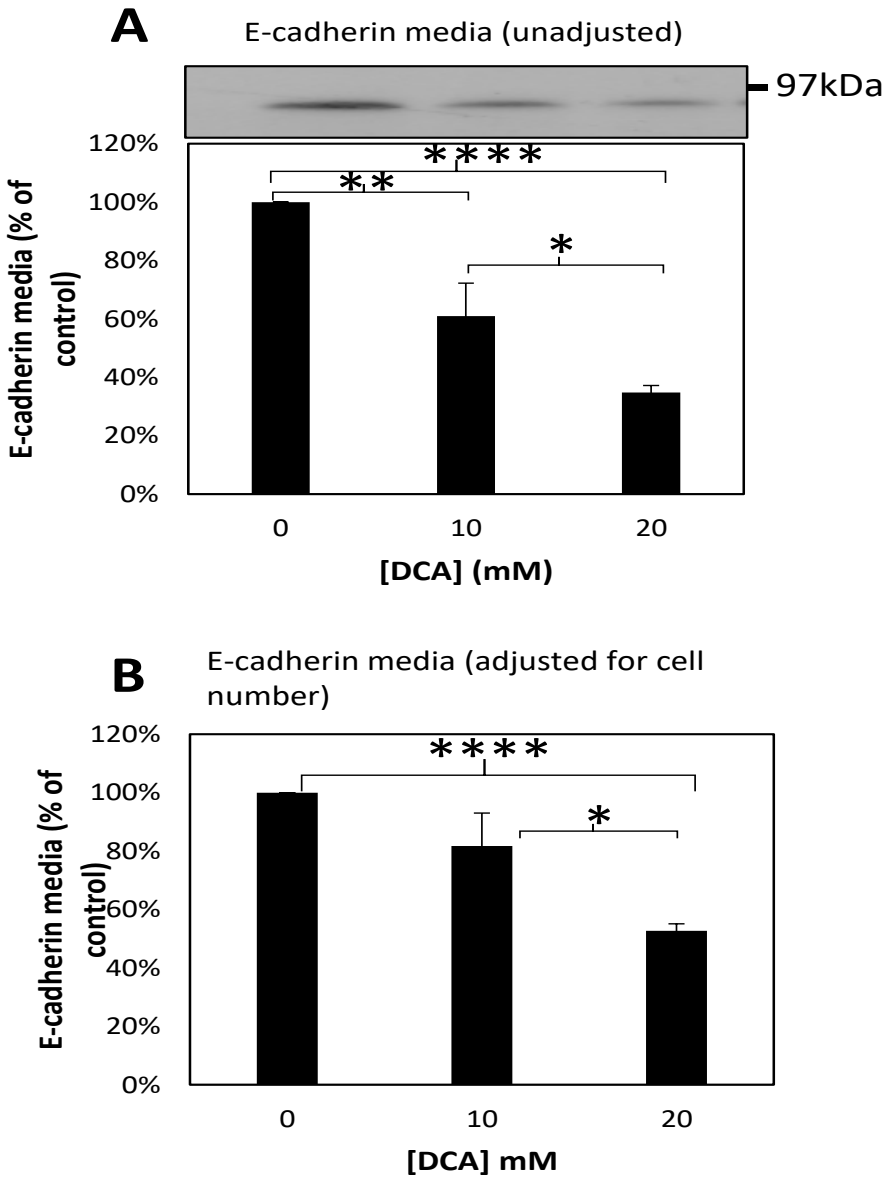

Figure 6.2.11. DCA decreases E-cadherin shedding from HEK Jagged1 cells. HEK Jagged1 cells were treated with 0, 10 and 20 mM DCA for 6 days, with conditioned media processed as per the Materials and Methods section. Immunoblot analysis of conditioned medium was carried out with anti-E-cadherin antibody. The results from the immunoblot were quantified by densitometric analysis **(A)**. Data was also adjusted for cell number determined by trypan blue assay **(B)**. Values are means ± S.D. (n=3). Unless indicated otherwise, results were not significantly different; * P≤ 0.05, ** P≤ 0.01 & **** P≤ 0.0001.

6.3 Summary

The experiments with the three SH-SY5Y cell lines indicated that DCA alters APP proteolysis in favour of alpha shedding over beta shedding. As ADAM enzymes (specifically

ADAM10) are responsible for alpha shedding, it was hypothesized that alpha shedding increased due to stimulation of the alpha pathway by increased ADAM expression/activity. SW480 and HEK Jagged1 cells were used to model the effects of DCA on other ADAM substrates – E-cadherin and Jagged1. The cell viability and metabolism results showed similar trends to those observed in the SH-SY5Y cells, but with a greater impact on SW480 cell proliferation and a lesser impact on HEK Jagged1 cell proliferation. Protein analysis indicated that APP levels increased in response to DCA treatment in both cell lines and a concurrent increase in the CTF and sAPPα levels was also seen. It was not possible to detect sAPPβ in any of the media samples tested for either cell line. As with the SH-SY5Y cell lines, p53 levels increased. E-cadherin expression decreased in both SW480 and HEK Jagged1 cells, accompanied by a decrease in E-cadherin shedding from HEK Jagged1 cells but not SW480 cells. Endogenous Jagged1 expression increased slightly in SW480 cells along with an increase in Jagged1 CTF and Jagged1 shedding. Interestingly, in HEK Jagged1 cells, Jagged1 and NT Jagged levels were unaltered by DCA treatment but there was an increase in Jagged1 CTF.

Chapter 7: Discussion

7.1 Introduction

Previous experiments with PC3 cells and SW480 cells indicated that dichloroacetate (DCA) affects APP and stimulates neurite-like growth, thought to be due to an increase in α-secretase activity (Parkin, unpublished data). The results here show that DCA alters proteolysis of APP in SH-SY5Y cells, shifting proteolysis towards the non-amyloidogenic pathway with reciprocal impairment of the amyloidogenic pathway. DCA also had a morphoregulatory impact on cells, altered metabolism and slowed cell proliferation. The effect of DCA on APP was not common to all ADAM substrates as different shedding and expression of Jagged1 and E-cadherin was seen in SW480 and HEK Jagged1 cells.

7.2 DCA stimulates neurite-like outgrowth

Morphological analysis of all the cell lines treated with DCA including the non-neuronal cell lines SW480 and HEK Jagged1, demonstrated an increase in neurite-like extensions. The number of extensions increased with higher doses and after a longer exposure to DCA. Neurite-like extensions were also observed after 24 hours in 24-hour DCA treated confluent SH-SY5Y cells (Fig. 3.2.1), indicating these changes happen within 24 hours of DCA treatment. This suggests DCA has a morphoregulatory influence on cells, possible by impacting on APP. These data reflect the morphological changes seen by our research group in PC3 and SW480 cells (Parkin, unpublished data). The two major proteins involved in the development of neurite growth are APP and its metabolite sAPPα. Neurite outgrowth is inhibited when APP is downregulated (Allinquant *et al*., 1995), and sAPPα produced from APP cleavage controls neurite outgrowth in association with integrin beta-1, which is dependent on the presence of APP holoprotein (Young-Pearse *et al*., 2008). It was suggested that sAPPα is responsible for the development of neurite-like extensions following DCA treatment, and immunoblot analysis of conditioned media indicated that across all the cell lines a significant increase in sAPPα levels was observed. The results here are similar to experiments with differentiated neural precursor cells, where treatment with exogenous sAPPα induced neurite elongation (Gakhar-Koppole *et al*., 2008). Furthermore, sAPPα is known to regulate neuritic outgrowth in neuroblastoma cells (Arcangeli *et al*., 1993, Mattson, 1994). Together these data demonstrate DCA induces neurite-like outgrowth in cells via increased sAPPα shedding.

The increase in neurite-like extensions may also have occurred due to increased p53 expression in response to DCA. DCA treatment increases p53 levels (Allende-Vega *et al*., 2015), and immunoblot analysis of p53 levels across the cell lines used here also reflect an increase

in p53 expression in response to DCA. p53 induces neurite outgrowth by acting as a transcription factor for Coronin 1b and Rab13, two proteins involved in neurite outgrowth (Di Giovanni *et al*., 2006). The importance of p53 in this process is demonstrated by siRNA targeting of p53 which inhibits neurite production. Therefore, increased sAPPα and increased p53 levels could work synergistically to increase neurite-like outgrowth. However, a limitation of this study is that the extensions are assumed to represent neurite outgrowth. Immunofluorescence staining for neuronal markers (Kim and Lee, 2012) like Growth Associated Protein 43 (GAP-43), a key protein involved in neuritogenesis (Aarts *et al*., 1998) would confirm whether or not the extensions are neurite outgrowths.

7.3 DCA decreases cell proliferation without inducing apoptosis

DCA inhibits cell proliferation and induces apoptosis in a range of cancer cell lines whilst sparing somatic cells (Madhok *et al*., 2010). Data from the trypan blue assays for the three SH-SY5Y cell lines confirm a reduction in cell proliferation following DCA treatment (Figs. 3.1.2, 4.2 & 5.2). Visual observations during DCA treatment showed few cells in suspension, suggesting that the difference in cell number was not due to apoptosis. This is in contrast to other experiments conducted with SH-SY5Y cells and DCA where 5 mM DCA induced apoptosis (Pajuelo-Reguera *et al*., 2015). However, they did not quantify this and assumptions were made on the basis of cells being present in suspension. SH-SY5Y cells are known to grow as a mixture of suspended and adherent cells under certain culture conditions which could explain the presence of cells in suspension (Biedler *et al*., 1978). Additionally, experiments with human colorectal cancer cells showed little to no apoptosis with DCA treatment (Lin *et al*., 2014). DCA is known to alter metabolism and inhibit growth rate as well as induce apoptosis, so DCA exhibited a growth inhibitory effect rather than a cytotoxic effect in these experiments.

To confirm DCA does not induce apoptosis in SH-SY5Y cells, flow cytometry analysis of apoptosis-specific markers like annexin-V could be employed (Koopman *et al*., 1994). This could also be used to determine the proportions of cells going through specific stages of the cell cycle as DCA increases the proportion of cells in G1 phase (Agnoletto *et al*., 2014). DCA exerts this growth inhibitory effect by inducing phosphorylation of AMP kinase (AMPK) which then increases p53 levels and p53 arrests the cell cycle through its transcription factor role (Allende-Vega *et al*., 2015). Levels of p53 were elevated following DCA treatment in each of the cell lines treated with DCA.

Further evidence that DCA is growth-inhibitory as opposed to cytotoxic is that following 24-hour treatment with DCA of confluent SH-SY5Y cells, no significant change in viable cell

count was seen (Fig. 3.1.2). Confluent SH-SY5Y cells are undergoing less proliferation than sub-confluent cells, as SH-SY5Y cells do exhibit some contact-inhibition. No significant change in live cell count was observed after 24H DCA treatment of confluent SH-SY5Y cells, confirming DCA is growth-inhibitory rather than cytotoxic. However, there was a considerable time-difference in exposure to DCA (6 days compared to 24 hours) so further cell proliferation and viability assays that examine the effects of DCA over a range of time points is necessary to confirm this.

SW480 cells were more susceptible to inhibition of cell proliferation (Fig. 6.1.2) than the SH-SY5Y cell lines. This is similar to another study which showed that different cancer cell lines have varying susceptibilities to DCA treatment; in response to DCA HTC116 and LS174T colorectal cancer cell lines showed no significant increase in apoptosis, whilst apoptosis in SW480 cells increased 6-fold relative to the control (Shahrzad *et al*., 2010). Other experiments with colorectal cancer cells and DCA suggest that the impact of DCA on apoptosis and cell growth is correlated to how metastatic the cell line is (Madhok *et al*., 2010), which could explain why SW480 cells are more susceptible to DCA treatment.

Cell proliferation was halted in the HEK-Jagged 1 cells used here (Fig. 6.2.2). This is in contrast to experiments with DCA and untransfected HEK cells were 20 mM DCA did not alter growth (Madhok *et al*., 2010). HEK cells and HEK-Jagged1 cells are not identical so the small decrease in cell proliferation may be due to an effect of Jagged1 overexpression. However, as Jagged1 is a ligand for Notch, a key protein involved in cell growth and proliferation, an increase in cell proliferation would be expected which suggests that the action of DCA on cell proliferation may have an impact on notch signalling (Capaccione and Pine, 2013). Together, these findings demonstrate that DCA inhibits cell proliferation but is not cytotoxic, therefore if it was to be used as a treatment for AD it may not affect neuronal viability as the majority of neurons are terminally differentiated.

7.4 Metabolic activity increases in response to DCA

DCA increases oxidative phosphorylation in cells by inactivating pyruvate dehydrogenase kinases (PDKs) (Stacpoole, 1989). The metabolic activity of DCA-treated cell lines increased, with the exception of the 24-hour treatment of SH-SY5Y cells. The data was not adjusted for reduced cell proliferation, so when taking into account the reduced cell numbers seen with DCA treatment, there is an even greater increase in metabolic activity. Although the trend was the same across the different cell lines, the relative magnitude of the increases varied. A possible reason for this is that DCA has different affinity for the four

different PDK isoenzymes, and the distribution of these isoenzymes varies in tissues (Bonnet *et al*., 2007) and could therefore account for the differing levels of metabolic activity between cell lines. Numerous studies have shown that DCA increases metabolic activity (through up-regulation of p53) in cancer cell lines including leukaemia cell lines (Allende-Vega *et al*., 2015) as well as *in vivo* in glioblastoma patients (Michelakis *et al*., 2010) confirming the changes seen here. Changes to mitochondrial function and glucose metabolism are observed in AD, sometimes years prior to clinical presentation of the disease (Stacpoole, 2012), if DCA was used at this stage to increase mitochondrial activity and glucose metabolism, then it may prevent impaired neuronal functioning. However, it is worth noting that resistance to Aβ can be induced by reversion to glycolysis in a small subset of cells, so increasing oxidative phosphorylation in these cells may make them more sensitive to Aβ (Newington *et al*., 2011).

7.5 DCA and APP expression

From the morphological observations, it was hypothesized that DCA increases APP expression (thereby increasing sAPPα) to induce neurite-like outgrowth or alters the proteolysis of APP in favour of sAPPα. No investigation into a direct link between DCA and APP expression or proteolysis has been published (according to a thorough search of literature). Endogenous APP in SH-SY5Y cells and SH-SY5Y BACE1 cells was essentially unchanged following DCA treatment. In contrast, endogenous APP expression in HEK Jagged1 and SW480 cells increased suggesting the mechanism by which DCA increases APP expression is cell-specific. This is of particular interest as overexpression of APP can lead to development of cancer (Takayama *et al*., 2009) and has also been associated with memory impairment in mice (Simon *et al*., 2009). APP regulates gene expression via the APP intracellular domain (AICD) and microarray analysis of HEK cells overexpressing human APP suggests APP significantly alters the expression of 2304 genes (Wu *et al*., 2016). Due to the large number of interactions of APP with other genes and the lack of literature on DCA and APP there are numerous factors that may alter APP expression following DCA treatment. However, it is of note that p53 decreases APP gene expression by preventing binding of SP1 to the APP promoter (Cuesta *et al*., 2009) and p53 levels are elevated in response to DCA treatment. It is surprising that APP levels are not decreased in response to DCA given that p53 levels increase. As APP inhibits p53 activation at the post-translational level (Xu *et al*., 1999), it is possible that a feedback loop exists between the two, altering APP and p53 levels accordingly.

APP expression is increased in AD patients and APP has been proposed as a cell surface receptor for Aβ, resulting in stress-induced apoptosis (Deyts *et al*., 2016). APP overexpressing SH-SY5Y cells were used to model the elevated APP levels in AD brains. In DCA-treated SH-SY5Y APP_{695} cells, APP expression increased, as did the levels of the CTF fragment of APP, an indication of increased proteolysis (Nunan *et al*., 2001). This is in contrast to endogenous APP where APP expression was not altered much by DCA treatment (Figs. 3.1.4, 3.2.4 & 5.4). The increase in APP expression in response to DCA may be an artefactual response of the cytomegalovirus (CMV) promoter sequence which is the promoter used in these cells to overexpress APP_{695}. The CMV promoter is inhibited by p53 and stimulated by c-jun so it is possible that DCA increases c-jun thereby increasing APP expression in response to DCA (Rodova *et al*., 2013). High doses of DCA can induce the tumorigenesis in rats and the majority of the tumours are c-jun positive suggesting DCA may increase c-jun levels (Stauber *et al*., 1998). The increased neurite-like outgrowth may also be an indicator of increased c-jun expression as c-jun phosphorylated at serine 73 (in PC12 cells) induces neurite-like outgrowth (Dragunow *et al*., 2000). The BACE1 overexpressing cells also contain the CMV promoter and levels of BACE1 increased in response to DCA in the SH-SY5Y BACE1 cells, again suggesting artefactual stimulation of the CMV promoter induced by DCA treatment. Another reason for increased APP expression following DCA treatment is that transfected APP_{695} is known to self-regulate its expression (von Rotz *et al*., 2004) and this could be stimulated by DCA thus increasing APP expression.

The CTF of APP is released when APP is cleaved by either an alpha or beta secretase and so increased CTF is indicative of increased proteolysis and/or increased APP holoprotein expression. As APP expression increased in the SH-SY5Y APP_{695} cells it was not possible to determine whether the CTF production reflected increased APP expression or increased proteolysis.

7.6 DCA shifts APP proteolysis towards non-amyloidogenic processing

Endogenous levels of APP in SH-SY5Y cells were essentially unaltered by DCA treatment, suggesting that if sAPPα is the cause for the neurite-like extensions then it must be due to alteration in APP proteolysis. DCA increased sAPPα (695 and 751/770) shedding from untransfected SH-SY5Y cells (Fig. 3.1.5) and decreased sAPPβ levels (Fig. 3.1.6). The change in APP proteolysis may be due to stimulation the non-amyloidogenic pathway, inhibition of the amyloidogenic pathway or a combination of the two. As no previous work with APP and DCA

has been published, the mechanism by which DCA alters APP proteolysis is unknown. It was suggested that increased ADAM10 levels would indicate stimulation of the alpha secretase pathway and explain the increased levels of sAPPα seen following DCA treatment, as ADAM10 is responsible for alpha cleavage of APP (Deuss *et al*., 2008). The results here mirrored those seen in ADAM10 overexpressing cells and mice models which show increased sAPPα levels and decreased BACE1 proteolysis (Haass *et al*., 2012, Postina *et al*., 2004), indicating that increased ADAM10 expression may be the mechanism by which DCA alters APP proteolysis. Immunoblot analysis of cell lysates were inconclusive for ADAM10, ADAM17 and presenilin-1 due to poor specificity of the antibodies, but there was an indication of increased ADAM10 levels (Fig. 3.1.8A). The use of alternative antibodies that show higher specificity would allow for investigation into the relative expression of these proteins in response to DCA treatment and confirm whether DCA up-regulates ADAM10.

It is also possible that the decrease in sAPPβ and increase in sAPPα is due to reduction of BACE1 expression/activity induced by DCA. BACE1 expression is influenced by the APP intracellular domain (AICD) (Kimberly *et al*., 2001), so DCA may modulate the specific AICD isoform generated and repress BACE1 expression via AICD. However, the majority of APP is usually subject to alpha cleavage (Koo and Squazzo, 1994), so inhibition of all BACE1 activity would not account for the significant increases in alpha shedding given that APP holoprotein levels are essentially unchanged. Furthermore, there was still some $sAPP\beta_{751/770}$ produced indicating that not all BACE1 activity is abolished by DCA. This suggests an alternative mechanism such as increased ADAM expression is responsible for increased alpha shedding.

It is worth noting that APP proteolysis was altered in the 24 h DCA-treated confluent SH-SY5Y cells, suggesting that DCA alters processing within 24 hours and is not limited to proliferating cells. The levels of sAPPβ were not completely ablated after 24 hour DCA treatment, suggesting that it is a gradual process.

The shift in proteolysis is of particular significance as stimulation of the alpha pathway may result in reduced production of toxic Aβ peptides, the major culprit in neurodegeneration seen in AD (Ittner and Gotz, 2011). Depletion of sAPPβ in theory should correspond to a decrease in Aβ production as BACE1 cleavage of APP must occur to produce C99 which is then subsequently cleaved to produced Aβ (Zacchetti *et al*., 2007). In contrast to the effects seen with alpha shedding, the decrease in beta shedding differentially affects the sAPPβ isoforms; $sAPP\beta_{751/770}$ levels decreased whilst a complete ablation of $sAPP\beta_{695}$ was seen (Fig 3.1.6). The ablation of $sAPP\beta_{695}$ is of most significance as APP_{695} is primarily expressed in neurons with

lower levels of APP_{751} and APP_{770} also expressed (Nalivaeva and Turner, 2013). APP_{695} differs from APP_{751} and APP70 by the absence of a Kunitz-type protease inhibitor (KPI) domain in 695 that is present in the other two isoforms. The KPI domain inhibits trypsin, plasmin and other serine proteases (Godfroid and Octave, 1990) but is also thought to be involved in APP dimerization and its role as a receptor (Ben Khalifa *et al*., 2012). It is possible that the KPI domain exerts limited protection against the mechanism by which DCA exerts reduced BACE1 cleavage, as KPI-containing APP isoforms are associated with decreased sAPPα and increased Aβ production (Ho *et al*., 1996). The salient point of these results is the overall decrease in sAPPβ production. The inhibition of BACE1 activity has been a therapeutic goal for AD treatment as BACE1 knockout mice show no detectable forms of Aβ in the brain (Sathya *et al*., 2012) and BACE1 deficiency stops the progression of memory less and neurodegeneration (Ohno *et al*., 2004). These data suggest that down-regulation of the amyloidogenic pathway would prevent Aβ production and therefore prevent disease progression. To confirm that Aβ levels are depleted following DCA treatment, an Aβ assay of the media from DCA-treated cells is necessary.

Increased sAPPα shedding was also observed from SW480 and HEK Jagged1 cells, demonstrating that increased alpha shedding is not specific to neuronal-like cells, however it was not possible to detect sAPPβ in these cells. As APP expression was altered in both cell lines, the increased sAPPα levels shed from these cells is not necessarily due to increased alpha cleavage and may just reflect the increased APP levels.

DCA shifts APP proteolysis towards non-amyloidogenic processing, implying a reduction in Aβ levels generated. Preventing Aβ generation as well as the neuroprotective and neurotrophic attributes of sAPPα suggest DCA is a novel therapeutic for AD and warrants further investigation.

7.7 Over-expression of APP and BACE1 alter the effects of DCA on APP proteolysis

7.7.1 APP_{695} overexpression saturates the alpha secretase pathway

It was hypothesized that if DCA increases alpha shedding, overexpression of APP would saturate the alpha pathway and counteract the effect of DCA on APP proteolysis. DCA increased sAPPα levels as expected from the APP expression data, but also increased levels of $sAPP\beta_{695}$ showing that overexpression of APP negates the effect of DCA on sAPPβ ablation (Figs 4.5 & 4.6). There was still a significant decrease in $sAPP\beta_{751/770}$, which is endogenous protein. This is similar to results seen in transgenic mice overexpressing wildtype human APP

which produced more C83 than C99 suggesting increased alpha cleavage (Simon *et al*., 2009), and it would appear that DCA further increases alpha cleavage. Together this suggests that overexpression of APP_{695} saturates the alpha pathway leaving a proportion of APP_{695} to undergo proteolysis via the beta pathway, as evidenced by the increase in $sAPP\beta_{695}$. Furthermore, the increased levels of $sAPP\beta_{695}$ with DCA treatment suggest that BACE1 is not inhibited by DCA.

7.7.2 BACE1 overexpression alters DCA action on APP proteolysis

BACE1 levels are elevated in AD patients, as indicated by elevated protein levels and BACE1 mRNA expression in AD brains post-mortem (Coulson *et al*., 2010). BACE1 overexpressing SH-SY5Y cells were used to model the effects of DCA treatment in the presence of high levels of BACE1. It was thought that high levels of BACE1 would negate the effect of DCA on APP proteolysis as, if alpha shedding is stimulated by DCA, increasing BACE1 levels could counterbalance this by stimulating the beta pathway. This was partially confirmed; $sAPP\beta_{751/770}$ increased in response to DCA but so did $sAPP\alpha$, however this was only significant at 20 mM for the $sAPP\alpha_{751/770}$ band. Furthermore, ablation of $sAPP\beta_{695}$ occurred. This is in contrary to expectations, suggesting that overexpression of BACE1 is not sufficient to fully overcome the increased alpha shedding stimulated by DCA. The neuronal relevant $sAPP\beta_{695}$ was depleted with DCA treatment despite excess BACE1 being present. This indicates that although sufficient BACE1 was present to cleave APP via the amyloidogenic pathway, this was not the case. It also demonstrates DCA may alter the delivery of APP to BACE1, as BACE1 overexpressing H4 neuroglioma cells show increased C99 (and therefore $sAPP\beta$) generation (Repetto *et al*., 2004), so it would be expected that BACE1 overexpressing cells have increased beta cleavage of APP. As BACE1 cleavage and ADAM cleavage of APP take place at separate spatial locations in the cell (BACE1 cleavage takes place in 'lipid rafts' or endocytic compartments whereas ADAM cleavage takes place at the plasma membrane or Trans-golgi membrane), this suggests that DCA may work by impairing delivery of APP to BACE1 lipid rafts, thus stimulating the alpha pathway (Harris *et al*., 2009). This would not necessarily require an increase in ADAM expression but may work as an adjuvant to increased ADAM expression.

DCA also increased the expression of BACE1 in BACE1 overexpressing cells (Fig. 5.7) Interestingly the increase in BACE1 did not have a huge impact on $sAPP\beta$ production, which again could be due to the impaired delivery of APP to BACE1. Alternatively, DCA may inhibit the activity of BACE1 thus overexpression of BACE1 can negate DCA effects on amyloidogenic processing to some extent by increasing the amount of BACE1 present and therefore increase the amount of active BACE1. It is possible that the elevated $sAPP\alpha$ levels directly cause

reduced amyloidogenic processing, as sAPPα associates with BACE1 via a unique BACE1 recognition sequence preventing APP association with BACE1 and thus inhibiting amyloidogenic processing (Obregon *et al*., 2012). Conducting BACE1 activity assays may help shed light on this.

7.8 DCA modulation of ectodomain shedding extends to other ADAM substrates

ADAMs are expressed throughout the body acting on E-cadherin (Maretzky *et al*., 2005) and Jagged1 shedding (LaVoie and Selkoe, 2003). As stimulation of the alpha pathway is the proposed mechanism for DCA mediation of APP proteolysis, it is likely that DCA affects ADAM expression or activity in some manner. As ADAMs have other substrates, the effect of DCA on shedding of other ADAM substrates was investigated using SW480 cells and HEK Jagged1 cells as endogenous E-cadherin and Jagged1 are not detectable via immunoblot in SH-SY5Y cells.

7.8.1 DCA alters Jagged1 expression and shedding

In response to DCA, Jagged1 expression increased in SW480 cells along with increased levels of Jagged1 CTF (Fig. 6.1.8). The shedding of Jagged1 also increased as expected from the CTF increase. However, Jagged1 shedding increased ~9-fold in response to 20 mM DCA (Fig. 6.1.9), a larger increase than expected from the ~1.2fold increase in Jagged1 holoprotein expression alone. These data demonstrate that DCA increases shedding of another ADAM substrate – Jagged1. The common moiety between Jagged1 ectodomain shedding and APP shedding is ADAM10 and ADAM17 (Allinson *et al*., 2004, Parr-Sturgess *et al*., 2010, LaVoie and Selkoe, 2003), further supporting the idea that DCA stimulates the alpha pathway by increasing ADAM expression or activity. However, as Jagged1 has also been shown to be cleaved by BACE1 (He *et al*., 2014), it is possible that increased soluble Jagged1 (sJAG1) is due to increased BACE1 activity, as overexpression of BACE1 in HEK cells increases Jagged1 CTF levels (Hu *et al*., 2013). The anti-Jagged1 antibody used here does not discriminate between sJAG1 cleaved by an alpha secretase and sJAG1 cleaved by BACE1 so it is not possible to confirm which sheddase is responsible for increased sJAG1.

The expression and shedding of Jagged1 was not altered in HEK-Jagged1 cells treated with DCA, but an increase in CTF was observed suggesting increased proteolysis (Figs 6.2.8 & 6.2.9). This suggests that DCA has a biphasic effect in HEK Jagged1 cells as increased CTF levels should correspond to increased sJAg1 but sJag1 is not significantly increased suggesting a possible clearance of sJag1. As sJag1 is a paracrine signalling molecule (Yamamoto *et al*., 2013), it is possible that although increased shedding is observed, sJag1 is re-internalised in

neighbouring cells stimulating signalling pathways resulting in altered E-cadherin expression for example (Delury *et al*., 2013).

Although it was not possible to examine β-cleavage in HEK Jagged1 and SW480 cells, it is likely that ADAM activity is stimulated or ADAM expression increased as indicated by increased sAPPα levels and shed Jagged1 as Jagged1 is primarily shed by ADAM enzymes.

7.8.2 DCA alters shedding and expression of E-cadherin

E-cadherin is another ADAM substrate (ADAM10 or 15) that undergoes ectodomain shedding and RIP. The expression of endogenous E-cadherin decreased in HEK Jagged1 and SW480 cells in response to DCA (Figs. 6.2.10 & 6.1.10). Reduced expression of E-Cadherin is likely a response to increased sJag1 (stimulated by DCA) in both cell lines as sJag1 reduces E-cadherin expression (Delury *et al*., 2013). Shedding of E-cadherin decreased in HEK Jagged1 cells as expected, however shedding of E-cadherin increased in SW480 cells. This was unexpected as less E-cadherin was expressed and therefore less available to undergo shedding. It is possible that stimulation of ADAM10 resulted in increased cleavage of the available E-cadherin in SW480 cells but not in HEK Jagged1 cells due to the abundance of Jagged1 as a substrate for ADAM10. Increased E-cadherin shedding may be beneficial, as the CTF of E-cadherin (analogous to AICD) is thought to promote degradation of C99 and C83, preventing formation of Aβ (Agiostratidou *et al*., 2006). Together, these data suggest that the effect of DCA on ADAM substrates is not universal, but that ADAM10 is the likely candidate increased by DCA as it is common to APP, Jagged1 and E-cadherin shedding.

7.9 DCA increases p53 expression

The expression of p53 increased in all cell lines treated with DCA in a dose-dependent manner. These data confirm that DCA increases expression of p53 as seen in numerous cell lines (Michelakis *et al*., 2010, Agnoletto *et al*., 2014, Kumar *et al*., 2012, Morfouace *et al*., 2012, Sutendra *et al*., 2013). It also demonstrates that there is continuous mitochondrial activity following DCA treatment as p53 translocates to the mitochondria in response to stress (Vaseva and Moll, 2009). The mechanism via which this occurs is through DCA-stimulation of phosphorylation of the metabolic sensor AMP-activated protein kinase (AMPK) which increases p53 transcriptional activity. This is the proposed cause of growth inhibition with DCA treatment as p53 arrests the cell cycle at G1, in response to AMPK.

Interestingly, an additional band was observed in the untransfected SH-SY5Y immunoblots for p53 (Fig 3.1.7). The band located at approximately 50 kDa is only present in the control cells, suggesting DCA treatment reduces levels of this supposed p53 isoform. No additional bands were present in p53 immunoblots from other cells lines. Characterisation of the protein (using p53 isoform specific antibodies) from the band in question would allow for further insight into the mechanistic action of DCA on p53 as there are at least 12 human p53 isoforms and expression of the isoforms can alter p53 transcription activity (Bourdon *et al*., 2005).

7.10 Summary of findings

DCA has pleiotropic effects influencing cell proliferation, cell metabolism, protein expression and proteolysis. DCA stimulates the development of neurite-like outgrowth in a range of cells, thought to be in response to increased sAPPα levels from altered APP proteolysis and increased p53 levels. Increased p53 levels induced by DCA also halt cell proliferation without inducing apoptosis and promote oxidative phosphorylation over glycolysis as seen by increased metabolic activity. Metabolic activity also increases due to the inhibition of PDK by DCA, causing an increase in active PDC. The extent of the increase varied across cell lines due to the different distribution of PDK isoforms and the different binding kinetics of DCA with each of the four isoforms. DCA does not alter endogenous APP expression in SH-SY5Y cells but does alter APP proteolysis in favour of the non-amyloidogenic pathway, reducing sAPPβ production. Overexpression of APP saturates the non-amyloidogenic pathway resulting in some sAPPβ production. DCA also increases shedding of Jagged1 in HEK Jagged1 cells and increases E-cadherin shedding in SW480 cells suggesting increased ADAM activity, specifically ADAM10. A number of suggestions for further work have been suggested throughout this section, however the most interesting analysis is the determination of Aβ levels following DCA treatment given its direct role in AD pathology. Further work could also extend to treating primary neuronal cultures with DCA, with a long-term goal of treating APP transgenic mice with DCA. Treating the other cell lines for 24 hours whilst confluent and repeating the analysis would be of use, as would quantitative RT-PCR to see whether mRNA levels correspond to the changes seen at the protein level.

7.11 Conclusion

Dichloroacetate is a small, cheap PDK inhibitor that crosses the blood brain barrier and shows up to 100% bioavailability. The change in metabolic activity induced by DCA has

important applications for the treatment of AD as oxidative phosphorylation and glucose metabolism are reduced in AD brains, often several decades prior to clinical presentation. It is therefore possible that DCA could have benefits at preventing the onset of AD by maintaining mitochondrial function. It is clear that DCA has pleiotropic effects beyond modulation of metabolism, including altering proliferation, increasing p53 expression and altering ADAM-mediated proteolysis. The most important finding was the alteration to APP proteolysis. Reduction of sAPPβ in response to DCA is an indication of reduced Aβ generation and it is hoped analysis of Aβ levels generated by DCA treated cells reflects this. DCA is proposed as a novel therapeutic for Alzheimer's disease given its ability to increase non-amyloidogenic processing over amyloidogenic processing thought to be due to increased ADAM10 expression. DCA has safely been used in humans for over 40 years and has several attributes conducive to a good pharmaceutical. This study provides the basis of further investigation into a novel AD treatment that is cheap, safe and addresses the underlying pathogenic cause of AD.

Acknowledgements

I would like to thank Ed for his guidance, knowledge, and assistance throughout the project (including the attempt to save cells from Storm Desmond!). I would like to express my gratitude to The Liz And Terry Bramall Foundation for the funding which made this project possible. I would also like to thank Rachael Smith for valuable scientific discussions (and listening to me complain!) and Anna Lee for her continued support. Thanks also to the various technicians, staff and students that helped along the way as well as my family for putting up with me being hundreds of miles away. Lastly, I would like to dedicate this work to my grandmother Jean Dysart; a great lady who sadly succumbed to Alzheimer's Disease.

References

AARTS, L. H. J., SCHOTMAN, P., VERHAAGEN, J., SCHRAMA, L. H. & GISPEN, W. H. 1998. The Role of The Neural Growth Associated Protein B-50/Gap-43 in Morphogenesis. *In:* EHRLICH, Y. H. (ed.) *Molecular and Cellular Mechanisms of Neuronal Plasticity: Basic and Clinical Implications.* Boston, MA: Springer US.

ABEMAYOR, E., KOVACHICH, G. B. & HAUGAARD, N. 1984. Effects of dichloroacetate on brain pyruvate dehydrogenase. *J Neurochem,* 42**,** 38-42.

ABUSHAKRA, S., VELLAS, B., CUMMINGS, J., HEY, J., TOLAR, M. & POWER, A. 2016. Tramiprosate, an oral amyloid anti-aggregation agent, shows robust cognitive efficacy in APOE4/4 homozygous ad patients: efficacy and safety analyses from two Phase 3 trials. *Neurobiology of Aging,* 39, Supplement 1**,** S22.

ACEVEDO, K. M., HUNG, Y. H., DALZIEL, A. H., LI, Q. X., LAUGHTON, K., WIKHE, K., REMBACH, A., ROBERTS, B., MASTERS, C. L., BUSH, A. I. & CAMAKARIS, J. 2011. Copper promotes the trafficking of the amyloid precursor protein. *J Biol Chem,* 286**,** 8252-62.

AGIOSTRATIDOU, G., MUROS, R. M., JUNICHI, S., MARAMBAUD, P. & ROBAKIS, N. K. 2006. The cytoplasmic sequence of E-cadherin promotes non-amyloidogenic degradation of Aβ precursors. *Journal of Neurochemistry,* 96**,** 1182-1188.

AGNOLETTO, C., MELLONI, E., CASCIANO, F., RIGOLIN, G. M., RIMONDI, E., CELEGHINI, C., BRUNELLI, L., CUNEO, A., SECCHIERO, P. & ZAULI, G. 2014. Sodium dichloroacetate exhibits anti-leukemic activity in B-chronic lymphocytic leukemia (B-CLL) and synergizes with the p53 activator Nutlin-3. *Oncotarget,* 5**,** 4347-4360.

AISEN, P. S., GAUTHIER, S., FERRIS, S. H., SAUMIER, D., HAINE, D., GARCEAU, D., DUONG, A., SUHY, J., OH, J., LAU, W. C. & SAMPALIS, J. 2011. Tramiprosate in mild-to-moderate Alzheimer's disease – a randomized, double-blind, placebo-controlled, multi-centre study (the Alphase Study). *Archives of Medical Science : AMS,* 7**,** 102-111.

ALLENDE-VEGA, N., KRZYWINSKA, E., ORECCHIONI, S., LOPEZ-ROYUELA, N., REGGIANI, F., TALARICO, G., ROSSI, J.-F., ROSSIGNOL, R., HICHERI, Y., CARTRON, G., BERTOLINI, F. & VILLALBA, M. 2015. The presence of wild type p53 in hematological cancers improves the efficacy of combinational therapy targeting metabolism. *Oncotarget,* 6**,** 19228-19245.

ALLINQUANT, B., HANTRAYE, P., MAILLEUX, P., MOYA, K., BOUILLOT, C. & PROCHIANTZ, A. 1995. Downregulation of amyloid precursor protein inhibits neurite outgrowth in vitro. *The Journal of Cell Biology,* 128**,** 919-927.

ALLINSON, T. M., PARKIN, E. T., CONDON, T. P., SCHWAGER, S. L., STURROCK, E. D., TURNER, A. J. & HOOPER, N. M. 2004. The role of ADAM10 and ADAM17 in the ectodomain shedding of angiotensin converting enzyme and the amyloid precursor protein. *Eur J Biochem,* 271**,** 2539-47.

ALLINSON, T. M. J., PARKIN, E. T., TURNER, A. J. & HOOPER, N. M. 2003. ADAMs family members as amyloid precursor protein α-secretases. *Journal of Neuroscience Research,* 74**,** 342-352.

ALPAR, A., UEBERHAM, U., BRUCKNER, M. K., ARENDT, T. & GARTNER, U. 2006. The expression of wild-type human amyloid precursor protein affects the dendritic phenotype of neocortical pyramidal neurons in transgenic mice. *Int J Dev Neurosci,* 24**,** 133-40.

ALTMEPPEN, H. C., PROX, J., KRASEMANN, S., PUIG, B., KRUSZEWSKI, K., DOHLER, F., BERNREUTHER, C., HOXHA, A., LINSENMEIER, L., SIKORSKA, B., LIBERSKI, P. P., BARTSCH, U., SAFTIG, P. & GLATZEL, M. 2015. The sheddase ADAM10 is a potent modulator of prion disease. *Elife,* 4.

ANAND, R., GILL, K. D. & MAHDI, A. A. 2014. Therapeutics of Alzheimer's disease: Past, present and future. *Neuropharmacology,* 76, Part A**,** 27-50.

ANDERS, A., GILBERT, S., GARTEN, W., POSTINA, R. & FAHRENHOLZ, F. 2001. Regulation of the alpha-secretase ADAM10 by its prodomain and proprotein convertases. *Faseb j,* 15**,** 1837-9.

ANDREASSEN, O. A., FERRANTE, R. J., HUANG, H. M., DEDEOGLU, A., PARK, L., FERRANTE, K. L., KWON, J., BORCHELT, D. R., ROSS, C. A., GIBSON, G. E. & BEAL, M. F. 2001. Dichloroacetate exerts therapeutic effects in transgenic mouse models of Huntington's disease. *Ann Neurol,* 50**,** 112-7.

ARCANGELI, A., BECCHETTI, A., MANNINI, A., MUGNAI, G., DE FILIPPI, P., TARONE, G., DEL BENE, M. R., BARLETTA, E., WANKE, E. & OLIVOTTO, M. 1993. Integrin-mediated neurite outgrowth in neuroblastoma cells depends on the activation of potassium channels. *J Cell Biol,* 122**,** 1131-43.

ARIKKATH, J. & REICHARDT, L. F. 2008. Cadherins and catenins at synapses: roles in synaptogenesis and synaptic plasticity. *Trends Neurosci,* 31**,** 487-94.

ATRI, A., HENDRIX, S. B., PEJOVIĆ, V., HOFBAUER, R. K., EDWARDS, J., MOLINUEVO, J. L. & GRAHAM, S. M. 2015. Cumulative, additive benefits of memantine-donepezil combination over component monotherapies in moderate to severe Alzheimer's dementia: a pooled area under the curve analysis. *Alzheimer's Research & Therapy,* 7**,** 1-12.

AULD, D. S., KORNECOOK, T. J., BASTIANETTO, S. & QUIRION, R. 2002. Alzheimer's disease and the basal forebrain cholinergic system: relations to beta-amyloid peptides, cognition, and treatment strategies. *Prog Neurobiol,* 68**,** 209-45.

BARGER, S. W. & HARMON, A. D. 1997. Microglial activation by Alzheimer amyloid precursor protein and modulation by apolipoprotein E. *Nature,* 388**,** 878-881.

BARNES, C. A., MELTZER, J., HOUSTON, F., ORR, G., MCGANN, K. & WENK, G. L. 2000. Chronic treatment of old rats with donepezil or galantamine: effects on memory, hippocampal plasticity and nicotinic receptors. *Neuroscience,* 99**,** 17-23.

BECHERER, J. D. & BLOBEL, C. P. 2003. Biochemical properties and functions of membrane-anchored metalloprotease-disintegrin proteins (ADAMs). *Current Topics in Developmental Biology.* Academic Press.

BECKETT, C., NALIVAEVA, N. N., BELYAEV, N. D. & TURNER, A. J. 2012. Nuclear signalling by membrane protein intracellular domains: the AICD enigma. *Cell Signal,* 24**,** 402-9.

BELL, H. & PARKIN, E. T. 2016. Pyruvate dehydrogenase kinase inhibition: Reversing the Warburg effect in cancer therapy. *International Journal of Cancer Therapy and Oncology; Vol 4, No 2 (2016): April - June*.

BELYAEV, N. D., KELLETT, K. A., BECKETT, C., MAKOVA, N. Z., REVETT, T. J., NALIVAEVA, N. N., HOOPER, N. M. & TURNER, A. J. 2010. The transcriptionally active amyloid precursor protein (APP) intracellular domain is preferentially produced from the 695 isoform of APP in a {beta}-secretase-dependent pathway. *J Biol Chem,* 285**,** 41443-54.

BEN KHALIFA, N., TYTECA, D., MARINANGELI, C., DEPUYDT, M., COLLET, J.-F., COURTOY, P. J., RENAULD, J.-C., CONSTANTINESCU, S., OCTAVE, J.-N. & KIENLEN-CAMPARD, P. 2012. Structural features of the KPI domain control APP dimerization, trafficking, and processing. *The FASEB Journal,* 26**,** 855-867.

BENTAHIR, M., NYABI, O., VERHAMME, J., TOLIA, A., HORRE, K., WILTFANG, J., ESSELMANN, H. & DE STROOPER, B. 2006. Presenilin clinical mutations can affect gamma-secretase activity by different mechanisms. *J Neurochem,* 96**,** 732-42.

BERRIDGE, M. V., HERST, P. M. & TAN, A. S. 2005. Tetrazolium dyes as tools in cell biology: new insights into their cellular reduction. *Biotechnol Annu Rev,* 11**,** 127-52.

BEYREUTHER, K., POLLWEIN, P., MULTHAUP, G., MONNING, U., KONIG, G., DYRKS, T., SCHUBERT, W. & MASTERS, C. L. 1993. Regulation and expression of the Alzheimer's beta/A4 amyloid protein precursor in health, disease, and Down's syndrome. *Ann N Y Acad Sci,* 695**,** 91-102.

BIEDLER, J. L., ROFFLER-TARLOV, S., SCHACHNER, M. & FREEDMAN, L. S. 1978. Multiple neurotransmitter synthesis by human neuroblastoma cell lines and clones. *Cancer Res,* 38**,** 3751-7.

BILLNITZER, A. J., BARSKAYA, I., YIN, C. & PEREZ, R. G. 2013. APP independent and dependent effects on neurite outgrowth are modulated by the receptor associated protein (RAP). *J Neurochem,* 124**,** 123-32.

BIRD, T. D. 2008. Genetic aspects of Alzheimer disease. *Genet Med,* 10**,** 231-239.

BLACK, R. A., RAUCH, C. T., KOZLOSKY, C. J., PESCHON, J. J., SLACK, J. L., WOLFSON, M. F., CASTNER, B. J., STOCKING, K. L., REDDY, P., SRINIVASAN, S., NELSON, N., BOIANI, N., SCHOOLEY, K. A., GERHART, M., DAVIS, R., FITZNER, J. N., JOHNSON, R. S., PAXTON, R. J., MARCH, C. J. & CERRETTI, D. P. 1997. A metalloproteinase disintegrin that releases tumour-necrosis factor-alpha from cells. *Nature,* 385**,** 729-33.

BLENNOW, K., DE LEON, M. J. & ZETTERBERG, H. 2006. Alzheimer's disease. *The Lancet,* 368**,** 387-403.

BONNET, S., ARCHER, S. L., ALLALUNIS-TURNER, J., HAROMY, A., BEAULIEU, C., THOMPSON, R., LEE, C. T., LOPASCHUK, G. D., PUTTAGUNTA, L., BONNET, S., HARRY, G., HASHIMOTO, K., PORTER, C. J., ANDRADE, M. A., THEBAUD, B. & MICHELAKIS, E. D. 2007. A Mitochondria-K+ Channel Axis Is Suppressed in Cancer and Its Normalization Promotes Apoptosis and Inhibits Cancer Growth. *Cancer Cell,* 11**,** 37-51.

BOURDON, J. C., FERNANDES, K., MURRAY-ZMIJEWSKI, F., LIU, G., DIOT, A., XIRODIMAS, D. P., SAVILLE, M. K. & LANE, D. P. 2005. p53 isoforms can regulate p53 transcriptional activity. *Genes Dev,* 19**,** 2122-37.

BOWKER-KINLEY, M. M., DAVIS, W. I., WU, P., HARRIS, R. A. & POPOV, K. M. 1998. Evidence for existence of tissue-specific regulation of the mammalian pyruvate dehydrogenase complex. *Biochem J,* 329 (Pt 1)**,** 191-6.

BRAAK, H. & BRAAK, E. 1991. Neuropathological stageing of Alzheimer-related changes. *Acta Neuropathologica,* 82**,** 239-259.

BRANCA, C., SARNICO, I., RUOTOLO, R., LANZILLOTTA, A., VISCOMI, A. R., BENARESE, M., PORRINI, V., LORENZINI, L., CALZÀ, L., IMBIMBO, B. P., OTTONELLO, S. & PIZZI, M. 2014. Pharmacological targeting of the β-amyloid precursor protein intracellular domain. *Scientific Reports,* 4**,** 4618.

BREEN, K. C., BRUCE, M. & ANDERTON, B. H. 1991. Beta amyloid precursor protein mediates neuronal cell-cell and cell-surface adhesion. *J Neurosci Res,* 28**,** 90-100.

BRINKMALM, G., BRINKMALM, A., BOURGEOIS, P., PERSSON, R., HANSSON, O., PORTELIUS, E., MERCKEN, M., ANDREASSON, U., PARENT, S., LIPARI, F., OHRFELT, A., BJERKE, M., MINTHON, L., ZETTERBERG, H., BLENNOW, K. & NUTU, M. 2013. Soluble amyloid precursor protein alpha and beta in CSF in Alzheimer's disease. *Brain Res,* 1513**,** 117-26.

CAPACCIONE, K. M. & PINE, S. R. 2013. The Notch signaling pathway as a mediator of tumor survival. *Carcinogenesis,* 34**,** 1420-1430.

CEGLIA, I., REITZ, C., GRESACK, J., AHN, J.-H., BUSTOS, V., BLECK, M., ZHANG, X., MARTIN, G., SIMON, S. M., NAIRN, A. C., GREENGARD, P. & KIM, Y. 2015. APP intracellular domain-WAVE1 pathway reduces amyloid-β production. *Nature Medicine,* 21**,** 1054-1059.

CHANG, W.-P., HUANG, X., DOWNS, D., CIRRITO, J. R., KOELSCH, G., HOLTZMAN, D. M., GHOSH, A. K. & TANG, J. 2011. β-Secretase inhibitor GRL-8234 rescues age-related cognitive decline in APP transgenic mice. *The FASEB Journal,* 25**,** 775-784.

CHASSEIGNEAUX, S. & ALLINQUANT, B. 2012. Functions of Aβ, sAPPα and sAPPβ : similarities and differences. *Journal of Neurochemistry,* 120**,** 99-108.

CHENG, G., YU, Z., ZHOU, D. & MATTSON, M. P. 2002. Phosphatidylinositol-3-kinase-Akt kinase and p42/p44 mitogen-activated protein kinases mediate neurotrophic and

excitoprotective actions of a secreted form of amyloid precursor protein. *Exp Neurol,* 175**,** 407-14.

CHERET, C., WILLEM, M., FRICKER, F. R., WENDE, H., WULF-GOLDENBERG, A., TAHIROVIC, S., NAVE, K.-A., SAFTIG, P., HAASS, C., GARRATT, A. N., BENNETT, D. L. & BIRCHMEIER, C. 2013. Bace1 and Neuregulin-1 cooperate to control formation and maintenance of muscle spindles. *The EMBO Journal,* 32**,** 2015-2028.

CHEUNG, Z. H. & IP, N. Y. 2012. Cdk5: a multifaceted kinase in neurodegenerative diseases. *Trends Cell Biol,* 22**,** 169-75.

CHYUNG, A. S. C., GREENBERG, B. D., COOK, D. G., DOMS, R. W. & LEE, V. M. Y. 1997. Novel β-Secretase Cleavage of β-Amyloid Precursor Protein in the Endoplasmic Reticulum/Intermediate Compartment of NT2N Cells. *The Journal of Cell Biology,* 138**,** 671-680.

COHEN, A. D. & KLUNK, W. E. 2014. Early detection of Alzheimer's disease using PiB and FDG PET. *Neurobiology of Disease,* 72, Part A**,** 117-122.

COLOMBO, A., WANG, H., KUHN, P. H., PAGE, R., KREMMER, E., DEMPSEY, P. J., CRAWFORD, H. C. & LICHTENTHALER, S. F. 2013. Constitutive alpha- and beta-secretase cleavages of the amyloid precursor protein are partially coupled in neurons, but not in frequently used cell lines. *Neurobiol Dis,* 49**,** 137-47.

COULSON, D. T., BEYER, N., QUINN, J. G., BROCKBANK, S., HELLEMANS, J., IRVINE, G. B., RAVID, R. & JOHNSTON, J. A. 2010. BACE1 mRNA expression in Alzheimer's disease postmortem brain tissue. *J Alzheimers Dis,* 22**,** 1111-22.

CUESTA, A., ZAMBRANO, A., ROYO, M. & PASCUAL, A. 2009. The tumour suppressor p53 regulates the expression of amyloid precursor protein (APP). *Biochemical Journal,* 418**,** 643-650.

DAS, V. & MILLER, J. H. 2012. Microtubule stabilization by peloruside A and paclitaxel rescues degenerating neurons from okadaic acid-induced tau phosphorylation. *Eur J Neurosci,* 35**,** 1705-17.

DASILVA, K. A., BROWN, M. E., COUSINS, J. E., RAPPAPORT, R. V., AUBERT, I., WESTAWAY, D. & MCLAURIN, J. 2009. scyllo-inositol (ELND005) ameliorates amyloid pathology in an aggressive mouse model of Alzheimer's disease. *Alzheimer's & Dementia,* 5**,** P425.

DE STROOPER, B. 2003. Aph-1, Pen-2, and Nicastrin with Presenilin generate an active gamma-Secretase complex. *Neuron,* 38**,** 9-12.

DE STROOPER, B. & ANNAERT, W. 2000. Proteolytic processing and cell biological functions of the amyloid precursor protein. *J Cell Sci,* 113 (Pt 11)**,** 1857-70.

DE STROOPER, B., ANNAERT, W., CUPERS, P., SAFTIG, P., CRAESSAERTS, K., MUMM, J. S., SCHROETER, E. H., SCHRIJVERS, V., WOLFE, M. S., RAY, W. J., GOATE, A. & KOPAN, R. 1999. A presenilin-1-dependent gamma-secretase-like protease mediates release of Notch intracellular domain. *Nature,* 398**,** 518-22.

DELURY, C., TINKER, C., RIVERS, S., HODGES, M., BROUGHTON, S. & PARKIN, E. 2013. Differential regulation of E-cadherin expression by the soluble ectodomain and intracellular domain of jagged1. *International Journal of Biochemistry Research and Review,* 3**,** 278-290.

DEUSS, M., REISS, K. & HARTMANN, D. 2008. Part-time alpha-secretases: the functional biology of ADAM 9, 10 and 17. *Curr Alzheimer Res,* 5**,** 187-201.

DEVI, L., TANG, J. & OHNO, M. 2015. Beneficial Effects of the β-Secretase Inhibitor GRL-8234 in 5XFAD Alzheimer's Transgenic Mice Lessen during Disease Progression. *Current Alzheimer research,* 12**,** 13-21.

DEYTS, C., THINAKARAN, G. & PARENT, A. T. 2016. APP Receptor? To Be or Not To Be. *Trends in Pharmacological Sciences,* 37**,** 390-411.

DI GIOVANNI, S., KNIGHTS, C. D., RAO, M., YAKOVLEV, A., BEERS, J., CATANIA, J., AVANTAGGIATI, M. L. & FADEN, A. I. 2006. The tumor suppressor protein p53 is

required for neurite outgrowth and axon regeneration. *The EMBO Journal,* 25**,** 4084-4096.

DOODY, R. S., RAMAN, R., FARLOW, M., IWATSUBO, T., VELLAS, B., JOFFE, S., KIEBURTZ, K., HE, F., SUN, X., THOMAS, R. G., AISEN, P. S., SIEMERS, E., SETHURAMAN, G. & MOHS, R. 2013. A Phase 3 Trial of Semagacestat for Treatment of Alzheimer's Disease. *New England Journal of Medicine,* 369**,** 341-350.

DRAGUNOW, M., XU, R., WALTON, M., WOODGATE, A., LAWLOR, P., MACGIBBON, G. A., YOUNG, D., GIBBONS, H., LIPSKI, J., MURAVLEV, A., PEARSON, A. & DURING, M. 2000. c-Jun promotes neurite outgrowth and survival in PC12 cells. *Brain Res Mol Brain Res,* 83**,** 20-33.

DRIES, D. R., SHAH, S., HAN, Y. H., YU, C., YU, S., SHEARMAN, M. S. & YU, G. 2009. Glu-333 of nicastrin directly participates in gamma-secretase activity. *J Biol Chem,* 284**,** 29714-24.

DUNBAR, E. M., COATS, B. S., SHROADS, A. L., LANGAEE, T., LEW, A., FORDER, J. R., SHUSTER, J. J., WAGNER, D. A. & STACPOOLE, P. W. 2014. Phase 1 trial of dichloroacetate (DCA) in adults with recurrent malignant brain tumors. *Invest New Drugs,* 32**,** 452-64.

EDBAUER, D., WILLEM, M., LAMMICH, S., STEINER, H. & HAASS, C. 2002. Insulin-degrading Enzyme Rapidly Removes the β-Amyloid Precursor Protein Intracellular Domain (AICD). *Journal of Biological Chemistry,* 277**,** 13389-13393.

EHEHALT, R., MICHEL, B., DE PIETRI TONELLI, D., ZACCHETTI, D., SIMONS, K. & KELLER, P. 2002. Splice variants of the beta-site APP-cleaving enzyme BACE1 in human brain and pancreas. *Biochem Biophys Res Commun,* 293**,** 30-7.

ELLAWANDA, F. & WALLACE, R. 2013. Can Infections Cause Alzheimer's Disease? *Epidemiologic Reviews,* 35**,** 161-180.

ERCOLI, L. M., SIDDARTH, P., DUNKIN, J. J., BRAMEN, J. & SMALL, G. W. 2003. MMSE Items Predict Cognitive Decline in Persons with Genetic Risk for Alzheimer's Disease. *Journal of Geriatric Psychiatry and Neurology,* 16**,** 67-73.

FARRER, L. A., CUPPLES, L. A., HAINES, J. L., HYMAN, B., KUKULL, W. A., MAYEUX, R., MYERS, R. H., PERICAK-VANCE, M. A., RISCH, N. & VAN DUIJN, C. M. 1997. Effects of age, sex, and ethnicity on the association between apolipoprotein E genotype and Alzheimer disease. A meta-analysis. APOE and Alzheimer Disease Meta Analysis Consortium. *Jama,* 278**,** 1349-56.

FINDLAY, J. A., HAMILTON, D. L. & ASHFORD, M. L. J. 2015. BACE1 activity impairs neuronal glucose oxidation: rescue by beta-hydroxybutyrate and lipoic acid. *Frontiers in Cellular Neuroscience,* 9**,** 382.

FREUDE, K. K., PENJWINI, M., DAVIS, J. L., LAFERLA, F. M. & BLURTON-JONES, M. 2011. Soluble amyloid precursor protein induces rapid neural differentiation of human embryonic stem cells. *J Biol Chem,* 286**,** 24264-74.

FUENTEALBA, R. A., BARRÍA, M. I., LEE, J., CAM, J., ARAYA, C., ESCUDERO, C. A., INESTROSA, N. C., BRONFMAN, F. C., BU, G. & MARZOLO, M.-P. 2007. ApoER2 expression increases Aβ production while decreasing Amyloid Precursor Protein (APP) endocytosis: Possible role in the partitioning of APP into lipid rafts and in the regulation of γ-secretase activity. *Molecular Neurodegeneration,* 2**,** 14-14.

FURUKAWA, K., SOPHER, B. L., RYDEL, R. E., BEGLEY, J. G., PHAM, D. G., MARTIN, G. M., FOX, M. & MATTSON, M. P. 1996. Increased activity-regulating and neuroprotective efficacy of alpha-secretase-derived secreted amyloid precursor protein conferred by a C-terminal heparin-binding domain. *J Neurochem,* 67**,** 1882-96.

GAKHAR-KOPPOLE, N., HUNDESHAGEN, P., MANDL, C., WEYER, S. W., ALLINQUANT, B., MULLER, U. & CICCOLINI, F. 2008. Activity requires soluble amyloid precursor protein alpha to promote neurite outgrowth in neural stem cell-derived neurons via activation of the MAPK pathway. *Eur J Neurosci,* 28**,** 871-82.

GAO, C., DING, Y., ZHONG, L., JIANG, L., GENG, C., YAO, X. & CAO, J. 2014. Tacrine induces apoptosis through lysosome- and mitochondria-dependent pathway in HepG2 cells. *Toxicology in Vitro,* 28**,** 667-674.

GERVAIS, F., PAQUETTE, J., MORISSETTE, C., KRZYWKOWSKI, P., YU, M., AZZI, M., LACOMBE, D., KONG, X., AMAN, A., LAURIN, J., SZAREK, W. A. & TREMBLAY, P. 2007. Targeting soluble Aβ peptide with Tramiprosate for the treatment of brain amyloidosis. *Neurobiology of Aging,* 28**,** 537-547.

GHISO, J. & FRANGIONE, B. 2002. Amyloidosis and Alzheimer's disease. *Adv Drug Deliv Rev,* 54**,** 1539-51.

GHOSAL, K., VOGT, D. L., LIANG, M., SHEN, Y., LAMB, B. T. & PIMPLIKAR, S. W. 2009. Alzheimer's disease-like pathological features in transgenic mice expressing the APP intracellular domain. *Proc Natl Acad Sci U S A,* 106**,** 18367-72.

GHOSH, A. K., KUMARAGURUBARAN, N., HONG, L., KULKARNI, S., XU, X., MILLER, H. B., REDDY, D. S., WEERASENA, V., TURNER, R., CHANG, W., KOELSCH, G. & TANG, J. 2008. Potent Memapsin 2 (β-Secretase) Inhibitors: Design, Synthesis, Protein-Ligand X-ray Structure and in vivo Evaluation. *Bioorganic & medicinal chemistry letters,* 18**,** 1031-1036.

GIACOBINI, E. 2003. Cholinergic function and Alzheimer's disease. *Int J Geriatr Psychiatry,* 18**,** S1-5.

GODFROID, E. & OCTAVE, J.-N. 1990. Glycosylation of the amyloid peptide precursor containing the Kunitz protease inhibitor domain improves the inhibition of trypsin. *Biochemical and Biophysical Research Communications,* 171**,** 1015-1021.

GODYŃ, J., JOŃCZYK, J., PANEK, D. & MALAWSKA, B. 2016. Therapeutic strategies for Alzheimer's disease in clinical trials. *Pharmacological Reports,* 68**,** 127-138.

GOLDE, T. E., KOO, E. H., FELSENSTEIN, K. M., OSBORNE, B. A. & MIELE, L. 2013. γ-Secretase inhibitors and modulators. *Biochimica et Biophysica Acta (BBA) - Biomembranes,* 1828**,** 2898-2907.

GOODGER, Z. V., RAJENDRAN, L., TRUTZEL, A., KOHLI, B. M., NITSCH, R. M. & KONIETZKO, U. 2009. Nuclear signaling by the APP intracellular domain occurs predominantly through the amyloidogenic processing pathway. *J Cell Sci,* 122**,** 3703-14.

GOOZ, M. 2010. ADAM-17: The Enzyme That Does It All. *Critical reviews in biochemistry and molecular biology,* 45**,** 146-169.

GRALLE, M. & FERREIRA, S. T. 2007. Structure and functions of the human amyloid precursor protein: the whole is more than the sum of its parts. *Prog Neurobiol,* 82**,** 11-32.

GROCHOWSKI, C. M., LOOMES, K. M. & SPINNER, N. B. 2016. Jagged1 (JAG1): Structure, expression, and disease associations. *Gene,* 576**,** 381-384.

GUENETTE, S., CHANG, Y., HIESBERGER, T., RICHARDSON, J. A., ECKMAN, C. B., ECKMAN, E. A., HAMMER, R. E. & HERZ, J. 2006. Essential roles for the FE65 amyloid precursor protein-interacting proteins in brain development. *Embo j,* 25**,** 420-31.

HAAPASALO, A. & KOVACS, D. M. 2011. The many substrates of presenilin/γ-secretase. *Journal of Alzheimer's Disease,* 25**,** 3-28.

HAASS, C., KAETHER, C., THINAKARAN, G. & SISODIA, S. 2012. Trafficking and Proteolytic Processing of APP. *Cold Spring Harbor Perspectives in Medicine,* 2**,** a006270.

HAASS, C., SCHLOSSMACHER, M. G., HUNG, A. Y., VIGO-PELFREY, C., MELLON, A., OSTASZEWSKI, B. L., LIEBERBURG, I., KOO, E. H., SCHENK, D., TEPLOW, D. B. & ET AL. 1992. Amyloid beta-peptide is produced by cultured cells during normal metabolism. *Nature,* 359**,** 322-5.

HAMID, R., KILGER, E., WILLEM, M., VASSALLO, N., KOSTKA, M., BORNHOVD, C., REICHERT, A. S., KRETZSCHMAR, H. A., HAASS, C. & HERMS, J. 2007. Amyloid precursor protein intracellular domain modulates cellular calcium homeostasis and ATP content. *J Neurochem,* 102**,** 1264-75.

HAN, W., JI, T., MEI, B. & SU, J. 2011. Peptide p3 may play a neuroprotective role in the brain. *Medical Hypotheses,* 76**,** 543-546.

HARDY, J. & HIGGINS, G. 1992. Alzheimer's disease: the amyloid cascade hypothesis. *Science,* 256**,** 184-185.

HARRIS, B., PEREIRA, I. & PARKIN, E. 2009. Targeting ADAM10 to lipid rafts in neuroblastoma SH-SY5Y cells impairs amyloidogenic processing of the amyloid precursor protein. *Brain Res,* 1296**,** 203-15.

HARTL, D., KLATT, S., ROCH, M., KONTHUR, Z., KLOSE, J., WILLNOW, T. E. & ROHE, M. 2013. Soluble alpha-APP (sAPPalpha) regulates CDK5 expression and activity in neurons. *PLoS One,* 8**,** e65920.

HARTMAN, R. E., LAURER, H., LONGHI, L., BALES, K. R., PAUL, S. M., MCINTOSH, T. K. & HOLTZMAN, D. M. 2002. Apolipoprotein E4 influences amyloid deposition but not cell loss after traumatic brain injury in a mouse model of Alzheimer's disease. *The Journal of neuroscience,* 22**,** 10083-10087.

HARTMANN, D., DE STROOPER, B., SERNEELS, L., CRAESSAERTS, K., HERREMAN, A., ANNAERT, W., UMANS, L., LUBKE, T., LENA ILLERT, A., VON FIGURA, K. & SAFTIG, P. 2002. The disintegrin/metalloprotease ADAM 10 is essential for Notch signalling but not for alpha-secretase activity in fibroblasts. *Hum Mol Genet,* 11**,** 2615-24.

HE, W., HU, J., XIA, Y. & YAN, R. 2014. β-Site Amyloid Precursor Protein Cleaving Enzyme 1(BACE1) Regulates Notch Signaling by Controlling the Cleavage of Jagged 1 (Jag1) and Jagged 2 (Jag2) Proteins. *Journal of Biological Chemistry,* 289**,** 20630-20637.

HELLSTROM-LINDAHL, E., VIITANEN, M. & MARUTLE, A. 2009. Comparison of Abeta levels in the brain of familial and sporadic Alzheimer's disease. *Neurochem Int,* 55**,** 243-52.

HEWITT, R. E., MCMARLIN, A., KLEINER, D., WERSTO, R., MARTIN, P., TSOKOS, M., STAMP, G. W. & STETLER-STEVENSON, W. G. 2000. Validation of a model of colon cancer progression. *J Pathol,* 192**,** 446-54.

HICKS, D. A., MAKOVA, N. Z., GOUGH, M., PARKIN, E. T., NALIVAEVA, N. N. & TURNER, A. J. 2013. The Amyloid Precursor Protein Represses Expression of Acetylcholinesterase in Neuronal Cell Lines. *Journal of Biological Chemistry,* 288**,** 26039-26051.

HICKS, D. A., NALIVAEVA, N. N. & TURNER, A. J. 2012. Lipid Rafts and Alzheimer's Disease: Protein-Lipid Interactions and Perturbation of Signaling. *Frontiers in Physiology,* 3**,** 189.

HO, A. & SUDHOF, T. C. 2004. Binding of F-spondin to amyloid-beta precursor protein: a candidate amyloid-beta precursor protein ligand that modulates amyloid-beta precursor protein cleavage. *Proc Natl Acad Sci U S A,* 101**,** 2548-53.

HO, L., FUKUCHI, K.-I. & YOUNKIN, S. G. 1996. The Alternatively Spliced Kunitz Protease Inhibitor Domain Alters Amyloid β Protein Precursor Processing and Amyloid β Protein Production in Cultured Cells. *Journal of Biological Chemistry,* 271**,** 30929-30934.

HOAREAU, C., BORRELL, V., SORIANO, E., KREBS, M. O., PROCHIANTZ, A. & ALLINQUANT, B. 2008. Amyloid precursor protein cytoplasmic domain antagonizes reelin neurite outgrowth inhibition of hippocampal neurons. *Neurobiology of Aging,* 29**,** 542-553.

HOLMES, C., BOCHE, D., WILKINSON, D., YADEGARFAR, G., HOPKINS, V., BAYER, A., JONES, R. W., BULLOCK, R., LOVE, S., NEAL, J. W., ZOTOVA, E. & NICOLL, J. A. 2008. Long-term effects of Abeta42 immunisation in Alzheimer's disease: follow-up of a randomised, placebo-controlled phase I trial. *Lancet,* 372**,** 216-23.

HOLTZMAN, D. M., BALES, K. R., TENKOVA, T., FAGAN, A. M., PARSADANIAN, M., SARTORIUS, L. J., MACKEY, B., OLNEY, J., MCKEEL, D., WOZNIAK, D. & PAUL, S. M. 2000. Apolipoprotein E isoform-dependent amyloid deposition and neuritic degeneration in a mouse model of Alzheimer's disease. *Proc Natl Acad Sci U S A,* 97**,** 2892-7.

HORWITZ, S. B. 1994. Taxol (paclitaxel): mechanisms of action. *Ann Oncol,* 5 Suppl 6**,** S3-6.

HU, X., HE, W., LUO, X., TSUBOTA, K. E. & YAN, R. 2013. BACE1 regulates hippocampal astrogenesis via the Jagged1-Notch pathway. *Cell Rep,* 4**,** 40-9.

HUGHES, R. E., NIKOLIC, K. & RAMSAY, R. R. 2016. One for All? Hitting Multiple Alzheimer's Disease Targets with One Drug. *Frontiers in Neuroscience,* 10**,** 177.

HUSSAIN, I., POWELL, D., HOWLETT, D. R., TEW, D. G., MEEK, T. D., CHAPMAN, C., GLOGER, I. S., MURPHY, K. E., SOUTHAN, C. D., RYAN, D. M., SMITH, T. S., SIMMONS, D. L., WALSH, F. S., DINGWALL, C. & CHRISTIE, G. 1999. Identification of a novel aspartic protease (Asp 2) as beta-secretase. *Mol Cell Neurosci,* 14**,** 419-27.

HUTTON, M. & HARDY, J. 1997. The presenilins and Alzheimer's disease. *Hum Mol Genet,* 6**,** 1639-46.

ITTNER, L. M. & GOTZ, J. 2011. Amyloid-beta and tau--a toxic pas de deux in Alzheimer's disease. *Nat Rev Neurosci,* 12**,** 65-72.

JACOBSEN, K. T. & IVERFELDT, K. 2009. Amyloid precursor protein and its homologues: a family of proteolysis-dependent receptors. *Cellular and Molecular Life Sciences,* 66**,** 2299-2318.

JACOBSON, S. A. & SABBAGH, M. N. 2011. Investigational drugs for the treatment of AD: what can we learn from negative trials? *Alzheimer's Research & Therapy,* 3**,** 73-80.

JAGUST, W. J. & LANDAU, S. M. 2012. Apolipoprotein E, not fibrillar beta-amyloid, reduces cerebral glucose metabolism in normal aging. *J Neurosci,* 32**,** 18227-33.

JAVIER MIGUEL-HIDALGO, J., PAUL, I. A., WANZO, V. & BANERJEE, P. K. 2012. Memantine prevents cognitive impairment and reduces Bcl-2 and caspase 8 immunoreactivity in rats injected with amyloid β1–40. *European Journal of Pharmacology,* 692**,** 38-45.

JHA, M. K., JEON, S. & SUK, K. 2012. Pyruvate Dehydrogenase Kinases in the Nervous System: Their Principal Functions in Neuronal-glial Metabolic Interaction and Neuro-metabolic Disorders. *Current Neuropharmacology,* 10**,** 393-403.

JIAN, X. Q., WANG, K. S., WU, T. J., HILLHOUSE, J. J. & MULLERSMAN, J. E. 2011. Association of ADAM10 and CAMK2A polymorphisms with conduct disorder: evidence from family-based studies. *J Abnorm Child Psychol,* 39**,** 773-82.

KANEMARU, K., TAKIO, K., MIURA, R., TITANI, K. & IHARA, Y. 1992. Fetal-Type Phosphorylation of the τ in Paired Helical Filaments. *Journal of Neurochemistry,* 58**,** 1667-1675.

KANKOTIA, S. & STACPOOLE, P. W. 2014. Dichloroacetate and cancer: new home for an orphan drug? *Biochim Biophys Acta,* 1846**,** 617-29.

KAUFMANN, P., ENGELSTAD, K., WEI, Y., JHUNG, S., SANO, M. C., SHUNGU, D. C., MILLAR, W. S., HONG, X., GOOCH, C. L., MAO, X., PASCUAL, J. M., HIRANO, M., STACPOOLE, P. W., DIMAURO, S. & DE VIVO, D. C. 2006. Dichloroacetate causes toxic neuropathy in MELAS: a randomized, controlled clinical trial. *Neurology,* 66**,** 324-30.

KIM, M., SUH, J., ROMANO, D., TRUONG, M. H., MULLIN, K., HOOLI, B., NORTON, D., TESCO, G., ELLIOTT, K., WAGNER, S. L., MOIR, R. D., BECKER, K. D. & TANZI, R. E. 2009. Potential late-onset Alzheimer's disease-associated mutations in the ADAM10 gene attenuate α-secretase activity. *Human Molecular Genetics,* 18**,** 3987-3996.

KIM, Y.-G. & LEE, Y.-I. 2012. Differential Expressions of Synaptogenic Markers between Primary Cultured Cortical and Hippocampal Neurons. *Experimental Neurobiology,* 21**,** 61-67.

KIMBERLY, W. T., ZHENG, J. B., GUENETTE, S. Y. & SELKOE, D. J. 2001. The intracellular domain of the beta-amyloid precursor protein is stabilized by Fe65 and translocates to the nucleus in a notch-like manner. *J Biol Chem,* 276**,** 40288-92.

KNOECHEL, T. R., TUCKER, A. D., ROBINSON, C. M., PHILLIPS, C., TAYLOR, W., BUNGAY, P. J., KASTEN, S. A., ROCHE, T. E. & BROWN, D. G. 2006. Regulatory Roles of the N-Terminal Domain Based on Crystal Structures of Human Pyruvate Dehydrogenase Kinase 2 Containing Physiological and Synthetic Ligands. *Biochemistry,* 45**,** 402-415.

KNOPMAN, D. S., PARISI, J. E., SALVIATI, A., FLORIACH-ROBERT, M., BOEVE, B. F., IVNIK, R. J., SMITH, G. E., DICKSON, D. W., JOHNSON, K. A., PETERSEN, L. E., MCDONALD, W. C.,

BRAAK, H. & PETERSEN, R. C. 2003. Neuropathology of Cognitively Normal Elderly. *Journal of Neuropathology & Experimental Neurology,* 62**,** 1087-1095.
KOO, E. H. & SQUAZZO, S. L. 1994. Evidence that production and release of amyloid beta-protein involves the endocytic pathway. *J Biol Chem,* 269**,** 17386-9.
KOOPMAN, G., REUTELINGSPERGER, C. P., KUIJTEN, G. A., KEEHNEN, R. M., PALS, S. T. & VAN OERS, M. H. 1994. Annexin V for flow cytometric detection of phosphatidylserine expression on B cells undergoing apoptosis. *Blood,* 84**,** 1415-20.
KOVALEVICH, J. & LANGFORD, D. 2013. Considerations for the Use of SH-SY5Y Neuroblastoma Cells in Neurobiology. *In:* AMINI, S. & WHITE, K. M. (eds.) *Neuronal Cell Culture: Methods and Protocols.* Totowa, NJ: Humana Press.
KRAUSE, K., KARGER, S., SHEU, S. Y., AIGNER, T., KURSAWE, R., GIMM, O., SCHMID, K. W., DRALLE, H. & FUHRER, D. 2008. Evidence for a role of the amyloid precursor protein in thyroid carcinogenesis. *J Endocrinol,* 198**,** 291-9.
KRISHNASWAMY, S., VERDILE, G., GROTH, D., KANYENDA, L. & MARTINS, R. N. 2009. The structure and function of Alzheimer's gamma secretase enzyme complex. *Crit Rev Clin Lab Sci,* 46**,** 282-301.
KUHN, P.-H., WANG, H., DISLICH, B., COLOMBO, A., ZEITSCHEL, U., ELLWART, J. W., KREMMER, E., ROßNER, S. & LICHTENTHALER, S. F. 2010. ADAM10 is the physiologically relevant, constitutive α-secretase of the amyloid precursor protein in primary neurons. *The EMBO Journal,* 29**,** 3020-3032.
KUMAR, A., KANT, S. & SINGH, S. M. 2012. Novel molecular mechanisms of antitumor action of dichloroacetate against T cell lymphoma: Implication of altered glucose metabolism, pH homeostasis and cell survival regulation. *Chemico-Biological Interactions,* 199**,** 29-37.
KUMAR, A., SINGH, A. & EKAVALI 2015. A review on Alzheimer's disease pathophysiology and its management: an update. *Pharmacological Reports,* 67**,** 195-203.
LACOR, P. N., BUNIEL, M. C., FURLOW, P. W., CLEMENTE, A. S., VELASCO, P. T., WOOD, M., VIOLA, K. L. & KLEIN, W. L. 2007. Abeta oligomer-induced aberrations in synapse composition, shape, and density provide a molecular basis for loss of connectivity in Alzheimer's disease. *J Neurosci,* 27**,** 796-807.
LAMMICH, S., KOJRO, E., POSTINA, R., GILBERT, S., PFEIFFER, R., JASIONOWSKI, M., HAASS, C. & FAHRENHOLZ, F. 1999. Constitutive and regulated α-secretase cleavage of Alzheimer's amyloid precursor protein by a disintegrin metalloprotease. *Proceedings of the National Academy of Sciences of the United States of America,* 96**,** 3922-3927.
LANDMAN, N. & KIM, T.-W. 2004. Got RIP? *Cytokine and Growth Factor Reviews,* 15**,** 337-351.
LAVOIE, M. J. & SELKOE, D. J. 2003. The Notch ligands, Jagged and Delta, are sequentially processed by alpha-secretase and presenilin/gamma-secretase and release signaling fragments. *J Biol Chem,* 278**,** 34427-37.
LEE, V. M. Y., GOEDERT, M. & TROJANOWSKI, J. Q. 2001. NEURODEGENERATIVE TAUOPATHIES. *Annual Review of Neuroscience,* 24**,** 1121-1159.
LEWCZUK, P., KAMROWSKI-KRUCK, H., PETERS, O., HEUSER, I., JESSEN, F., POPP, J., BURGER, K., HAMPEL, H., FROLICH, L., WOLF, S., PRINZ, B., JAHN, H., LUCKHAUS, C., PERNECZKY, R., HULL, M., SCHRODER, J., KESSLER, H., PANTEL, J., GERTZ, H. J., KLAFKI, H. W., KOLSCH, H., REULBACH, U., ESSELMANN, H., MALER, J. M., BIBL, M., KORNHUBER, J. & WILTFANG, J. 2010. Soluble amyloid precursor proteins in the cerebrospinal fluid as novel potential biomarkers of Alzheimer's disease: a multicenter study. *Mol Psychiatry,* 15**,** 138-45.
LI, D., MASIERO, M., BANHAM, A. H. & HARRIS, A. L. 2014. The Notch Ligand Jagged1 as a Target for Anti-Tumor Therapy. *Frontiers in Oncology,* 4**,** 254.
LI, L., CAO, D., KIM, H., LESTER, R. & FUKUCHI, K.-I. 2006. Simvastatin enhances learning and memory independent of amyloid load in mice. *Annals of Neurology,* 60**,** 729-739.

LI, W., JAMES, M. O., MCKENZIE, S. C., CALCUTT, N. A., LIU, C. & STACPOOLE, P. W. 2011. Mitochondrion as a novel site of dichloroacetate biotransformation by glutathione transferase zeta 1. *J Pharmacol Exp Ther,* 336**,** 87-94.

LICHTENTHALER, S. F., HAASS, C. & STEINER, H. 2011. Regulated intramembrane proteolysis - lessons from amyloid precursor protein processing. *Journal of Neurochemistry,* 117**,** 779-796.

LIN, G., HILL, D. K., ANDREJEVA, G., BOULT, J. K., TROY, H., FONG, A. C., ORTON, M. R., PANEK, R., PARKES, H. G., JAFAR, M., KOH, D. M., ROBINSON, S. P., JUDSON, I. R., GRIFFITHS, J. R., LEACH, M. O., EYKYN, T. R. & CHUNG, Y. L. 2014. Dichloroacetate induces autophagy in colorectal cancer cells and tumours. *Br J Cancer,* 111**,** 375-85.

LIU, C. C., KANEKIYO, T., XU, H. & BU, G. 2013. Apolipoprotein E and Alzheimer disease: risk, mechanisms and therapy. *Nat Rev Neurol,* 9**,** 106-18.

LO SARDO, V., ZUCCATO, C., GAUDENZI, G., VITALI, B., RAMOS, C., TARTARI, M., MYRE, M. A., WALKER, J. A., PISTOCCHI, A., CONTI, L., VALENZA, M., DRUNG, B., SCHMIDT, B., GUSELLA, J., ZEITLIN, S., COTELLI, F. & CATTANEO, E. 2012. An evolutionary recent neuroepithelial cell adhesion function of huntingtin implicates ADAM10-Ncadherin. *Nat Neurosci,* 15**,** 713-21.

LOPES, F. M., SCHRÖDER, R., JÚNIOR, M. L. C. D. F., ZANOTTO-FILHO, A., MÜLLER, C. B., PIRES, A. S., MEURER, R. T., COLPO, G. D., GELAIN, D. P., KAPCZINSKI, F., MOREIRA, J. C. F., FERNANDES, M. D. C. & KLAMT, F. 2010. Comparison between proliferative and neuron-like SH-SY5Y cells as an in vitro model for Parkinson disease studies. *Brain Research,* 1337**,** 85-94.

LUO, W. J., WANG, H., LI, H., KIM, B. S., SHAH, S., LEE, H. J., THINAKARAN, G., KIM, T. W., YU, G. & XU, H. 2003. PEN-2 and APH-1 coordinately regulate proteolytic processing of presenilin 1. *J Biol Chem,* 278**,** 7850-4.

MA, Q.-L., ZUO, X., YANG, F., UBEDA, O. J., GANT, D. J., ALAVERDYAN, M., TENG, E., HU, S., CHEN, P.-P., MAITI, P., TETER, B., COLE, G. M. & FRAUTSCHY, S. A. 2013. Curcumin Suppresses Soluble Tau Dimers and Corrects Molecular Chaperone, Synaptic, and Behavioral Deficits in Aged Human Tau Transgenic Mice. *Journal of Biological Chemistry,* 288**,** 4056-4065.

MADHOK, B. M., YELURI, S., PERRY, S. L., HUGHES, T. A. & JAYNE, D. G. 2010. Dichloroacetate induces apoptosis and cell-cycle arrest in colorectal cancer cells. *Br J Cancer,* 102**,** 1746-52.

MAELICKE, A., HOEFFLE-MAAS, A., LUDWIG, J., MAUS, A., SAMOCHOCKI, M., JORDIS, U. & KOEPKE, A. K. E. 2010. Memogain is a Galantamine Pro-drug having Dramatically Reduced Adverse Effects and Enhanced Efficacy. *Journal of Molecular Neuroscience,* 40**,** 135-137.

MAHER, B. A., AHMED, I. A. M., KARLOUKOVSKI, V., MACLAREN, D. A., FOULDS, P. G., ALLSOP, D., MANN, D. M. A., TORRES-JARDÓN, R. & CALDERON-GARCIDUENAS, L. 2016. Magnetite pollution nanoparticles in the human brain. *Proceedings of the National Academy of Sciences*.

MARAMBAUD, P., SHIOI, J., SERBAN, G., GEORGAKOPOULOS, A., SARNER, S., NAGY, V., BAKI, L., WEN, P., EFTHIMIOPOULOS, S., SHAO, Z., WISNIEWSKI, T. & ROBAKIS, N. K. 2002. A presenilin-1/γ-secretase cleavage releases the E-cadherin intracellular domain and regulates disassembly of adherens junctions. *The EMBO Journal,* 21**,** 1948-1956.

MARAMBAUD, P., WEN, P. H., DUTT, A., SHIOI, J., TAKASHIMA, A., SIMAN, R. & ROBAKIS, N. K. 2003. A CBP binding transcriptional repressor produced by the PS1/epsilon-cleavage of N-cadherin is inhibited by PS1 FAD mutations. *Cell,* 114**,** 635-45.

MARETZKY, T., REISS, K., LUDWIG, A., BUCHHOLZ, J., SCHOLZ, F., PROKSCH, E., DE STROOPER, B., HARTMANN, D. & SAFTIG, P. 2005. ADAM10 mediates E-cadherin shedding and regulates epithelial cell-cell adhesion, migration, and β-catenin translocation.

Proceedings of the National Academy of Sciences of the United States of America, 102**,** 9182-9187.

MATTSON, M. P. 1994. Secreted forms of beta-amyloid precursor protein modulate dendrite outgrowth and calcium responses to glutamate in cultured embryonic hippocampal neurons. *J Neurobiol,* 25**,** 439-50.

MCCLEAN, P. L., PARTHSARATHY, V., FAIVRE, E. & HOLSCHER, C. 2011. The diabetes drug liraglutide prevents degenerative processes in a mouse model of Alzheimer's disease. *J Neurosci,* 31**,** 6587-94.

MICHELAKIS, E. D., SUTENDRA, G., DROMPARIS, P., WEBSTER, L., HAROMY, A., NIVEN, E., MAGUIRE, C., GAMMER, T.-L., MACKEY, J. R., FULTON, D., ABDULKARIM, B., MCMURTRY, M. S. & PETRUK, K. C. 2010. Metabolic Modulation of Glioblastoma with Dichloroacetate. *Science Translational Medicine,* 2**,** 31ra34-31ra34.

MICHELAKIS, E. D., WEBSTER, L. & MACKEY, J. R. 2008. Dichloroacetate (DCA) as a potential metabolic-targeting therapy for cancer. *Br J Cancer,* 99**,** 989-94.

MIQUEL, E., CASSINA, A., MARTÍNEZ-PALMA, L., BOLATTO, C., TRÍAS, E., GANDELMAN, M., RADI, R., BARBEITO, L. & CASSINA, P. 2012. Modulation of Astrocytic Mitochondrial Function by Dichloroacetate Improves Survival and Motor Performance in Inherited Amyotrophic Lateral Sclerosis. *PLoS ONE,* 7**,** e34776.

MORFOUACE, M., LALIER, L., BAHUT, M., BONNAMAIN, V., NAVEILHAN, P., GUETTE, C., OLIVER, L., GUEGUEN, N., REYNIER, P. & VALLETTE, F. M. 2012. Comparison of Spheroids Formed by Rat Glioma Stem Cells and Neural Stem Cells Reveals Differences in Glucose Metabolism and Promising Therapeutic Applications. *Journal of Biological Chemistry,* 287**,** 33664-33674.

MORI, M., YAMAGATA, T., GOTO, T., SAITO, S. & MOMOI, M. Y. 2004. Dichloroacetate treatment for mitochondrial cytopathy: long-term effects in MELAS. *Brain & development,* 26**,** 453-458.

MOSCONI, L., BERTI, V., GLODZIK, L., PUPI, A., DE SANTI, S. & DE LEON, M. J. 2010. Pre-clinical detection of Alzheimer's disease using FDG-PET, with or without amyloid imaging. *J Alzheimers Dis,* 20**,** 843-54.

MOSCONI, L., DE SANTI, S., LI, J., TSUI, W. H., LI, Y., BOPPANA, M., LASKA, E., RUSINEK, H. & DE LEON, M. J. 2008. Hippocampal hypometabolism predicts cognitive decline from normal aging. *Neurobiol Aging,* 29**,** 676-92.

MOSS, M. L., BOMAR, M., LIU, Q., SAGE, H., DEMPSEY, P., LENHART, P. M., GILLISPIE, P. A., STOECK, A., WILDEBOER, D., BARTSCH, J. W., PALMISANO, R. & ZHOU, P. 2007. The ADAM10 Prodomain Is a Specific Inhibitor of ADAM10 Proteolytic Activity and Inhibits Cellular Shedding Events. *Journal of Biological Chemistry,* 282**,** 35712-35721.

MUKRASCH, M. D., BIBOW, S., KORUKOTTU, J., JEGANATHAN, S., BIERNAT, J., GRIESINGER, C., MANDELKOW, E. & ZWECKSTETTER, M. 2009. Structural Polymorphism of 441-Residue Tau at Single Residue Resolution. *PLoS Biol,* 7**,** e1000034.

MÜLLER, T., MEYER, H. E., EGENSPERGER, R. & MARCUS, K. 2008. The amyloid precursor protein intracellular domain (AICD) as modulator of gene expression, apoptosis, and cytoskeletal dynamics—Relevance for Alzheimer's disease. *Progress in Neurobiology,* 85**,** 393-406.

MURATORE, C. R., RICE, H. C., SRIKANTH, P., CALLAHAN, D. G., SHIN, T., BENJAMIN, L. N., WALSH, D. M., SELKOE, D. J. & YOUNG-PEARSE, T. L. 2014. The familial Alzheimer's disease APPV717I mutation alters APP processing and Tau expression in iPSC-derived neurons. *Hum Mol Genet,* 23**,** 3523-36.

NALIVAEVA, N. N. & TURNER, A. J. 2013. The amyloid precursor protein: a biochemical enigma in brain development, function and disease. *FEBS Lett,* 587**,** 2046-54.

NEEDHAM, B. E., WLODEK, M. E., CICCOTOSTO, G. D., FAM, B. C., MASTERS, C. L., PROIETTO, J., ANDRIKOPOULOS, S. & CAPPAI, R. 2008. Identification of the Alzheimer's disease

amyloid precursor protein (APP) and its homologue APLP2 as essential modulators of glucose and insulin homeostasis and growth. *J Pathol,* 215**,** 155-63.

NESTOR, S. M., RUPSINGH, R., BORRIE, M., SMITH, M., ACCOMAZZI, V., WELLS, J. L., FOGARTY, J., BARTHA, R. & THE ALZHEIMER'S DISEASE NEUROIMAGING, I. 2008. Ventricular enlargement as a possible measure of Alzheimer's disease progression validated using the Alzheimer's disease neuroimaging initiative database. *Brain,* 131**,** 2443-2454.

NEWINGTON, J. T., PITTS, A., CHIEN, A., ARSENEAULT, R., SCHUBERT, D. & CUMMING, R. C. 2011. Amyloid Beta Resistance in Nerve Cell Lines Is Mediated by the Warburg Effect. *PLoS ONE,* 6**,** e19191.

NICOLAS, M. & HASSAN, B. A. 2014. Amyloid precursor protein and neural development. *Development,* 141**,** 2543-8.

NIKOLAEV, A., MCLAUGHLIN, T., O'LEARY, D. & TESSIER-LAVIGNE, M. 2009. N-APP binds DR6 to cause axon pruning and neuron death via distinct caspases. *Nature,* 457**,** 981-989.

NUNAN, J., SHEARMAN, M. S., CHECLER, F., CAPPAI, R., EVIN, G., BEYREUTHER, K., MASTERS, C. L. & SMALL, D. H. 2001. The C-terminal fragment of the Alzheimer's disease amyloid protein precursor is degraded by a proteasome-dependent mechanism distinct from gamma-secretase. *Eur J Biochem,* 268**,** 5329-36.

O'BRIEN, J. T. & MARKUS, H. S. 2014. Vascular risk factors and Alzheimer's disease. *BMC Med,* 12**,** 218.

O'BRIEN, R. J. & WONG, P. C. 2011. Amyloid Precursor Protein Processing and Alzheimer's Disease. *Annual review of neuroscience,* 34**,** 185-204.

OBREGON, D., HOU, H., DENG, J., GIUNTA, B., TIAN, J., DARLINGTON, D., SHAHADUZZAMAN, M. D., ZHU, Y., MORI, T., MATTSON, M. P. & TAN, J. 2012. sAPP-α modulates β-secretase activity and amyloid-β generation. *Nature communications,* 3**,** 777-777.

OCTAVE, J.-N., PIERROT, N., FERAO SANTOS, S., NALIVAEVA, N. N. & TURNER, A. J. 2013. From synaptic spines to nuclear signaling: nuclear and synaptic actions of the amyloid precursor protein. *Journal of Neurochemistry,* 126**,** 183-190.

OHNO, M., SAMETSKY, E. A., YOUNKIN, L. H., OAKLEY, H., YOUNKIN, S. G., CITRON, M., VASSAR, R. & DISTERHOFT, J. F. 2004. BACE1 deficiency rescues memory deficits and cholinergic dysfunction in a mouse model of Alzheimer's disease. *Neuron,* 41**,** 27-33.

OSMAN, N. M. S., AMER, A. S. & ABDELWAHAB, S. 2016. Effects of Ginko biloba leaf extract on the neurogenesis of the hippocampal dentate gyrus in the elderly mice. *Anatomical Science International,* 91**,** 280-289.

PAJUELO-REGUERA, D., ALAN, L., OLEJAR, T. & JEZEK, P. 2015. Dichloroacetate stimulates changes in the mitochondrial network morphology via partial mitophagy in human SH-SY5Y neuroblastoma cells. *Int J Oncol,* 46**,** 2409-18.

PARIHAR, M. S. & BREWER, G. J. 2010. Amyloid-beta as a modulator of synaptic plasticity. *J Alzheimers Dis,* 22**,** 741-63.

PARKIN, E. & HARRIS, B. 2009. A disintegrin and metalloproteinase (ADAM)-mediated ectodomain shedding of ADAM10. *J Neurochem,* 108**,** 1464-79.

PARKIN, E. T., WATT, N. T., HUSSAIN, I., ECKMAN, E. A., ECKMAN, C. B., MANSON, J. C., BAYBUTT, H. N., TURNER, A. J. & HOOPER, N. M. 2007. Cellular prion protein regulates β-secretase cleavage of the Alzheimer's amyloid precursor protein. *Proceedings of the National Academy of Sciences,* 104**,** 11062-11067.

PARR-STURGESS, CATHERINE A., RUSHTON, DAVID J. & PARKIN, EDWARD T. 2010. Ectodomain shedding of the Notch ligand Jagged1 is mediated by ADAM17, but is not a lipid-raft-associated event. *Biochemical Journal,* 432**,** 283-294.

PARSONS, C., DANYSZ, W., DEKUNDY, A. & PULTE, I. 2013. Memantine and Cholinesterase Inhibitors: Complementary Mechanisms in the Treatment of Alzheimer's Disease. *Neurotoxicity Research,* 24**,** 358-369.

PARTHSARATHY, V., MCCLEAN, P. L., HÖLSCHER, C., TAYLOR, M., TINKER, C., JONES, G., KOLOSOV, O., SALVATI, E., GREGORI, M., MASSERINI, M. & ALLSOP, D. 2013. A Novel Retro-Inverso Peptide Inhibitor Reduces Amyloid Deposition, Oxidation and Inflammation and Stimulates Neurogenesis in the APPswe/PS1ΔE9 Mouse Model of Alzheimer's Disease. *PLoS ONE,* 8**,** e54769.

PASCIUTO, E., AHMED, T., WAHLE, T., GARDONI, F., D'ANDREA, L., PACINI, L., JACQUEMONT, S., TASSONE, F., BALSCHUN, D., DOTTI, CARLOS G., CALLAERTS-VEGH, Z., D'HOOGE, R., MÜLLER, ULRIKE C., DI LUCA, M., DE STROOPER, B. & BAGNI, C. 2015. Dysregulated ADAM10-Mediated Processing of APP during a Critical Time Window Leads to Synaptic Deficits in Fragile X Syndrome. *Neuron,* 87**,** 382-398.

PEDERSEN, W. A., KLOCZEWIAK, M. A. & BLUSZTAJN, J. K. 1996. Amyloid beta-protein reduces acetylcholine synthesis in a cell line derived from cholinergic neurons of the basal forebrain. *Proceedings of the National Academy of Sciences of the United States of America,* 93**,** 8068-8071.

PERL, D. P. 2010. Neuropathology of Alzheimer's Disease. *The Mount Sinai Journal of Medicine, New York,* 77**,** 32-42.

PERNECZKY, R., GUO, L. H., KAGERBAUER, S. M., WERLE, L., KURZ, A., MARTIN, J. & ALEXOPOULOS, P. 2013. Soluble amyloid precursor protein [beta] as blood-based biomarker of Alzheimer/'s disease. *Transl Psychiatry,* 3**,** e227.

PETERSEN, R. C. 2004. Mild cognitive impairment as a diagnostic entity. *J Intern Med,* 256**,** 183-94.

POSTINA, R., SCHROEDER, A., DEWACHTER, I., BOHL, J., SCHMITT, U., KOJRO, E., PRINZEN, C., ENDRES, K., HIEMKE, C., BLESSING, M., FLAMEZ, P., DEQUENNE, A., GODAUX, E., VAN LEUVEN, F. & FAHRENHOLZ, F. 2004. A disintegrin-metalloproteinase prevents amyloid plaque formation and hippocampal defects in an Alzheimer disease mouse model. *J Clin Invest,* 113**,** 1456-64.

PRINCE, M., WIMO, A., GUERCHET, M., ALI, G.-C., WU, Y.-T. & PRINA, M. 2015. World Alzheimer Report 2015: The Global Impact of Dementia An Analysis of Prevalence, Incidence and Trends. London: Alzheimer's Disease International.

PRINZEN, C., MULLER, U., ENDRES, K., FAHRENHOLZ, F. & POSTINA, R. 2005. Genomic structure and functional characterization of the human ADAM10 promoter. *Faseb j,* 19**,** 1522-4.

PUZZO, D., PRIVITERA, L., LEZNIK, E., FA, M., STANISZEWSKI, A., PALMERI, A. & ARANCIO, O. 2008. Picomolar amyloid-beta positively modulates synaptic plasticity and memory in hippocampus. *J Neurosci,* 28**,** 14537-45.

REDDY, P. H. & BEAL, M. F. 2008. Amyloid beta, mitochondrial dysfunction and synaptic damage: implications for cognitive decline in aging and Alzheimer's disease. *Trends Mol Med,* 14**,** 45-53.

REIMAN, E. M., CASELLI, R. J., YUN, L. S., CHEN, K., BANDY, D., MINOSHIMA, S., THIBODEAU, S. N. & OSBORNE, D. 1996. Preclinical evidence of Alzheimer's disease in persons homozygous for the epsilon 4 allele for apolipoprotein E. *N Engl J Med,* 334**,** 752-8.

REINHARDT, S., SCHUCK, F., GRÖSGEN, S., RIEMENSCHNEIDER, M., HARTMANN, T., POSTINA, R., GRIMM, M. & ENDRES, K. 2014. Unfolded protein response signaling by transcription factor XBP-1 regulates ADAM10 and is affected in Alzheimer's disease. *The FASEB Journal,* 28**,** 978-997.

REISBERG, B., DOODY, R., STOFFLER, A., SCHMITT, F., FERRIS, S. & MOBIUS, H. J. 2003. Memantine in moderate-to-severe Alzheimer's disease. *N Engl J Med,* 348**,** 1333-41.

REPETTO, E., RUSSO, C., VENEZIA, V., NIZZARI, M., NITSCH, R. M. & SCHETTINI, G. 2004. BACE1 Overexpression Regulates Amyloid Precursor Protein Cleavage and Interaction with the ShcA Adapter. *Annals of the New York Academy of Sciences,* 1030**,** 330-338.

ROCH, J. M., MASLIAH, E., ROCH-LEVECQ, A. C., SUNDSMO, M. P., OTERO, D. A., VEINBERGS, I. & SAITOH, T. 1994. Increase of synaptic density and memory retention by a peptide

representing the trophic domain of the amyloid beta/A4 protein precursor. *Proc Natl Acad Sci U S A,* 91**,** 7450-4.

RODOVA, M., JAYINI, R., SINGASANI, R., CHIPPS, E. & ISLAM, M. R. 2013. CMV promoter is repressed by p53 and activated by JNK pathway. *Plasmid,* 69**,** 223-30.

RODRIGUEZ-MARTIN, T., CUCHILLO-IBANEZ, I., NOBLE, W., NYENYA, F., ANDERTON, B. H. & HANGER, D. P. 2013. Tau phosphorylation affects its axonal transport and degradation. *Neurobiol Aging,* 34**,** 2146-57.

ROGERS, J. T., BUSH, A. I., CHO, H. H., SMITH, D. H., THOMSON, A. M., FRIEDLICH, A. L., LAHIRI, D. K., LEEDMAN, P. J., HUANG, X. & CAHILL, C. M. 2008. Iron and the translation of the amyloid precursor protein (APP) and ferritin mRNAs: riboregulation against neural oxidative damage in Alzheimer's disease. *Biochem Soc Trans,* 36**,** 1282-7.

SAKONO, M. & ZAKO, T. 2010. Amyloid oligomers: formation and toxicity of Abeta oligomers. *Febs j,* 277**,** 1348-58.

SALAY, L. C., QI, W., KESHET, B., TAMM, L. K. & FERNANDEZ, E. J. 2009. Membrane interactions of a self-assembling model peptide that mimics the self-association, structure and toxicity of Aβ(1-40). *Biochimica et biophysica acta,* 1788**,** 1714-1721.

SANCHEZ, W. Y., MCGEE, S. L., CONNOR, T., MOTTRAM, B., WILKINSON, A., WHITEHEAD, J. P., VUCKOVIC, S. & CATLEY, L. 2013. Dichloroacetate inhibits aerobic glycolysis in multiple myeloma cells and increases sensitivity to bortezomib. *British Journal of Cancer,* 108**,** 1624-1633.

SATHYA, M., PREMKUMAR, P., KARTHICK, C., MOORTHI, P., JAYACHANDRAN, K. S. & ANUSUYADEVI, M. 2012. BACE1 in Alzheimer's disease. *Clinica Chimica Acta,* 414**,** 171-178.

SCHELLER, J., CHALARIS, A., GARBERS, C. & ROSE-JOHN, S. 2011. ADAM17: a molecular switch to control inflammation and tissue regeneration. *Trends in Immunology,* 32**,** 380-387.

SCHOFIELD, P. W., TANG, M., MARDER, K., BELL, K., DOONEIEF, G., CHUN, M., SANO, M., STERN, Y. & MAYEUX, R. 1997. Alzheimer's disease after remote head injury: An incidence study. *Journal of Neurology Neurosurgery and Psychiatry,* 62**,** 119-124.

SEALS, D. F. & COURTNEIDGE, S. A. 2003. The ADAMs family of metalloproteases: multidomain proteins with multiple functions. *Genes Dev,* 17**,** 7-30.

SEUBERT, P., OLTERSDORF, T., LEE, M. G., BARBOUR, R., BLOMQUIST, C., DAVIS, D. L., BRYANT, K., FRITZ, L. C., GALASKO, D., THAL, L. J. & ET AL. 1993. Secretion of beta-amyloid precursor protein cleaved at the amino terminus of the beta-amyloid peptide. *Nature,* 361**,** 260-3.

SHAHRZAD, S., LACOMBE, K., ADAMCIC, U., MINHAS, K. & COOMBER, B. L. 2010. Sodium dichloroacetate (DCA) reduces apoptosis in colorectal tumor hypoxia. *Cancer Letters,* 297**,** 75-83.

SHAW, G., MORSE, S., ARARAT, M. & GRAHAM, F. L. 2002. Preferential transformation of human neuronal cells by human adenoviruses and the origin of HEK 293 cells. *The FASEB Journal*.

SHROADS, A. L., GUO, X., DIXIT, V., LIU, H.-P., JAMES, M. O. & STACPOOLE, P. W. 2008. Age-Dependent Kinetics and Metabolism of Dichloroacetate: Possible Relevance to Toxicity. *The Journal of pharmacology and experimental therapeutics,* 324**,** 1163-1171.

SHUKLA, M., HTOO, H. H., WINTACHAI, P., HERNANDEZ, J.-F., DUBOIS, C., POSTINA, R., XU, H., CHECLER, F., SMITH, D. R., GOVITRAPONG, P. & VINCENT, B. 2015. Melatonin stimulates the nonamyloidogenic processing of βAPP through the positive transcriptional regulation of ADAM10 and ADAM17. *Journal of Pineal Research,* 58**,** 151-165.

SHUKLA, V., SKUNTZ, S. & PANT, H. C. 2012. Deregulated Cdk5 activity is involved in inducing Alzheimer's disease. *Arch Med Res,* 43**,** 655-62.

SIMON, A. M., SCHIAPPARELLI, L., SALAZAR-COLOCHO, P., CUADRADO-TEJEDOR, M., ESCRIBANO, L., LOPEZ DE MATURANA, R., DEL RIO, J., PEREZ-MEDIAVILLA, A. & FRECHILLA, D. 2009. Overexpression of wild-type human APP in mice causes cognitive deficits and pathological features unrelated to Abeta levels. *Neurobiol Dis,* 33**,** 369-78.

SONG, P. & PIMPLIKAR, S. W. 2012. Knockdown of amyloid precursor protein in zebrafish causes defects in motor axon outgrowth. *PLoS One,* 7**,** e34209.

STACPOOLE, P. W. 1989. The pharmacology of dichloroacetate. *Metabolism,* 38**,** 1124-44.

STACPOOLE, P. W. 2012. The pyruvate dehydrogenase complex as a therapeutic target for age-related diseases. *Aging Cell,* 11**,** 371-7.

STACPOOLE, P. W., KERR, D. S., BARNES, C., BUNCH, S. T., CARNEY, P. R., FENNELL, E. M., FELITSYN, N. M., GILMORE, R. L., GREER, M., HENDERSON, G. N., HUTSON, A. D., NEIBERGER, R. E., O'BRIEN, R. G., PERKINS, L. A., QUISLING, R. G., SHROADS, A. L., SHUSTER, J. J., SILVERSTEIN, J. H., THERIAQUE, D. W. & VALENSTEIN, E. 2006. Controlled clinical trial of dichloroacetate for treatment of congenital lactic acidosis in children. *Pediatrics,* 117**,** 1519-31.

STACPOOLE, P. W., LORENZ, A. C., THOMAS, R. G. & HARMAN, E. M. 1988. Dichloroacetate in the treatment of lactic acidosis. *Ann Intern Med,* 108**,** 58-63.

STAUBER, A. J., BULL, R. J. & THRALL, B. D. 1998. Dichloroacetate and trichloroacetate promote clonal expansion of anchorage-independent hepatocytes in vivo and in vitro. *Toxicol Appl Pharmacol,* 150**,** 287-94.

STEINACKER, P., FANG, L., KUHLE, J., PETZOLD, A., TUMANI, H., LUDOLPH, A. C., OTTO, M. & BRETTSCHNEIDER, J. 2011. Soluble Beta-Amyloid Precursor Protein Is Related to Disease Progression in Amyotrophic Lateral Sclerosis. *PLoS ONE,* 6**,** e23600.

STERN, R. G., MOHS, R. C., DAVIDSON, M., SCHMEIDLER, J., SILVERMAN, J., KRAMER-GINSBERG, E., SEARCEY, T., BIERER, L. & DAVIS, K. L. 1994. A longitudinal study of Alzheimer's disease: measurement, rate, and predictors of cognitive deterioration. *Am J Psychiatry,* 151**,** 390-6.

SUTENDRA, G., DROMPARIS, P., KINNAIRD, A., STENSON, T. H., HAROMY, A., PARKER, J. M. R., MCMURTRY, M. S. & MICHELAKIS, E. D. 2013. Mitochondrial activation by inhibition of PDKII suppresses HIF1a signaling and angiogenesis in cancer. *Oncogene,* 32**,** 1638-1650.

TABNER, B. J., TURNBULL, S., EL-AGNAF, O. M. & ALLSOP, D. 2002. Formation of hydrogen peroxide and hydroxyl radicals from A(beta) and alpha-synuclein as a possible mechanism of cell death in Alzheimer's disease and Parkinson's disease. *Free Radic Biol Med,* 32**,** 1076-83.

TAKAYAMA, K., TSUTSUMI, S., SUZUKI, T., HORIE-INOUE, K., IKEDA, K., KANESHIRO, K., FUJIMURA, T., KUMAGAI, J., URANO, T., SAKAKI, Y., SHIRAHIGE, K., SASANO, H., TAKAHASHI, S., KITAMURA, T., OUCHI, Y., ABURATANI, H. & INOUE, S. 2009. Amyloid precursor protein is a primary androgen target gene that promotes prostate cancer growth. *Cancer Res,* 69**,** 137-42.

TAYLOR, C. J., IRELAND, D. R., BALLAGH, I., BOURNE, K., MARECHAL, N. M., TURNER, P. R., BILKEY, D. K., TATE, W. P. & ABRAHAM, W. C. 2008. Endogenous secreted amyloid precursor protein-alpha regulates hippocampal NMDA receptor function, long-term potentiation and spatial memory. *Neurobiol Dis,* 31**,** 250-60.

TAYLOR, M., MOORE, S., MAYES, J., PARKIN, E., BEEG, M., CANOVI, M., GOBBI, M., MANN, D. M. A. & ALLSOP, D. 2010. Development of a Proteolytically Stable Retro-Inverso Peptide Inhibitor of β-Amyloid Oligomerization as a Potential Novel Treatment for Alzheimer's Disease. *Biochemistry,* 49**,** 3261-3272.

THEUNIS, C., CRESPO-BIEL, N., GAFNER, V., PIHLGREN, M., LÓPEZ-DEBER, M. P., REIS, P., HICKMAN, D. T., ADOLFSSON, O., CHUARD, N., NDAO, D. M., BORGHGRAEF, P.,

DEVIJVER, H., VAN LEUVEN, F., PFEIFER, A. & MUHS, A. 2013. Efficacy and Safety of A Liposome-Based Vaccine against Protein Tau, Assessed in Tau.P301L Mice That Model Tauopathy. *PLoS ONE,* 8**,** e72301.

TIPPMANN, F., HUNDT, J., SCHNEIDER, A., ENDRES, K. & FAHRENHOLZ, F. 2009. Up-regulation of the α-secretase ADAM10 by retinoic acid receptors and acitretin. *The FASEB Journal,* 23**,** 1643-1654.

TOLIA, A. & DE STROOPER, B. 2009. Structure and function of γ-secretase. *Seminars in Cell & Developmental Biology,* 20**,** 211-218.

VAN KAMPEN, J., KAY, D., BARANOWSKI, D., MAELICKE, A. & KOPKE, A. 2012. Neurogenic effects of the galantamine prodrug, GLN-1062. *Alzheimer's & Dementia: The Journal of the Alzheimer's Association,* 8**,** P392-P393.

VAN ROY, F. & BERX, G. 2008. The cell-cell adhesion molecule E-cadherin. *Cellular and Molecular Life Sciences,* 65**,** 3756-3788.

VANDER HEIDEN, M. G., CANTLEY, L. C. & THOMPSON, C. B. 2009. Understanding the Warburg Effect: The Metabolic Requirements of Cell Proliferation. *Science (New York, N.Y.),* 324**,** 1029-1033.

VASEVA, A. V. & MOLL, U. M. 2009. The mitochondrial p53 pathway. *Biochimica et Biophysica Acta (BBA) - Bioenergetics,* 1787**,** 414-420.

VELLAS, B., BLACK, R., THAL, L. J., FOX, N. C., DANIELS, M., MCLENNAN, G., TOMPKINS, C., LEIBMAN, C., POMFRET, M. & GRUNDMAN, M. 2009. Long-term follow-up of patients immunized with AN1792: reduced functional decline in antibody responders. *Curr Alzheimer Res,* 6**,** 144-51.

VELLAS, B., COLEY, N., OUSSET, P.-J., BERRUT, G., DARTIGUES, J.-F., DUBOIS, B., GRANDJEAN, H., PASQUIER, F., PIETTE, F., ROBERT, P., TOUCHON, J., GARNIER, P., MATHIEX-FORTUNET, H. & ANDRIEU, S. 2012. Long-term use of standardised ginkgo biloba extract for the prevention of Alzheimer's disease (GuidAge): a randomised placebo-controlled trial. *The Lancet Neurology,* 11**,** 851-859.

VENKATARAMANI, V., ROSSNER, C., IFFLAND, L., SCHWEYER, S., TAMBOLI, I. Y., WALTER, J., WIRTHS, O. & BAYER, T. A. 2010. Histone Deacetylase Inhibitor Valproic Acid Inhibits Cancer Cell Proliferation via Down-regulation of the Alzheimer Amyloid Precursor Protein. *The Journal of Biological Chemistry,* 285**,** 10678-10689.

VON ARNIM, C. A., KINOSHITA, A., PELTAN, I. D., TANGREDI, M. M., HERL, L., LEE, B. M., SPOELGEN, R., HSHIEH, T. T., RANGANATHAN, S., BATTEY, F. D., LIU, C. X., BACSKAI, B. J., SEVER, S., IRIZARRY, M. C., STRICKLAND, D. K. & HYMAN, B. T. 2005. The low density lipoprotein receptor-related protein (LRP) is a novel beta-secretase (BACE1) substrate. *J Biol Chem,* 280**,** 17777-85.

VON ROTZ, R. C., KOHLI, B. M., BOSSET, J., MEIER, M., SUZUKI, T., NITSCH, R. M. & KONIETZKO, U. 2004. The APP intracellular domain forms nuclear multiprotein complexes and regulates the transcription of its own precursor. *Journal of Cell Science,* 117**,** 4435-4448.

WALLACE, R. A. & DALTON, A. J. 2011. What can we learn from study of Alzheimer's disease in patients with Down syndrome for early-onset Alzheimer's disease in the general population? *Alzheimer's Research & Therapy,* 3**,** 13-13.

WANG, H., LI, R. & SHEN, Y. 2013. β-Secretase: its biology as a therapeutic target in diseases. *Trends in Pharmacological Sciences,* 34**,** 215-225.

WANG, Y. & MANDELKOW, E. 2016. Tau in physiology and pathology. *Nat Rev Neurosci,* 17**,** 22-35.

WANG, Z., WANG, B., YANG, L., GUO, Q., AITHMITTI, N., SONGYANG, Z. & ZHENG, H. 2009. Presynaptic and postsynaptic interaction of the amyloid precursor protein promotes peripheral and central synaptogenesis. *J Neurosci,* 29**,** 10788-801.

WENK, G. L. 2003. Neuropathologic changes in Alzheimer's disease. *J Clin Psychiatry,* 64 Suppl 9**,** 7-10.

WEYER, S. W., KLEVANSKI, M., DELEKATE, A., VOIKAR, V., AYDIN, D., HICK, M., FILIPPOV, M., DROST, N., SCHALLER, K. L., SAAR, M., VOGT, M. A., GASS, P., SAMANTA, A., JASCHKE, A., KORTE, M., WOLFER, D. P., CALDWELL, J. H. & MULLER, U. C. 2011. APP and APLP2 are essential at PNS and CNS synapses for transmission, spatial learning and LTP. *Embo j,* 30**,** 2266-80.

WHITEHOUSE, P. J., PRICE, D. L., CLARK, A. W., COYLE, J. T. & DELONG, M. R. 1981. Alzheimer disease: evidence for selective loss of cholinergic neurons in the nucleus basalis. *Ann Neurol,* 10**,** 122-6.

WILCOCK, G. K., BALLARD, C. G., COOPER, J. A. & LOFT, H. 2008. Memantine for agitation/aggression and psychosis in moderately severe to severe Alzheimer's disease: a pooled analysis of 3 studies. *J Clin Psychiatry,* 69**,** 341-8.

WINBLAD, B. & MACHADO, J. C. 2008. Use of rivastigmine transdermal patch in the treatment of Alzheimer's disease. *Expert Opin Drug Deliv,* 5**,** 1377-86.

WOLOZIN, B., KELLMAN, W., RUOSSEAU, P., CELESIA, G. G. & SIEGEL, G. 2000. DEcreased prevalence of alzheimer disease associated with 3-hydroxy-3-methyglutaryl coenzyme a reductase inhibitors. *Archives of Neurology,* 57**,** 1439-1443.

WONG, C. W. 2016. Pharmacotherapy for Dementia: A Practical Approach to the Use of Cholinesterase Inhibitors and Memantine. *Drugs & Aging,* 33**,** 451-460.

WOODRUFF-PAK, D. S., VOGEL, R. W. & WENK, G. L. 2001. Galantamine: Effect on nicotinic receptor binding, acetylcholinesterase inhibition, and learning. *Proceedings of the National Academy of Sciences,* 98**,** 2089-2094.

WU, Y., ZHANG, S., XU, Q., ZOU, H., ZHOU, W., CAI, F., LI, T. & SONG, W. 2016. Regulation of global gene expression and cell proliferation by APP. *Scientific Reports,* 6**,** 22460.

XINTAROPOULOU, C., WARD, C., WISE, A., MARSTON, H., TURNBULL, A. & LANGDON, S. P. 2015. A comparative analysis of inhibitors of the glycolysis pathway in breast and ovarian cancer cell line models. *Oncotarget,* 6**,** 25677-25695.

XU, X., YANG, D., WYSS-CORAY, T., YAN, J., GAN, L., SUN, Y. & MUCKE, L. 1999. Wild-type but not Alzheimer-mutant amyloid precursor protein confers resistance against p53-mediated apoptosis. *Proceedings of the National Academy of Sciences of the United States of America,* 96**,** 7547-7552.

YAMAMOTO, M., TAGUCHI, Y., ITO-KUREHA, T., SEMBA, K., YAMAGUCHI, N. & INOUE, J. 2013. NF-kappaB non-cell-autonomously regulates cancer stem cell populations in the basal-like breast cancer subtype. *Nat Commun,* 4**,** 2299.

YAMAZAKI, K., MIZUI, Y. & TANAKA, I. 1997. Radiation hybrid mapping of human ADAM10 gene to chromosome 15. *Genomics,* 45**,** 457-9.

YAO, J., HAMILTON, R. T., CADENAS, E. & BRINTON, R. D. 2010. Decline in Mitochondrial Bioenergetics and Shift to Ketogenic Profile in Brain During Reproductive Senescence. *Biochimica et biophysica acta,* 1800**,** 1121-1126.

YOUNG-PEARSE, T. L., CHEN, A. C., CHANG, R., MARQUEZ, C. & SELKOE, D. J. 2008. Secreted APP regulates the function of full-length APP in neurite outgrowth through interaction with integrin beta1. *Neural Dev,* 3**,** 15.

ZACCHETTI, D., CHIEREGATTI, E., BETTEGAZZI, B., MIHAILOVICH, M., SOUSA, V. L., GROHOVAZ, F. & MELDOLESI, J. 2007. BACE1 expression and activity: relevance in Alzheimer's disease. *Neurodegener Dis,* 4**,** 117-26.

ZANETTI, O., SOLERTE, S. B. & CANTONI, F. 2009. Life expectancy in Alzheimer's disease (AD). *Arch Gerontol Geriatr,* 49 Suppl 1**,** 237-43.

ZHANG, B., MAITI, A., SHIVELY, S., LAKHANI, F., MCDONALD-JONES, G., BRUCE, J., LEE, E. B., XIE, S. X., JOYCE, S., LI, C., TOLEIKIS, P. M., LEE, V. M.-Y. & TROJANOWSKI, J. Q. 2005. Microtubule-binding drugs offset tau sequestration by stabilizing microtubules and

reversing fast axonal transport deficits in a tauopathy model. *Proceedings of the National Academy of Sciences of the United States of America,* 102**,** 227-231.

ZHANG, J. & HERRUP, K. 2011. Nucleocytoplasmic Cdk5 is involved in neuronal cell cycle and death in post-mitotic neurons. *Cell Cycle,* 10**,** 1208-14.

ZHANG, S., ZHANG, M., CAI, F. & SONG, W. 2013. Biological function of Presenilin and its role in AD pathogenesis. *Translational Neurodegeneration,* 2**,** 1-13.

ZHANG, X., LI, Y., XU, H. & ZHANG, Y.-W. 2014. The γ-secretase complex: from structure to function. *Frontiers in Cellular Neuroscience,* 8**,** 427.

ZHOU, F., GONG, K., SONG, B., MA, T., VAN LAAR, T., GONG, Y. & ZHANG, L. 2012. The APP intracellular domain (AICD) inhibits Wnt signalling and promotes neurite outgrowth. *Biochimica et Biophysica Acta (BBA) - Molecular Cell Research,* 1823**,** 1233-1241.

ZOU, K., GONG, J. S., YANAGISAWA, K. & MICHIKAWA, M. 2002. A novel function of monomeric amyloid beta-protein serving as an antioxidant molecule against metal-induced oxidative damage. *J Neurosci,* 22**,** 4833-41.